Escola de Camins
Escola Tècnica Superior d'Enginyeria de Camins, Canals i Ports
UPC BARCELONATECH

FEASIBILITY OF A HYBRID BRIDGE: SUSPENSION AND CABLE – STAYED MODEL

Thesis made by:
Víctor Folqué Ceballos

Internal tutor:
Ángel Carlos Aparicio Bengoechea

External tutor:
Jiří Stráský

Master in:
Enginyeria de Camins, Canals i Ports

Barcelona, 22/06/16

Building constructions

MASTER THESIS

INDEX

1. INTRODUCTION

The aim of this thesis is to respond to a need every day more emerging which is to create links connecting to open trade and social routes. The challenge is to avoid a distance of about 2.000 meters by constructing a hybrid bridge, a fact that has not happened so far because of the limitations that the different types of bridges present.

Nowadays it is being built the 3rd Bosphorus Bridge and it is the most significant example of a hybrid bridge. The difficulty resides in becoming a motorway/railway bridge rising a total length of 2.164 m and being then the longest one in this category. The objective here will be to reproduce similar conditions of this superstructure but for this we will have to take into account some considerations.

Broadly speaking, this study will be divided into different parts: a first part that will present the different characteristics of both a suspension bridge and a cable-stayed bridge, a second part where we will present the two models that we will study (2D and 3D), a third part with the construction phases of the bridge and a final part where both static and dynamic equilibrium will be verified. Most of the parts will be interrelated between them so we will see that there is not a strict order in this thesis.

Anyway, for the first part we will be able to use all the existing information and we will just expose all the different variables in order to choose between them in the second part. In this second part we will use the Finite Element Method for the 3D Model and we will adapt this to a 2D Model choosing the final different cross – sections we will adopt, the required geometry for the different parts and the existing elements in ***SAP2000*** to model the whole structure. The third part will be divided in two parts: one focused on the theoretical explanation about how to carry out the construction process and another one focused on the necessary calculations to reach consistent results. Finally it will be verified firstly the static equilibrium of the main parts of the structure accomplishing the Service Limit State (S.L.S) and the Ultimate Limit State (U.L.S), and secondly it will be carried out the dynamic analysis introducing the concept of aero - elasticity and studying this phenomena for three different models (2D Model, Fish-Bone Beam Model and 3D Model).

However, we will be more focused on guarantee the static equilibrium designing and studying the different possibilities we can have in the different components of the bridge.

2. SUSPENSION BRIDGES

2.1 Brief history

The construction of the first suspension bridges dates from the Industrial revolution, when rough iron bars became available and chain cables were possible. The first example of this type of bridges was the Menai Bridge (1826) with length of 176 m in the central span.

During this period the USA was the main designer and builder of suspension bridges and John Roebling became the most famous engineer of that time. He managed the in situ spinning method for the construction of parallel wire cables applying it in the construction of Niagara Bridge (1855). For the next 50 years the span lengths in suspension bridges increased considerably until the construction of 1280 m span Golden Gate Bridge (1937).

The American engineers used to design heavy and deep stiffening trusses so there weren't problems of instability because of the wind but this changed with the development of the deflection theory. This enabled designers to adopt more slender deck structures so the bridges had lower torsional stiffness and this ended with the disaster of Tacoma Narrows Bridge (1940).

After the Second World War American engineers began to use preformed parallel wire strands (PPWS). This method was developed by Japanese engineers who used it for really long span bridges. The most significant example of the technological growth arrived with Akashi Kaikyo Bridge (1990), with a main span of 1990 m and still remaining the longest in the world.

2.2 Definition

It is called suspension bridge a structure that allows to cross, at different levels, an obstacle and is composed of a deck supported by vertical or inclined wire hangers, which are the supporting structure, and hang flat on two towers.

2.3 Classification

The first and the main classification we will do it will be related with the number of spans of the bridge. In the following chapters we will classify different types of bridges according to more specific parameters as the continuity of the stiffening girders or the type of cable anchorages, but in general we can consider: single-span, three-span with two towers or multi-span with three or more towers.

1. Single-Span *2. Three-Span* *3. Multi-Span*

Figure 1: Main classification of suspension bridges

2.4 General characteristics

The following figure shows the different parts of which comprises a suspension bridge.

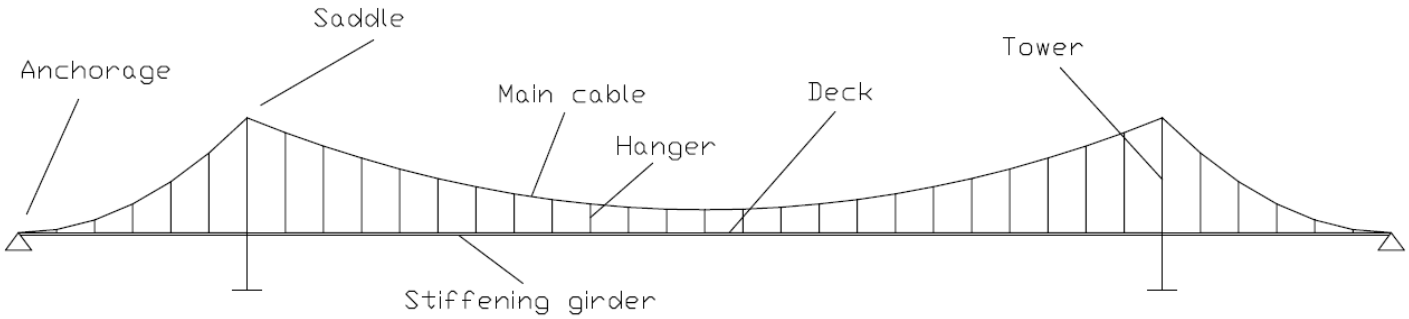

Figure 2: Main structural elements of a suspension bridge

Thus, the general characteristics of a suspension bridge are:

- Central span of length L plus two lateral spans the length of which ranges from 0.2*L to 0.5*L.
- Two main cables formed from high strength steel wires with certain flexibility supporting the whole structure.
- Two towers, which can be made by metal or reinforced concrete, situated between the central span and the two lateral spans providing a support to the cables.
- The deck with the stiffening girder that distribute concentrated traffic loading on this one avoiding local deformations of the structure and providing the torsional and bending stiffness to avoid dangerous oscillations by windage.
- Anchorages to secure cables to the ground, usually resisting horizontal forces that transmit these cables thanks to the force of gravity.

2.5 Cable arrangement

Generally, almost all suspension bridges has two main cables and then a disposition in two different planes. These cables drape in a parabolic curve between towers contributing to the overall visual impression. Anyway, a few suspension bridges employ a single cable, in which case the towers are usually tapered.

2.6 Materials and elements

2.6.1 Cables

For the cables we just only have to say that the main material will be used is high strength steel wire. The objective of this chapter is to describe briefly the different types of cables we can have and which we will use for our design. The problem appears in ***SAP2000***, where doesn't exist a database of the different cables we can choose so we will have to put directly the exact properties of our cable choice.

However, we can count with the following types of cables in suspensions bridges:

Name	Shape of section	Structure
Spiral Rope		Wires are stranded in several layers mainly in opposite lay directions
Parallel Wire Strand		The wires laid straight and parallel throughout the complete cable length
Strand Rope		Six strands made of several wires are closed around a core strand
Locked coil Rope		Deformed wires are used for the outside layers of Spiral Rope and the final layers are made up of interlocking Z-shapes wires

Table 1: Suspension bridge cable types

2.6.2 Suspended deck structure

The choice of the suspended deck is really important and the main reason is because the deck load is entirely supported by the cable, towers, and anchorages. From this point we have choose it trying to have the most economical deck with the best possible aerodynamic characteristics and with the highest torsional stiffness.

We know that the wind loading can affect the stability of the deck. On the one hand the deck structure only need to have a very low longitudinal stiffness because its continuously supported by the cable system in this direction, but on the other hand the torsional stiffness of the deck

can make a significant contribution to the overall structure stiffness, with an increase in the torsional natural frequency and improvement in aerodynamic properties.

Finally, the requirement for a low deck will suppose that we will have to choose a steel orthotropic deck. Then we have to take into account the possible solutions for the design of our suspended deck:

- Open trusses
- Plate girders
- Box girder

The first one comprises two vertical trusses positioned at the deck edges and connected by upper and lower plan bracing systems. This layout continues to be competitive to carry traffic on two levels and to carry rail traffic. Suspension bridges constructed with twin plate girders are another solution but are only suitable for shorter span lengths because of the poor aerodynamic characteristics. Finally we have the box girder which is the most common solution nowadays for the deck designing.

2.6.3 Hangers and cable bands

The main function of the hangers is to connect the deck and the stiffening girder to the main cables. In their design we have to select them in order to produce an economical and erected one. We have three types of hangers as we can see in the following figure:

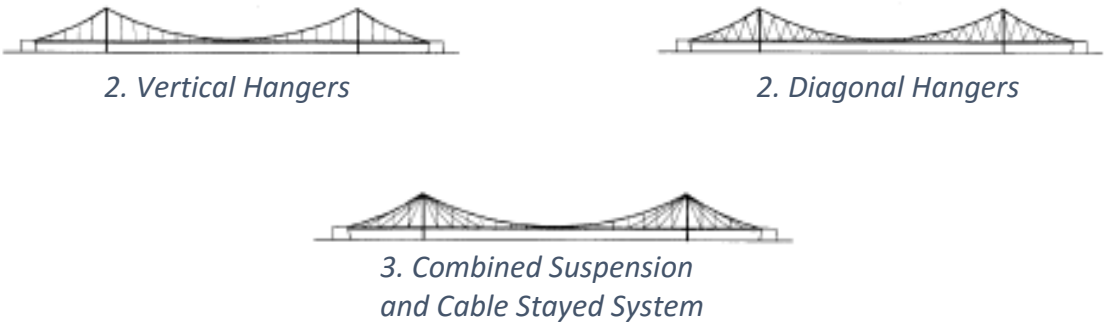

Figure 3: Types of hangers

The hangers should be as vertical as possible and equally spaced along the span but we have to note that the geometry of the deck is not the same as the cables so we can have difficulties in this way. We can have also diagonal hangers which are used to increase the damping of the suspended structure.

2.6.4 Towers

The towers are the primary responsible to provide supports to the ends of the main span with enough height to provide the required cable sag above the level of the stiffening girder and also to provide support to the deck.

In this case, we will be dealing with large spans in this cases tower base has to be relatively flexible with cable saddles fixed to the towers tops because the movement of the saddles due to varying traffic and temperatures produces longitudinal bending of the tower.

We have to be careful with the structural behavior of the tower and if we want to construct the most economical tower we will achieve this by using a tower with the highest practicable slenderness which will be our limiting factor. The limit is governed by the need for: an adequate margin against overall buckling of the tower and sufficient strength and stiffness for the tower to be safely erected as a free standing vertical cantilever subject to wind loading.

Tower design

Usually the towers of suspension bridges uses two vertical shafts and two planes of cables adopting for example an H shape but a few cable suspension bridges have also been designed with an A or an inverted Y form of towers.

Figure 4: Main shapes of suspension bridge towers

We also have to choose the material of construction, it could be steel or concrete. Taking into account that the tower is in general loaded in compression we should select concrete, but the considerably increased self-weight in comparison with an equivalent steel structure may result uneconomic.

Once we have chosen our material the tower cross-section must be arranged to produce the most effective column section, with the material placed at the maximum practical distance from the centroid. For a steel tower it's normally used a rectangular cross-section, made up of four stiffened plates whereas the appropriate cross-section for concrete towers is almost the same.

2.7 Connection with the structure

We can have two different ways of connecting the main cable with the structure, so we can have externally anchored or self-anchored types. The second ones are fixed to the deck instead of an external anchorage and in consequence the axial the axial compression is carried into the girders.

Figure 5: Externally-anchored type

Figure 6: Self-anchored type

2.8 Construction method - Erection of suspended deck

The deck structure will be divided into a series of prefabricated sections and the length of each one will be a multiple of the hanger spacing. The process of prefabrication and assembly must be very carefully controlled and the end of each abutting section must be accurately matched during assembly.

We have two different possibilities about how to erect the deck: the first one consists in initiate the erection of the deck at the centre of the main span working until the towers are reached and the second one consists in initiate this at the towers and continuing until the centre the main span is reached.

In this case we will choose the second option because of the wide maneuverability that provides us. This method allows the access along the already erected deck to the erection fronts and it exists a less reduction in the critical wind speed for the onset aerodynamic instability.

The equipment we will need to erect the deck will consist on a strand jack situated in a embarkation. The strand jack is a hollow hydraulic cylinder with a set of steel cables passing through the open centre, each one passing through two clamps. It operates climbing along the strands by releasing the clamp at one end, expanding the cylinder, clamping there, releasing the trailing end, contracting, and clamping the trailing end before starting over again.

The process will consist to lift each segment thanks to the strand jack and to put progressively the corresponding hanger.

Image 1: Example of strand jack

2.9 Analysis of suspension bridges

The suspension bridge differs from other bridge in that the cable geometry has to vary for each load combination in order to produce the equilibrium between the internal forces and the applied loading. Taking into account this is impossible to use standard methods of linear structural analysis.

Classical theories

So many theories about the construction of the complete suspension bridge has been made. The first who introduce us these systems was **Rankine**, based on the assumption that **the cable profile under dead load was parabolic**, and that the stiffening girder was sufficiently stiff to

distribute any imposed loading so that this profile remained parabolic. An improvement on this is the **elastic theory (Navier)** that retaining the same assumptions previously commented also uses a strain energy method to derive a more rational hanger loading due to imposed loads.

These two theories didn't take into account the cable displacements under the imposed load, assuming that these were small compared to the initial cable shape and consequently having large errors in the stiffening girder bending moments with large spans. Because of this it appeared the **deflection theory** developed by **Melan (1888)** that was based on combining the differential equations for both the cable and stiffening girder to derive an equation governing the behavior of the complete system. But this method was too much difficult to solve and **Bleich (1935)** developed the **linearized deflection theory**, assuming that the increase in cable tension due to imposed loading is small compared to that due to dead loading. Finally, **Crossthwaite (1947)** developed this into a practical method which could take into account non-uniform stiffening girder properties, hanger extensions, and horizontal cable movements.

3. CABLE-STAYED BRIDGES

3.1 History

Historically, cable-stayed bridges were born as a solution for large bridges but its aesthetic value has made their use has spread to structures with moderate and small spans. Despite the construction of these structures dates back many centuries the first modern cable-stayed bridges were constructed from the second half of twentieth century. The main responsible was **Dischinger**, who realized that higher stiffness and stability could be achieve with high strength pre-stressed cables.

In fact the **first bridge** its considered to be modern was built in **1955** in Sweden which is composed of three spans and has a **total length of 332 m**, and a main span of 182,6 m. The steel and concrete deck are sustained by four pairs of diagonal stay cables. Since then, there has been three generations of cable-stayed bridges.

The first generation used a small number of cables (between two and six pairs in the main span) separated by large distances (between 30 and 80 m). Due to the existing bending stiffness in the deck and the high tensions in the cables appeared the second generation of cable-stayed bridges. These ones adopted a partial suspension system and used a multiple-cable system allowing to decrease these parameters. The most important bridge of this generation was the **Brotonne Bridge**, constructed in France in **1977** with a **total length of 1.278 m** and a main span of 320 m. Finally, the third generation is characterized by the use of a large number of closely spaced stays (8-15 m) that support the deck, obtaining then very small bending moments and having to design the girder according to buckling and local deformations under concentrated loads. The most famous bridge of this generation is the **Normandy Bridge** in France in **1994** with a **total length of 2.141 m** and a main span of 856 m.

3.2 Definition

The cable-stayed bridges consist on a deck (superstructure) supported by straight and inclined cables which are connected to one or two towers. So the structural system is composed by these three main elements: the deck and the stiffening girder, the cables and the towers. In general, the design of these elements is closely related to the other so we will detail it and how they relate to each other.

3.3 General characteristics of a cable-stayed bridge

The following figure shows the different parts of which comprises a cable - stayed bridge.

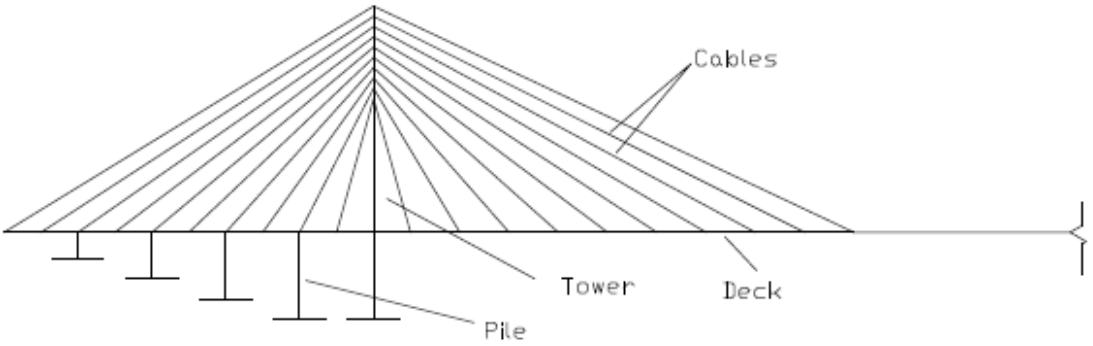

Figure 7: Main parts of cable – stayed bridge

Thus, the general characteristics of a suspension bridge are[1]:

- The length of a side span comes about 30-40 % of the main span.
- Cables formed from high strength steel wires with certain flexibility supporting the whole structure.
- Two towers, which can be made by metal or reinforced concrete, situated between the central span and the two lateral spans providing a support to the cables. Optimizations indicate that towers heights are about 1/5 of the main span.

3.4 Cable arrangement

We will classify cable-stayed bridges according to the cable disposition in the longitudinal and transversal direction. As it happens in suspension bridges the economical factor will be very important so we don't have to be careful only with the design of the cables in terms of structural performance. Thus, our layout will pretend to cover all the requirements (site conditions, aesthetic appearance…) with the best possible design.

In the longitudinal direction we have three possible designs:

[1] Characteristics referred to the deck and anchorages are the same and already explained in suspension bridges

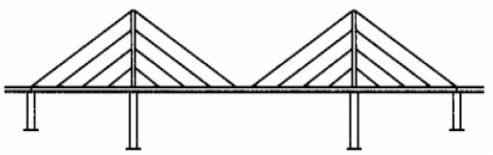

1. Harp system

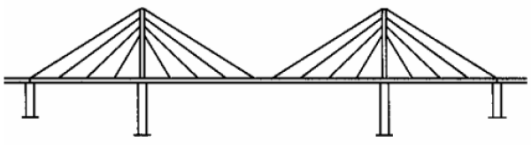

2. Semi-harp system

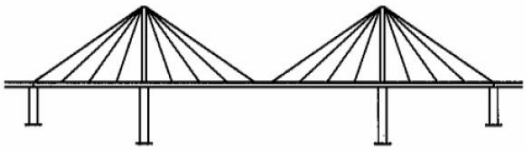

3. Fan system

Figure 8: Longitudinal classification of cable-stayed bridges

- **Harp system**: The cables are parallel to each other and are connected to the tower at different heights making the aesthetic of this kind of configuration very pleasant. However, with this system the towers should be higher and have more inclination, which increases the stiffness of the system. Therefore, the compression in the girder is very high and in terms of safety, this system is less efficient than the fan arrangement because the inclination of the cables is less pronounced.
- **Semi-harp system**: This system works almost as the fan configuration where all the cables are connected to the tower at convenient distances without being parallel. We achieve the maximum inclination of the cables rising then the maximum vertical force and consequently reducing the amount of material required in the girder.
- **Fan system**: the cables are anchored at the top of the towers, from the same point, which involves problems in the details of the anchorages because of the cable congestion and therefore in the construction and maintenance process which turns out to be complicated.

In the transversal direction we will classify them according to the plane where the cables are disposed: single central plane system, two lateral plane system and three plane system.

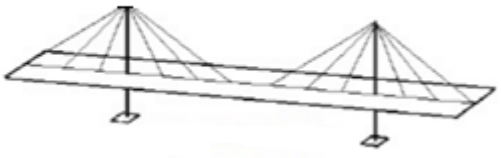

1. Single central plane system

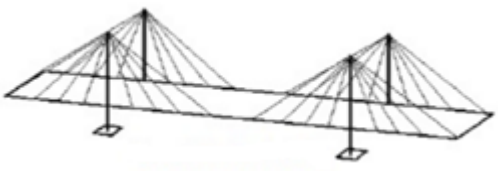

2. Two lateral plane system

3. Three plane system

Figure 9: Longitudinal classification of cable-stayed bridges

- **Single central plane system**: This type of system has only one vertical plane of stay cables along the middle longitudinal axis of the superstructure thus the space is used by the traffic. However the torsional forces are very significant in this layout conditioning the design of the girder and in this case his stiffness.
- **Two lateral plane system**: This arrangement has two planes situated in the lateral borders of the bridge and depending on the shape of the tower the layout can be vertical or inclined.
- **Three plane system**: This last layout is a combination of the two previous models. On the one hand we will achieve higher stiffness but on the other hand the economic cost of construction will be higher too.

3.5 Materials and elements

3.5.1 Cables

The cables offer us endless possibilities so we agree to limit their use and meaning in our specific case. They are responsible for supporting the loads of the deck and pass it through the towers to the substructure. Therefore, the physical integrity of the bridge depends on the quality with which the cables were made and flexibility.

The corresponding ***Eurocode (prEN 1993-1-11)***, defines a cable as an element that works fundamentally in tension, made of steel, and is adjustable and replaceable. This includes the key points of the behavior of a cable[2]:

- His load has a passive part that any other structural element would have and an active part which is introduced at the time of prestressing. We will consider the effects that this produce throughout the following chapters.
- His limited bending has consequences that will be addressed later.
- The need to reduce the weight of the cable has led to use steel cables with high elastic limit.
- His behavior, as passive element, produces important tensional variations that can lead to fatigue processes.

However, we will focus on the main elements and materials of the cable whose failure is a loss of the bearing capacity.

3.5.2 Deck structure

The deck is involved in the basic resistant scheme of the cable-stayed bridge structure because it must resist the horizontal components which the cables transmit. These components generally are balanced in the deck because its resultant, as in the tower, must be zero. We have to take

[2] The behavior of the cable in terms of protection, conservation and maintenance won't be taken into account

into account different factors to define the cross section of the deck as the cable layout, the span dimensions, the material used and other special requirements of the specific bridge.

In this case it's common also to use either steel or concrete cross – sections. For steel we can have: open cross-sections which are used for short and medium spans, box girders for long spans that may require to achieve the corresponding torsional stiffness and finally separate beams connected by cross girders. Open cross-sections and box girders are solutions also for concrete but with this material we will be able to use solid cross-sections too which will be used for smaller spans.

Finally, it exists composite cross-sections that use a concrete roadway slab as the top flange of the steel main and cross girders, connected by shear studs.

3.5.3 Towers

The physical integrity of the bridge depends on the stiffness of the tower which is the transferred from the load to the substructure, as mentioned before.

First of all we have known that the towers may be many shapes, but an H, an A or an inverted Y shape are the most popular. Towers of H shape has a simple and economic layout for medium-span bridges resulting the most logical shape with two plane of cables whereas towers of A shape and inverted Y are excellent choices for long span bridges with very flexible decks. The latter two also have higher torsional frequency than H shape and the two planes of cables can also be arranged in a symmetrical pattern.

The design parameters of the tower in this case both for the materials and the cross-section are the same as for suspension bridges.

3.6 Construction method

The construction method of a bridge must be selected taking into account the number of specific parameters related to the characteristics of the new bond to be built.

Because of its importance, both the construction process and the influence on the structural arrangement and the stresses during the construction phase, the subject receives a treatment of prominence within the technology of building bridges.

The main construction methods of cable-stayed bridges are:

- Construction on temporary supports
- Dovelas sucesivas
- Construction by cantilever method

In this case we will use the most widespread method is thus the construction by cantilever method. By this method the bridge is constructed with progressive concreting of segments with the help of rollers, and joined once hardened by prestressing the area already built. An alternative to concrete decks or the general technique in metal or composite decks is the use of prefabricated sections, transported and placed in position and subsequently joined by welding or prestressed in metal cases.

It is the most versatile technique, allowing suit any span length and height of the deck relative to the ground, although it is affected by the possibility of higher runtime errors, as well as the flexibility of the deck and deferred effects.

3.7 Analysis of cable-stayed bridges

3.7.1 Specific problems of cable-stayed bridges

The cables are one-dimensional elements with material behavior which is basically linear elastic but because of its constitution (parallel wires, strands or closed cables), the effect of its own weight and its small bending stiffness, have a global behavior rather more complicated. Thus it will appear a good number of mechanical and geometric non-linearities, rheological effects or execution errors. In this chapter we will deal with the geometric non-linearities but we won't delve into the mechanical problems that concrete or steel may cause.

3.7.1.1 Non - geometric linearities

Cable Sag

In this case the representation of the cables is carried out by biarticulated straight bars. In the presence of axial loads they will respond with a higher stiffness than the cables would do, so an apparent modulus of elasticity it will be defined, which is not other than the Modulus of Elasticity (E_T) in the permanent load stage. This module is given by the Ernst equation:

$$E_T = \frac{E}{1 + \frac{q^2 \cdot d^2 \cdot E \cdot A}{12 \cdot T^3}}$$

Where:

- **E** is the apparent modulus of elasticity that in this case is 200.000 N/mm^2.
- **q** is the linear weight of the cable, which in this case is 4.569 N/m.
- **d** is the horizontal projection of every cable.
- **A** is the cross section of the cable.
- **T** is the existing axial force in the cable.

As we can see we have three variables that will change depending of the each cable, the horizontal projection **d**, the axial force **T** and the area **A.** The program gives as the numbering cable in the order we have design the bridge and depending on the discretization we have chosen.

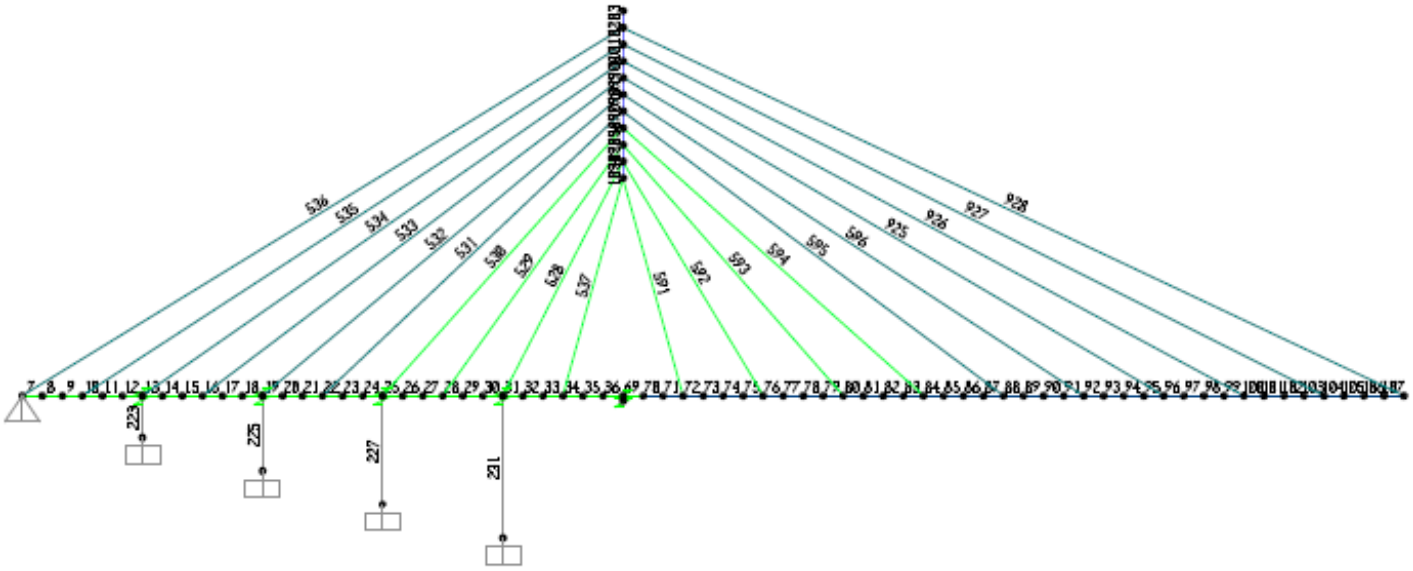

Image 2: Numbering cable

In order to simplify the process we will ordain the numbers according to the construction process, so then:

SAP nº	Construction nº
528	3
529	5
530	7
531	9
532	11
533	13
534	15
535	17
536	19
537	1

SAP nº	Construction nº
591	2
592	4
593	6
594	8
595	10
596	12
925	14
926	16
927	18
928	20

Table 2: New numbering cable

Since we know that to obtain the axial force we must have first a young modulus for each cable we will have to proceed by iteration knowing that we have to go *chapter nº4* in order to understand about what we are talking about when we talk about phases.

To determine the appropriate module of each of the cables we have considered the **phase 4** besides the **phase 1** and also we have made a weighted average of the results found. Thus in the following table we can see the apparent elasticity modulus of the cables according to the acting axial force both **phase 1** and **phase 4**:

E_T (Mpa)			
T1	199.776,00	T2	199.101,67
T3	47.322,53	T4	189.483,37
T5	197.483,31	T6	188.696,50
T7	187.130,36	T8	184.382,02
T9	195.462,68	T10	182.349,91
T11	178.263,40	T12	180.284,09
T13	194.135,48	T14	179.097,59
T15	169.110,71	T16	175.363,21
T17	194.879,67	T18	182.334,82
T19	56.391,39	T20	59.705,56

Table 3: Young modulus in each cable for phase 1

E_T (Mpa)			
T1	199.833,53	T2	199.009,01
T3	187.087,58	T4	189.269,42
T5	199.040,24	T6	188.736,21
T7	197.370,21	T8	184.435,20
T9	198.768,79	T10	182.421,74
T11	197.051,82	T12	180.415,69
T13	198.540,23	T14	180.126,33
T15	196.192,51	T16	178.599,09
T17	198.579,20	T18	185.899,74

Table 4: Young modulus in each cable for phase 4

Observing results obtained it was decided to add the straps in three groups each with an apparent different modulus: a first group with cables nº 3 and nº 19, a second group with only the number 20 and the last with the rest of cables. Finally we have:

E_T (Mpa)		
Group 1	T3, T19	120.093,85
Group 2	T20	78.962,71
Group 3	OTHER CABLES	180.314,70

Table 5: Summary table of the Young modulus adopted

Thus, by correcting the modulus of elasticity there will be a response of the cables to the geometric nonlinearity of the cables.

4. DEFINITION OF PHASES

4.1 Phase 1

This first phase only includes the staged construction of the cable – stayed bridge part. The construction of the lateral span it will be made thanks to a falsework being able to construct then the piles. After this it will be possible to prestress the cables of this part of the bridge and begin the construction of part of the deck belonging to the central span.

Figure 10: Parts involved in phase 1

4.2 Phase 2

This phase includes the execution of the deck in the suspended part of the bridge which is initially sustained by the main cable. It presents the following sub-phases:

- Cable laying supported on parallel tapes on both margins and lifting of the hangers in accordance with the guideline calculation.
- Lifting of the segment from the vessel until the lower level of the hanger thanks to the strand jack.
- Supporting of the segment from the hanger. The segment will be sustained by a temporary suspension system in order to reproduce the conditions of a falsework, ie not producing any stress over the segment.

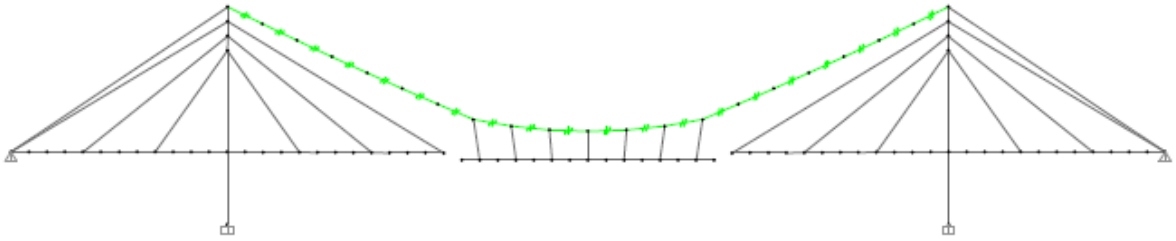

Figure 11: Parts involved in phase 2

4.2.1 Modeling in sap2000

Modeling in SAP2000 in this part consists in defining a group which contains the cable, the hangers and the segments that we will call phase 2.

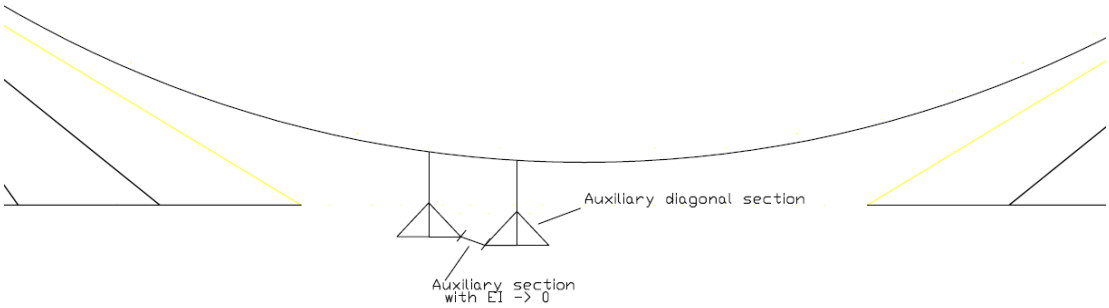

Figure 12: Auxiliary section detail

The process includes the following steps:

- We will introduce the hangers and the segments but we will leave a space between the segments with a very small length.
- In this space we will put an auxiliary section with the aim of stablishing a statically stable model. This section will have a lower stiffness in order to reproduce the real supporting conditions.
- Finally we will put more auxiliary sections because we don't want that the segment absorbs relevant stresses. We can sections in the ***figure 13*** as diagonals.

4.3 Phase 3

This phase involves placing the ends of both decks at the same level and has the following sub-phases:

- Lifting the segments until the same level of the end of the deck in phase 1.
- Connecting all the segments between them.
- Execution of the rest of all permanent loads corresponding to the pavement and the railings.
- Withdrawal of provisional suspension elements.

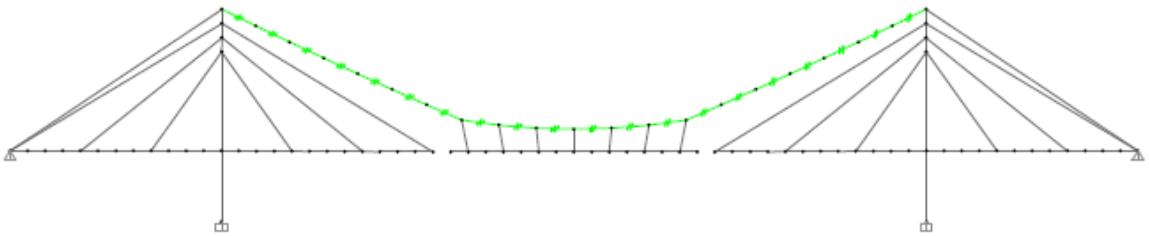

Figure 13: Parts involved in phase 3

4.3.1 Modeling in sap2000

The way to equalize the two levels with ***SAP2000*** consists in assign to the hangers an imposed deformation such that the two decks be placed at the same level. At the same time the suspended deck has to have all its points at the same level so that behaves as a continuous beam, so we will apply an additional deformation to achieve this.

In this moment we will make a change of section of the auxiliary section that is joining the segment by the real section of the deck. This change of section is an application of the program ***SAP2000.***

Then we will retire the diagonal auxiliary sections with the application "Remove" and finally, we will add the rest of permanent load adding another imposed deformation which in this case will be much reduced.

This modeling can be considered sufficiently approximate, at least, we have to keep in mind that the imposed deformation produces a vertical movement of the cable with negative sign as this plays like a spring at the top of the hanger and supports this and the deck. This scheme consisting in spring + hanger + deck gives us (stablishing the balance of vertical forces) axial forces in hangers that don't really exist and therefore we don't need to have they in mind. In relation to the additional vertical movements of the cable, are not significant, considering that the model is finally sufficiently estimated.

4.4 Phase 4

In this last phase we only have to take into account the final connection between the two decks with two small sections and the addition of some hangers in order to give more stability to the deck.

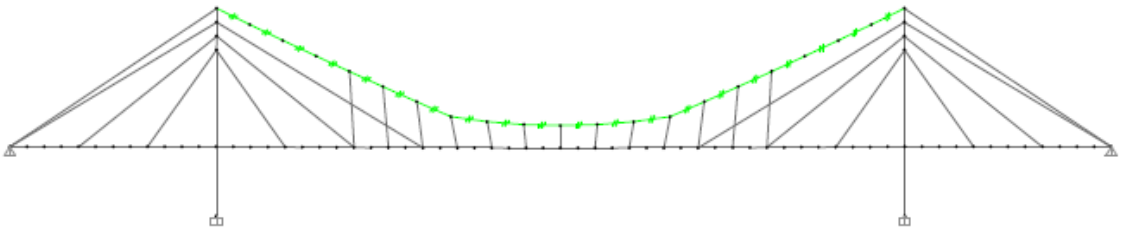

Figure 14: Parts involved in phase 4

5. PRESENTATION OF THE MODELS USED

5.1 3D Model

5.1.1 3D model analysis

The wide range of finite element method softwares has now rendered above the obsolete methods and it's because the complexity of the three-dimensional large displacement analysis of geometrically non-linear structures. This chapter is intended to show the methodology to be followed for the bridge design in 3D using the finite element method.

The mathematical theory and formulation of the FEM are well documented in many textbooks and explaining it is not the aim of this thesis. Regarding elements types, a structure can be modeled using line elements (1D), area elements (2D) or volume elements (3D) elements or even the combination of these three elements:

- **Line elements:** we have two different types for modeling the bridge members, the bar type and the beam element (frame element). The first one is used for modeling a truss member, a bearing or an individual member of the cross-frame and it has only one degree of freedom at each node with only axial tension or compression. The second one has six degrees of freedom and is used to model a beam or a column that has axial stiffness as well as bending stiffness.

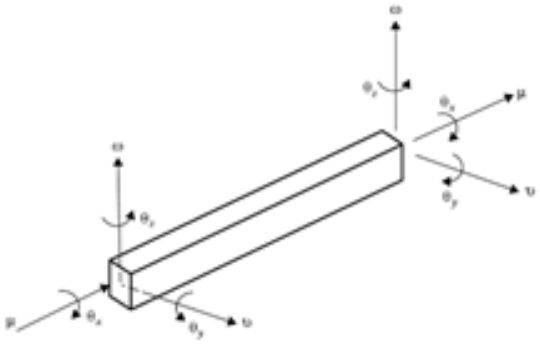

Figure 15: Degrees of freedom of a 3D element frame

- **Area elements**: these elements include two different types, elements with in-plane effects and out-of-plane effects. Regarding the first ones (referred as membrane elements) we have in each node two degrees of freedom (u,v) what has resulted in less use than the second one, which is used to simulate not only in-plane (membrane) but also plate bending (flexural) action with an additional three degrees of freedom (w,..) at each node. This type of combined plate element is often referred to as plane shell element, to differentiate a pure bending plate element. ***figure 16*** shows an example of how we have model our deck.

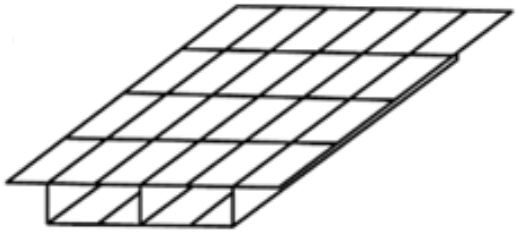

Figure 16: structure idealized by 3D plane Shell elements

- **Volume elements**: in bridge superstructures we rarely use them because its complicated usage and interpretation, so the model is usually built up from line or area elements or combinations of these two types.

The advantage of using FEM is that the analysis can be carried out for a transition area and a local area can be finely modeled separately from the whole model. However, for bridge structures is only recommended for failure analysis and not for a rapid design work.

In this global analysis, the three-dimensional analysis will be model by area elements regarding the stiffening girder. However, solution convergence can be difficult with this type of structures and that's why we won't be able to use the application cable in ***SAP2000*** and we will have to use line elements, and in this case frame elements. We could solve convergence problems by reducing the bending stiffness of the cables and hangers, rather as tension only elements but it won't be possible too

We have to note that the analysis of the stiffening girder will be made by segments of 48 m. The reality is that this is excessive but then we would have to put more cables so the calculation would become too complicated.

5.1.2 General geometrical characteristics of the bridge

Our bridge design consists in a three span bridge where the **main span** has a length of **1.416 m** and the two **lateral spans** have a length of **373 m.**

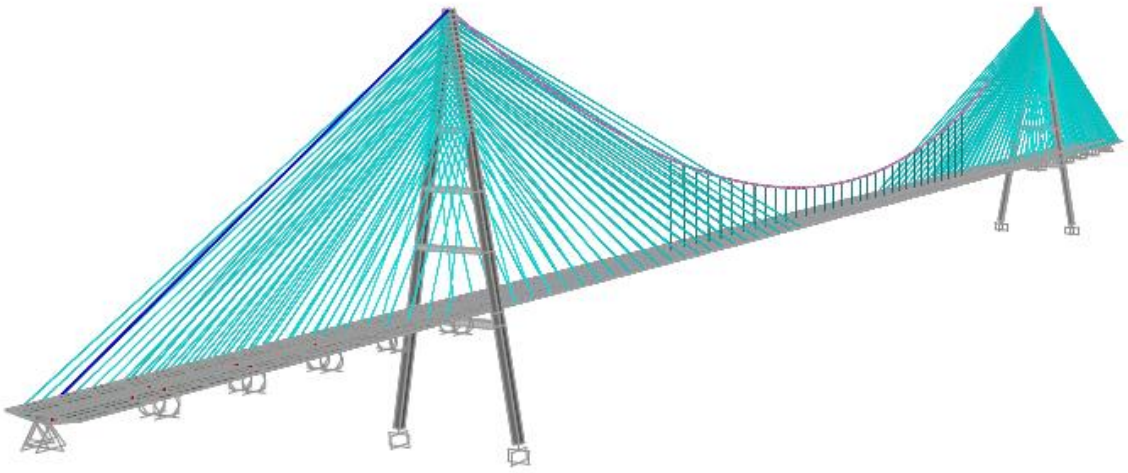

Image 3: Perspective view of the entire bridge

In the transversal direction the deck has total width of 60 meters consisting on[3]:

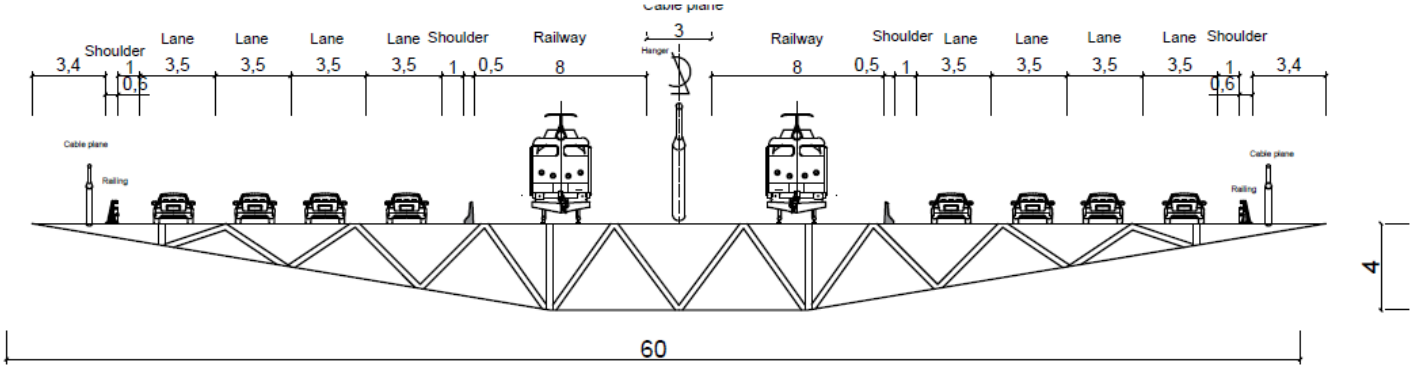

Figure 17: Detailed 3D deck cross-section

[3] Henceforth all the measurements in figures are in meters.

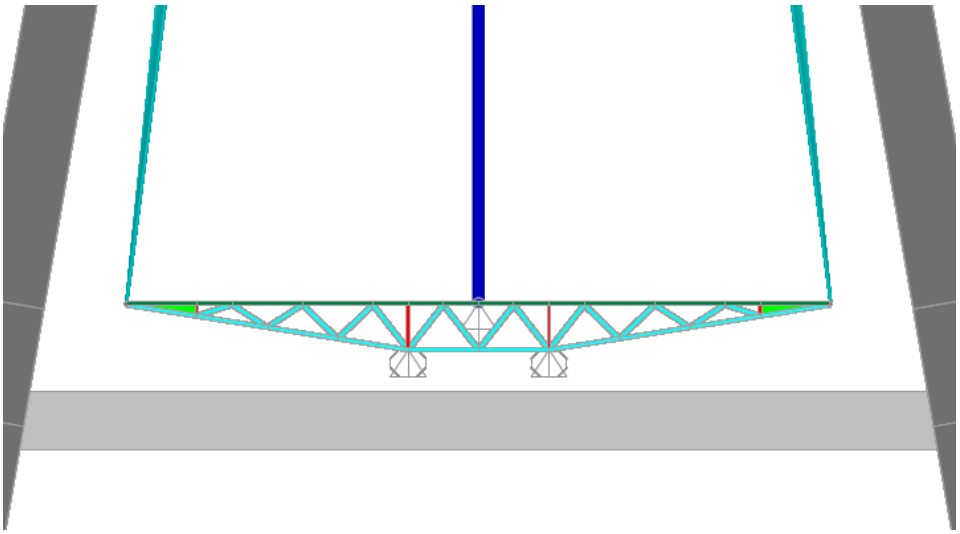

Image 4: 3D deck cross-section in SAP2000

5.1.3 Design of common elements for both parts of the bridge

Since we are dealing with a hybrid model the design of some of the elements composing the bridge must be the same.

5.1.3.1 Cables

In this case we will share the same material characteristic (not geometric) for all the cables in the structure. We will choose the Strand rope cables which count with these six strands of equal nominal diameter around a straight central wire which its diameter will be between 1.02 d and 1.05 d.

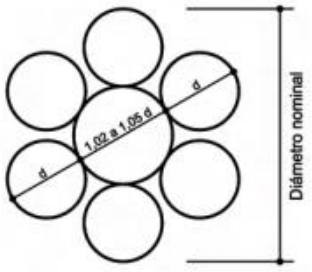

Figure 18: Strand Rope example

In 7 wire strands, the difference in diameter between the core wire and the periphery, serves to accommodate these during the tensioning process and prevent displacement of the core wire.

The strains must accomplish the technical requirements of *UNE 36094: 97* and must satisfy too the mechanical characteristics obtained from tensile test performed according to the *UNE 7326*: *88*. The following image shows the characteristics we have imposed according with the material chosen (Y1860s7) in ***SAP2000***:

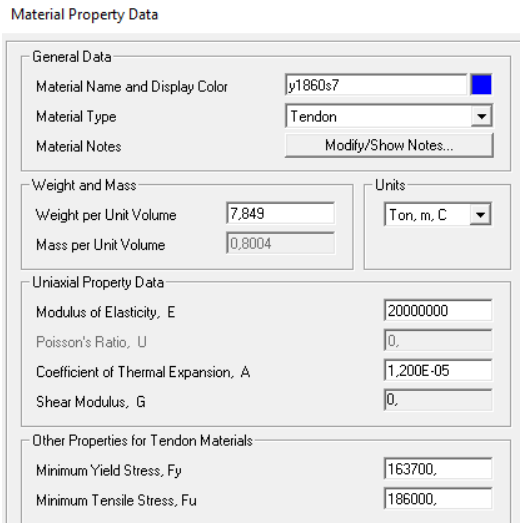

Image 5: Y1860 s7 strand characteristics

As we are dealing with frames and not with the cable application we have to give the value for an outside diameter and a wall thickness, this second one with the maximum possible value to have the minimum hole.

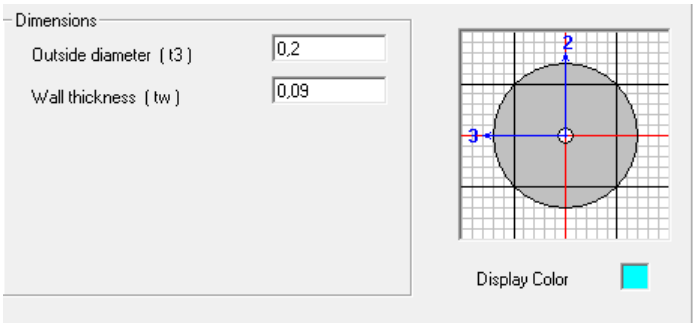

Image 6: SAP modeling of the cable cross-section

The following table shows us the diameter values adopted in the different types of cables we have in the structure:

Type of cable	Ø (m)
Main cables	1
Cables (Cable stayed bridge)	0,2
Hangers	0,1

Table 6: Diameters of the different cables in the bridge

5.1.3.2 Towers

Height

Our tower has a height of 330 meters which is approximately 1/5 of the length of the main span. As the tower has a considerable height this will allow us to reduce the required amount of cable steel and the compression forces in the bridge beam up to a cable inclination of 45º.

Material

In this model we will choose concrete as the tower is predominantly loaded in compression despite the considerably self-weight. As we can see in the ***image 7*** the tower will be connected with transversal cross beams. For the main structure of the tower (dark gray) it will be used RC 30 and for the cross beams RC 35.

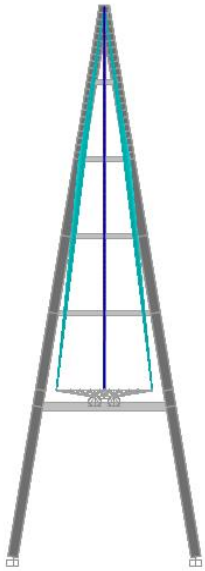

Image 7: 3D tower detail

Shape

Our tower in 3D model will have an "A" shape since we are dealing with long spans, proportioning us high torsional frequencies and permitting the two planes of cables be arranged in a symmetrical pattern.

Cross-section

As we have mentioned in previous chapters the most common cross-section for concrete towers is a rectangular cross-section and this is what we will used. We can see it in the following figure:

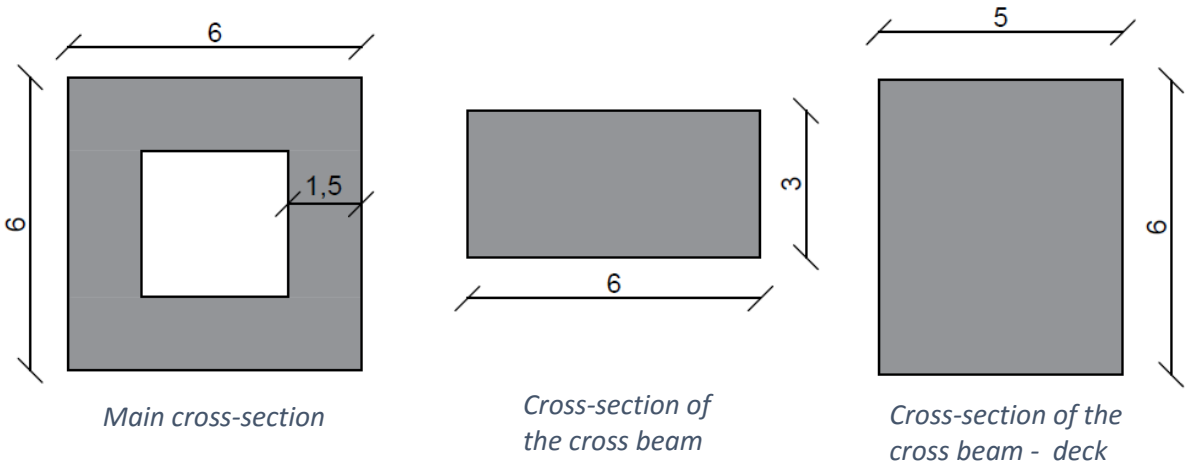

Figure 19: Details of the different cross-sections that the 3D tower has

The following table summarizes the main characteristics of the tower:

Main characteristics	
Height	330 m
Material	Concrete HA-30/HA-35
Shape	A
Cross-section	Rectangular

Table 7: Main characteristics of the tower

5.1.4 Design of the suspended structure

5.1.4.1 General characteristics

We will adopt a self-anchored model where the connection between the main cable and the deck will be made by rigid biarticulated hangers. We can see in the ***image 8*** the part of the main cable corresponding to the central span in pink. It will be connected with the two towers (320 m of height) having a cable sag of 200 m. The hanger length varies between 30 and 88 meters for the longest one counting with a total of 33 of them.

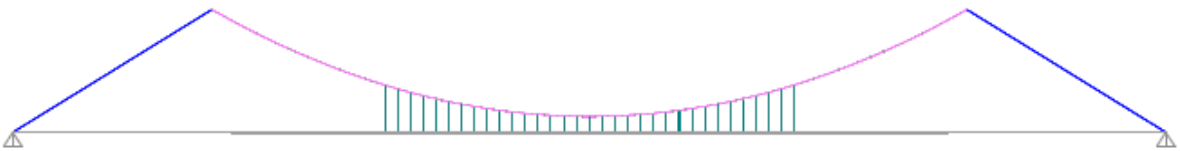

Image 8: Cross-section of the bridge in plane y = 0

5.1.4.2 Cable arrangement

Since the tower has an "A" shape it will must be employed a single cable, obviously on the central axis of the bridge.

5.1.4.3 Deck

In order to minimize the weight of the structure we will use a steel stiffening girder with his concrete slab (RC 30) just above it. This composite deck allow a faster and more effective construction phase than a concrete deck while being overall cheaper than a fully steel solution. Our design will be based in a box girder of an orthotropic deck of conventional arrangement as we can see in the ***image 9*** with 3 longitudinal trough stiffeners (in red) in the central part of the bridge with 30 cm of thickness and 2 more (in green) for the anchoring zone of the cables justifying this because these are critical zones. Therefore we will dispose a system of upper and lower plan bracing systems to increase the total stiffness. These will correspond to HEB 400 sections.

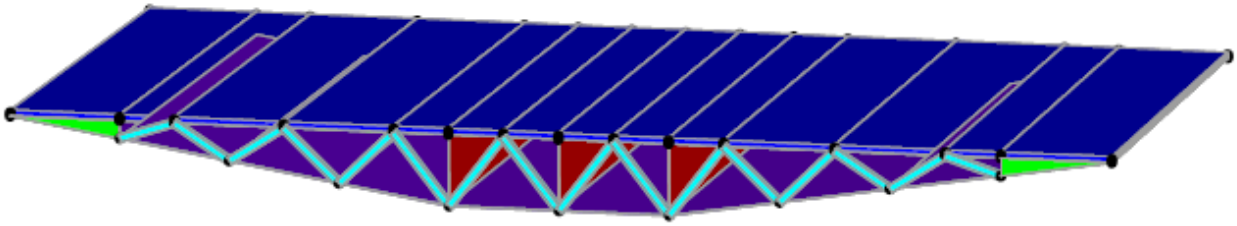

Image 9: Detail of the metallic segment of the bridge

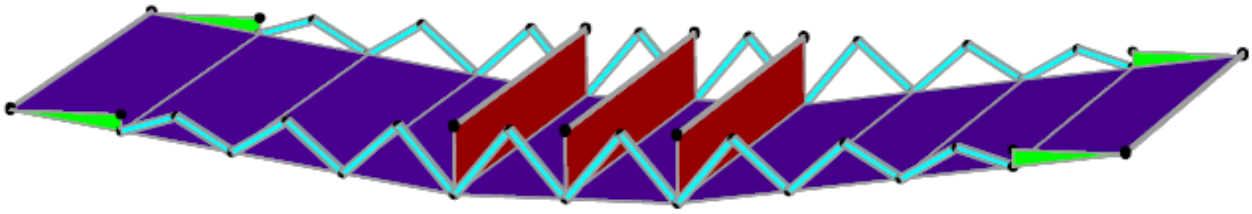

Image 10: Interior detail of the metallic segment of the bridge

We will discard plate girders and open trusses due to the lower self-weight of the box girder in comparison with these two options and the facility to maintain this because of its low exposed area and smooth external surfaces.

5.1.5 Design of the cable-stayed structure

5.1.5.1 Cable arrangement

For the cable arrangement we will make use of a semi-harp system in the longitudinal direction and a two plane system arranged in a symmetrical pattern. For very long spans where the tower is very high and needs high lateral stiffness it's better to use the two lateral plane system.

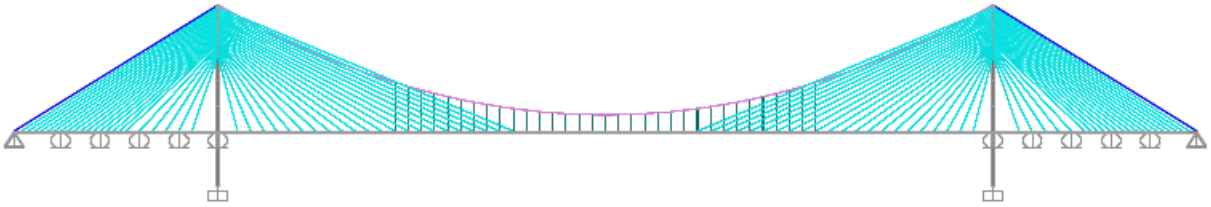

Image 11: Longitudinal elevation of the bridge design in 3D

Therefore, in the transversal direction, taking into account the problems that the other systems cause selecting the semi-harp system seems to be the best solution.

Thus, the disposition of the cables is given by the angle that these conform to the tower and the deck. A lower angle with the tower and higher with the board will provide greater vertical force (which is what really interests us) but in turn we need to have a larger number of cables. It is therefore estimate through trial and error the optimal point of connection between cables and towers.

The angles between the cables and the deck goes from 22,71º until 75,38 º and the total length of the cables varies between 143,31 m for the shorter cable and 586 m for the larger one. The quantity of cables employed rises to 22 cables on both sides of the tower and in the two planes of arrangement.

5.1.5.2 Deck

There will be two different types of deck depending if we are on the main span or on one of the lateral spans. We have already described the cross-section of the deck in the main span since is obviously the same than the suspension deck cross-section. For the lateral span we will choose a concrete box girder RC 30 because we want to create a counterweight in this area. Both the top and the bottom area have 30 cm of thickness.

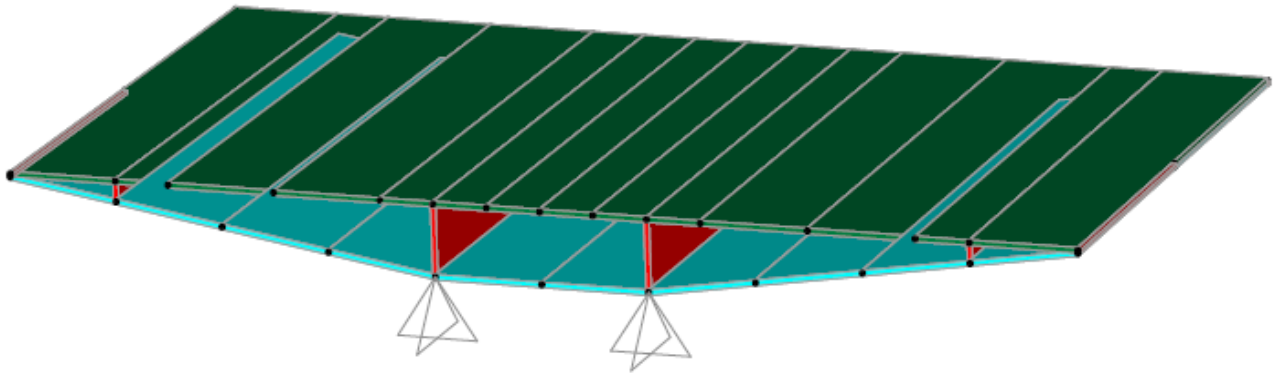

Image 12: Detail of the concrete segment of the bridge

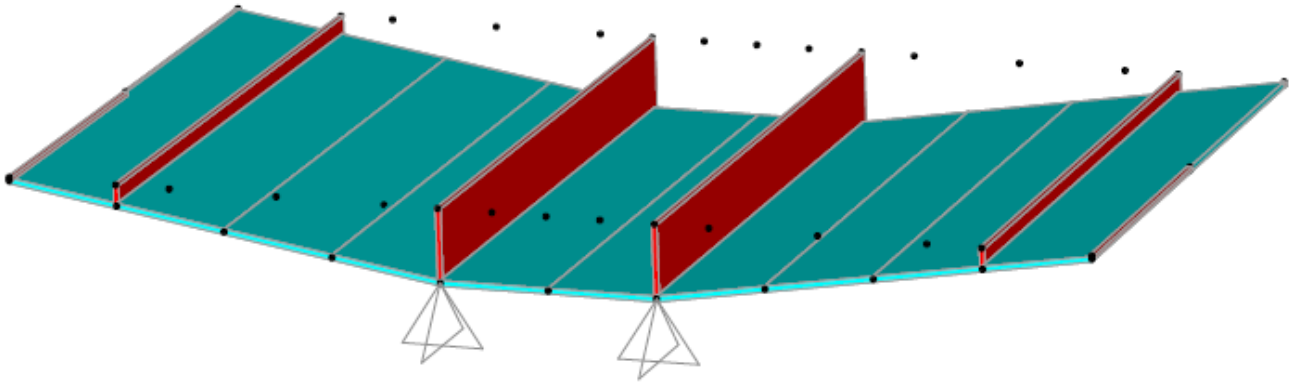

Image 13: Interior detail of the concrete segment of the bridge

In this case we will have 2 longitudinal through stiffeners (in red) in the central part of the bridge and 2 more (in red too) for the anchoring zone of the cable with 30 cm of thickness.

5.1.6 Summary

Finally a table with the main characteristics of the bridge in 3D it's shown:

General characteristics	
Main span length	1.416 m
Lateral span length	373 m
Width	60 m
Tower height	330 m
Suspension bridge part	

Cable arrangement	Single cable plane
Cable sag of main cable	200 m
Nº of hangers	33
Hanger length	30 – 80 m
Deck	Composite box girder section
Cable-stayed bridge part	
Cable arrangement	Semi-harp/two lateral system
Nº of cables	176
Cable length	143-586 m
Deck	Composite box girder section/Concrete box section

Table 8: Characteristics of the 3D model adopted

5.2 2D Model

5.2.1 2D Model analysis – Model comparison

We have already described the elements to model the structure. Since we are dealing in this case with a 2D model we will use frame elements for the deck, hangers and the cables of the cable-stayed bridge part. The problem appears with the main cable and its connection with the deck. This chapter will seek to find the right tool for modeling main suspension cable. We will propose different models trying to expose the problems that each of them entails.

5.2.1.1 Cable connected to the deck by hangers

SAP 2000 allows us to use the cable tool so use it for modeling of it might seem the most logical option. This is when a first model with **the cable connected to the deck by hangers** is proposed. It seems that this should be the prototype par excellence because it is the most faithful representation of reality but the program does not allow the solution reaches to converge. From here different solutions are sought and the first proposal is to adjust the suspension cables inserting a spring as you can see in the ***image 14***.

Actually, putting springs in the hangers the solution converges and we have consistent results. The problem occurs in **phase 3** when it is required to raise the central part of the deck to carry the same level of **phase 1**, this is where the program does not allow imposed directly deformations in springs (or n-link).

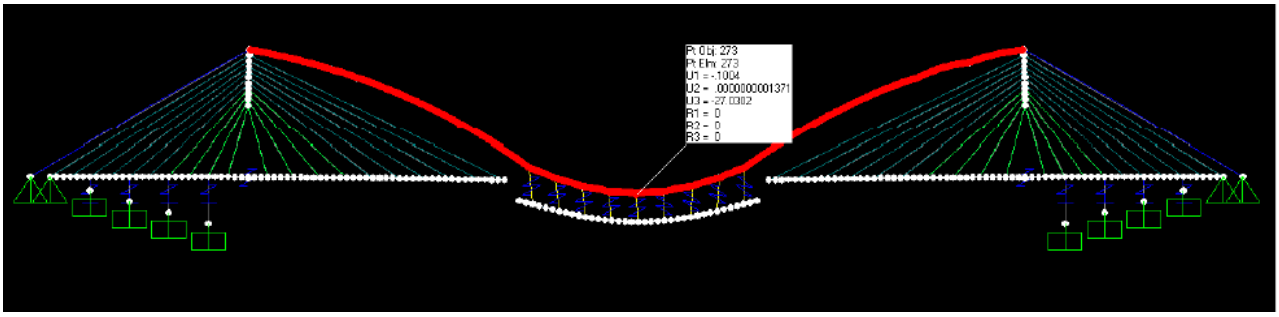

Image 14: Deflection of the cable for the case "Cable connected to the deck by hangers"

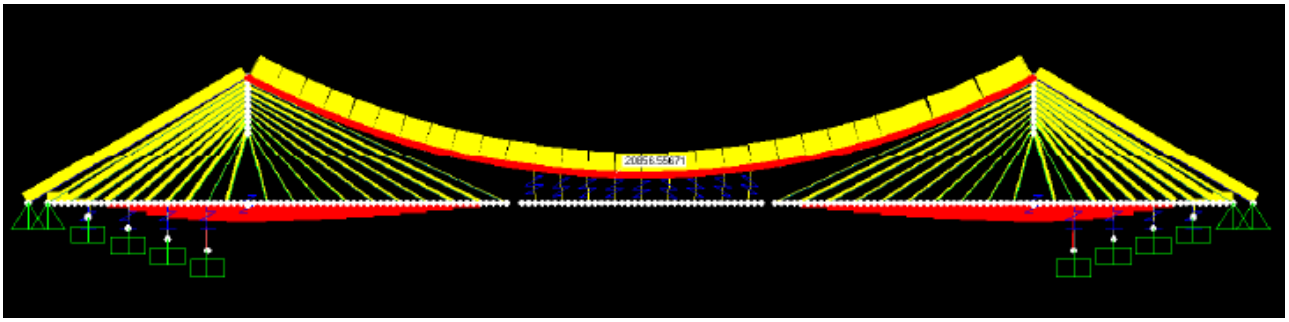

Image 15: Axial force diagram for the case "Cable connected to the deck by hangers"

5.2.1.2 Cable without connection to the deck

Knowing what have happened with the previous model we can think that the problem is in the hangers so we decide to try a new configuration in which they are not involved. We will call this second model as **cable without connection to the deck**. In this case the loads that were originally distributed along the central section of the board shall be transmitted directly to the cable. The deformed can be displayed in the ***image 16*** It is worth mentioning that it have been placed a series of supports where theoretically would have to be located hangers because the program cannot calculate items that are not supported, ie, that are not connected to any other point of the structure.

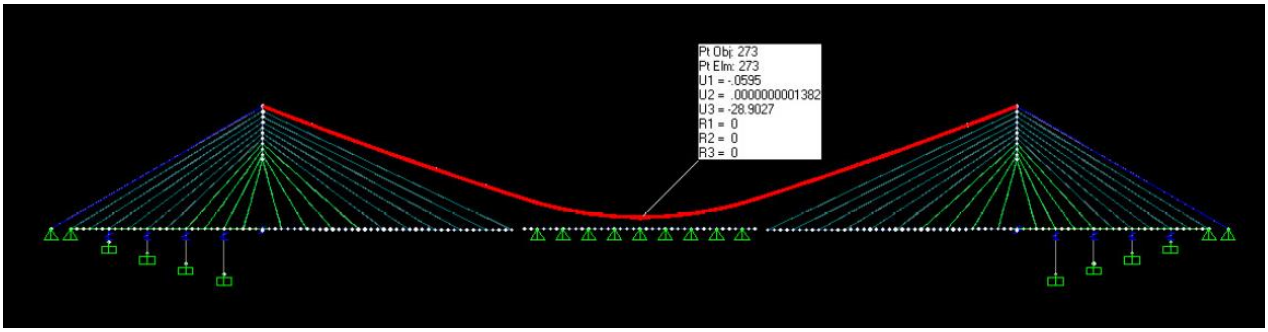

Image 16: Deflection of the cable for the case "Cable without connection to the deck"

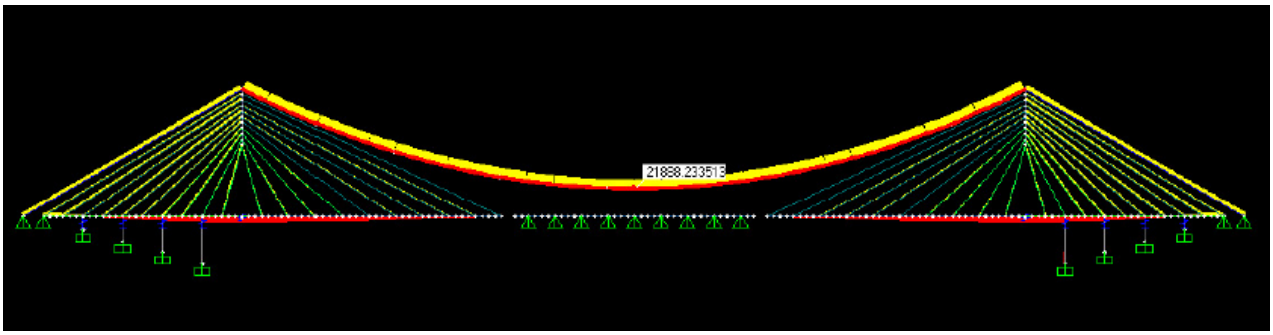

Image 17: Axial force diagram for the case "Cable without connection to the deck"

With this prototype we get results but we turn away a lot of what would become the real bridge. What we have achieved is to determine that the problem is given by the connection between the cable and suspension cables.

5.2.1.3 Model with springs connected to the deck by hangers

Finally we got to our third prototype, which we will call model with **springs connected to the deck by hangers** as shown in the ***image 18***. With this model we try to equate the most of the mechanical characteristics of the cable. Having this layout permits: on the one hand having hangers thus achieving connection with the deck and on the other hand, the solution converges without having to enter springs in the suspension cables.

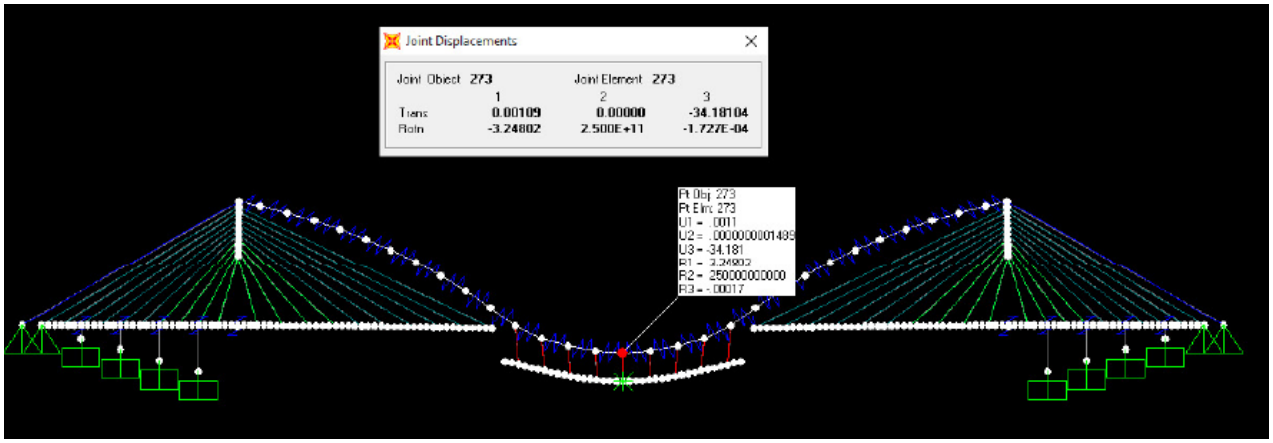

Image 18: Deflection of the cable for the case "Springs connected to the deck by hangers"

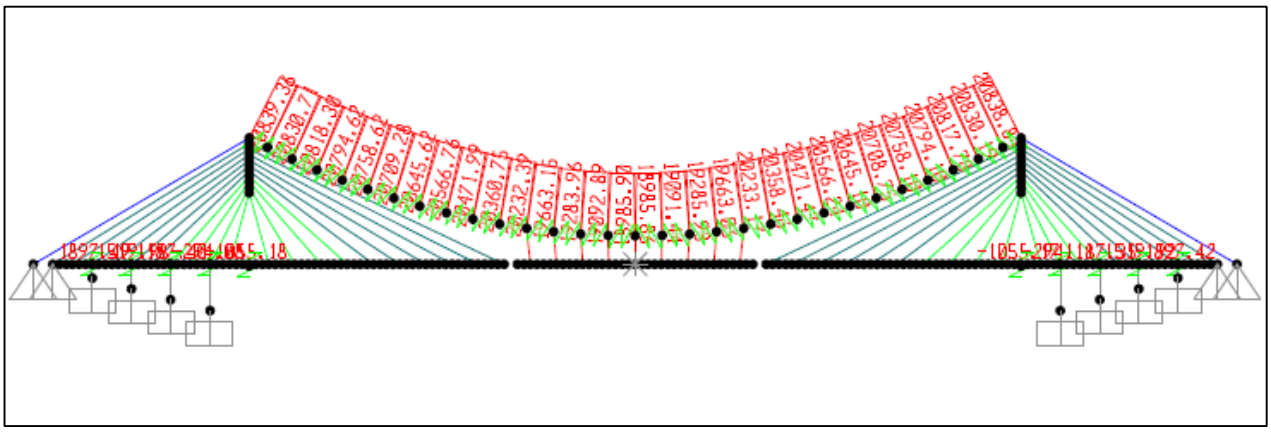

Image 19: Axial force diagram for the case "Springs connected to the deck by hangers"

5.2.1.4 Conclusions

Considering what we have seen in this chapter it can be concluded that the cable tool is not valid for the structure is being proposed and is raised for much simpler bridges. The problem lies in the moment when other elements attached to the cable (in this case hangers) generating convergence problems in the program. Therefore, this tool is intended for isolated models and in any case evolutionary models.

Below there is a summary table with the results of the three cases we have presented:

	Cable connected to the deck by hangers	Cable without connection to the deck	Springs connected to the deck by hangers
Vertical movement (m)	-27,02	-28,9	-34,181
Variation (%)	-	-	26,50
Axial force in the center (Tn)	20.856,55	21.838,23	18.985,90

Table 9: Summary with the results of the three studied cases

Knowing that we can't use the Cable tool the only solution is to make use of the springs. Comparing the first case with the third, which is what really interests us, we do not see too disparate results regarding the axial forces, while for the deflection we see a slightly more

noticeable difference. Despite this we have to deal with this problem and assume that the model developed with springs is a little more flexible.

As a last point also comment that has tested the model with the Frames tool (bars) but in any case it reproduced the cable due to the appearance of additional stresses despite impose the same mechanical characteristics of the cable.

5.2.2 General geometrical characteristics of the bridge

As in the 3D model our bridge design consists in a three span bridge where the main span has a length of 1.416 m and the two lateral spans have a length of 373 m.

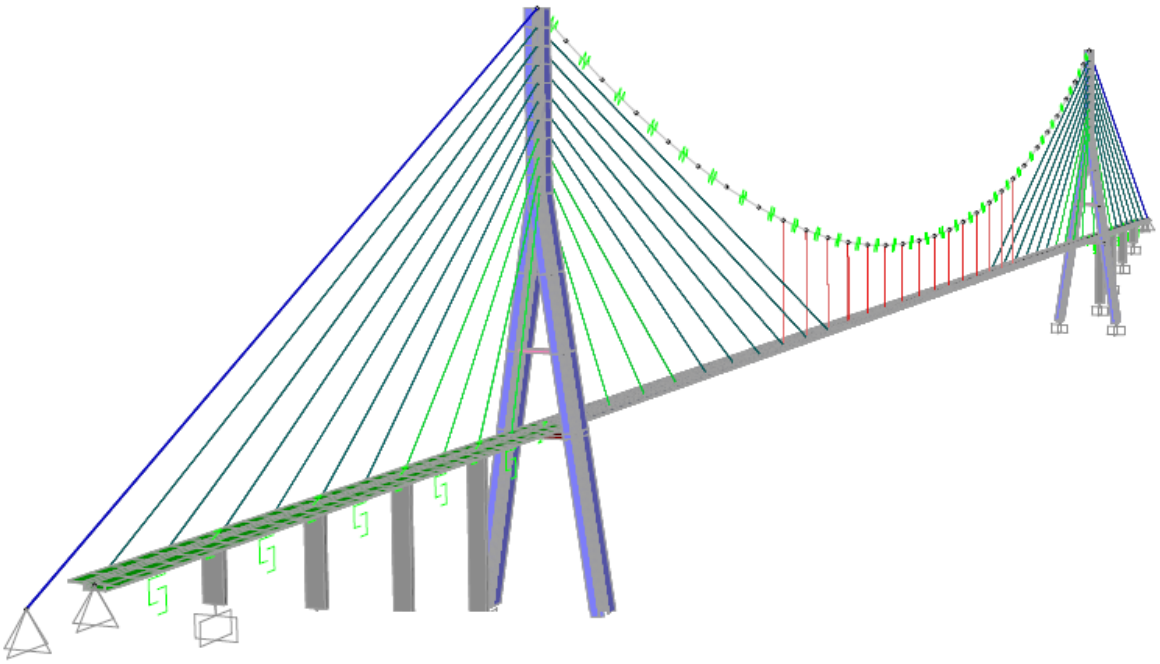

Image 20: Perspective view of the 2D model

In the transversal direction the deck has total width of 24 meters consisting on: space for cables (1,5x2 m) + railings (0,6x2 m) + lanes (3,5x4 m) + shoulders (2x0,5 m) + median strip (2,8 m).

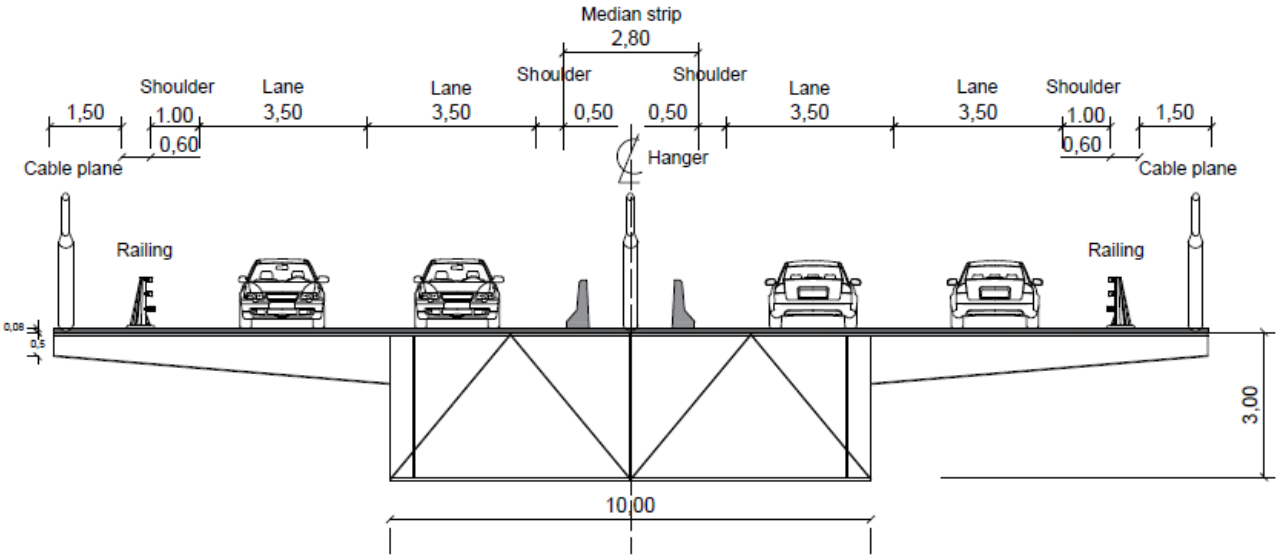

Figure 20: Detailed deck cross-section of the 2D model

5.2.3 Design of common elements for both parts of the bridge

5.2.3.1 Cables

For the cables we will choose the same material as in the 3D model (strand rope Y1860s7). But in this case the diameters will vary having then:

Type of cable	Ø (m)
Main cable	0,6
Cables type 1	0,2
Cables type 2	0,275
Hanger 1	0,350
Hanger 2	0,1

Table 10: Diameters of the different type of cables

5.2.3.2 Towers

Height

We will have again a tower of 330 m.

Material

In this case we will choose steel and the main reason is because the program gives us problems with the non-linear analysis according to the geometrical and mechanical characteristics. Steel

will give us a lower self-weight and we will be able to calculate all the considerations thanks to the Eurocde-3 whereas we would have more problems with the mechanical problems that concrete could generate.

The tower will be connected with transversal cross beams too so we will have different cross-sections. In red it can be seen the cross - section of the cross beam – deck and in pink the other cross beam sections.

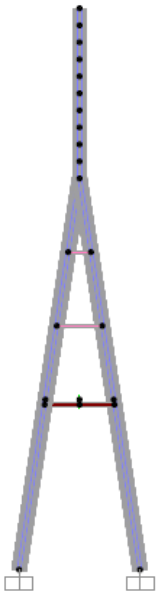

Image 21: 2D tower detail

Shape

In this 2D model the tower will have an inverted "Y" shape. The inverted "Y" proportion us similar advantages that the "A" shape does but we will select it because we are working in two dimensions and it would be impossible to anchor the cables in an "A" shape.

Cross-section

The most common cross-section for steel has the shape of a rectangle too so we present here the different existing cross-sections in the tower made of S355j2g3.

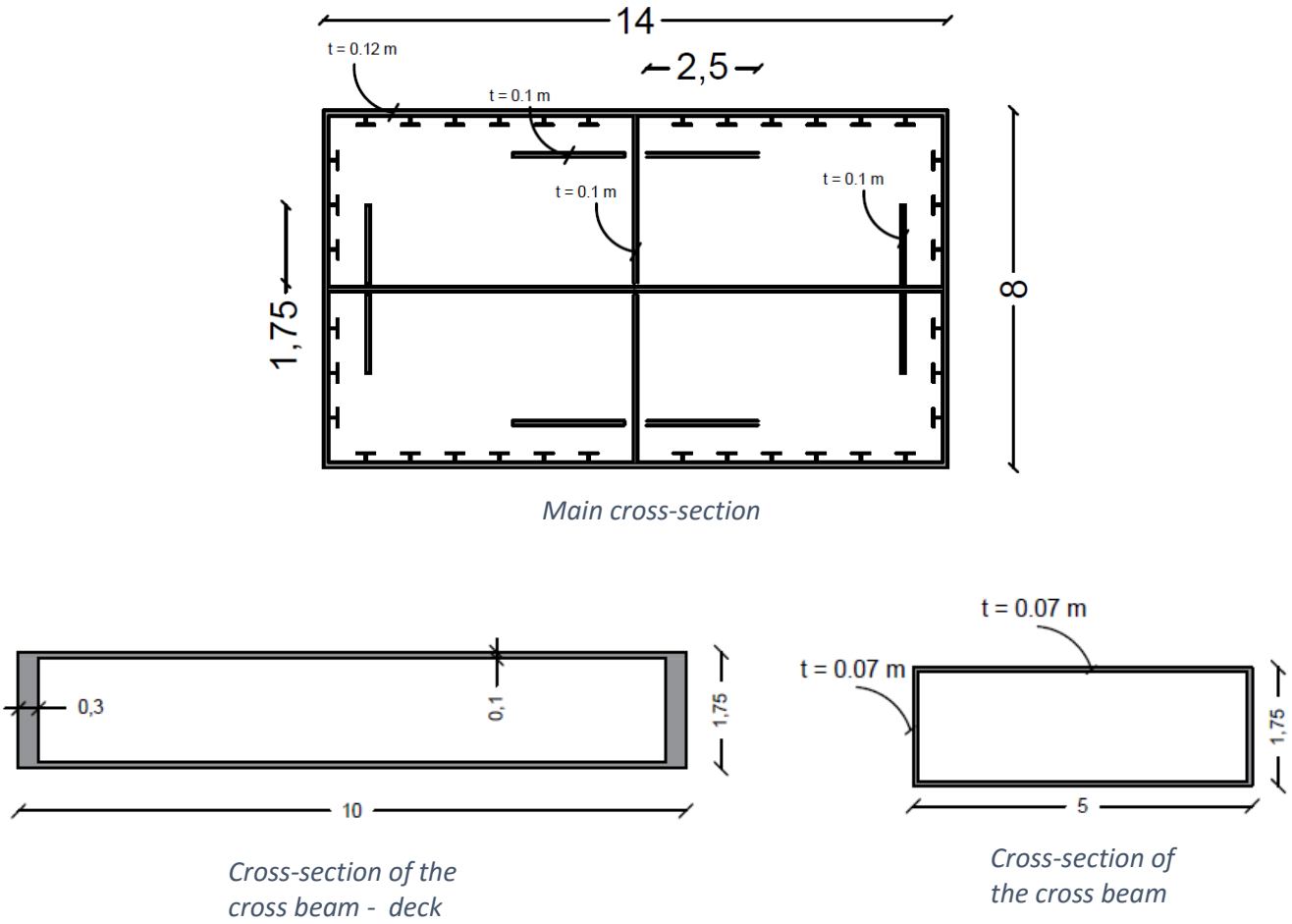

Main cross-section

Cross-section of the cross beam - deck

Cross-section of the cross beam

Figure 21: Details of the different cross-sections that the 2D tower has

5.2.4 Design of the suspended structure

5.2.4.1 General characteristics

We will decide to adopt an externally-anchored model where the connection between the main cable and the deck will be made again by rigid biarticulated hangers. This decision is based on the fact that we need a total control without the appearance of eccentricities and high bending moments.

We can see in the ***image 22*** the part of the main cable corresponding to the central span drawn as springs. It will be connected with the two towers (320 m of height) having a cable sag of 178

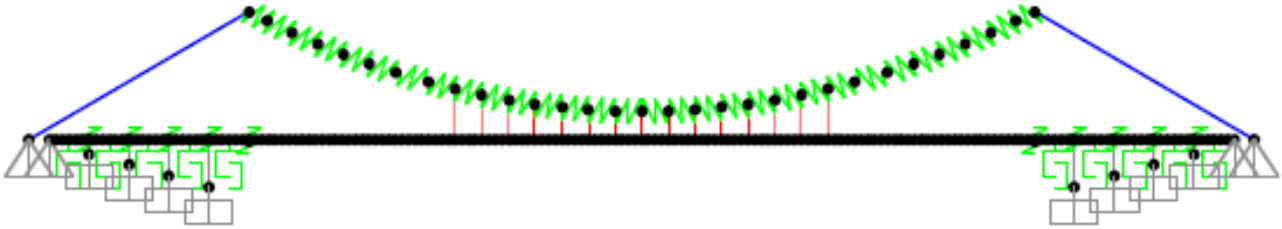

Image 22: Suspension structure of the 2D model

m. The hanger length varies between 55 and 91 meters for the longest one counting with a total of 15 of them and having two different types of hangers separating them in **type 1** (9) or **type 2** (6, corresponding to the most remote hangers from the center.

5.2.4.2 Cable arrangement

Since we are in a 2D model we will only have one plane in the transversal direction.

5.2.4.3 Deck

For this part of the deck we will try different cross-sections until we reach one that accomplish the S.L.S and the U.L.S. It's important to note that here the section is only made of steel. Then:

- Section nº 1

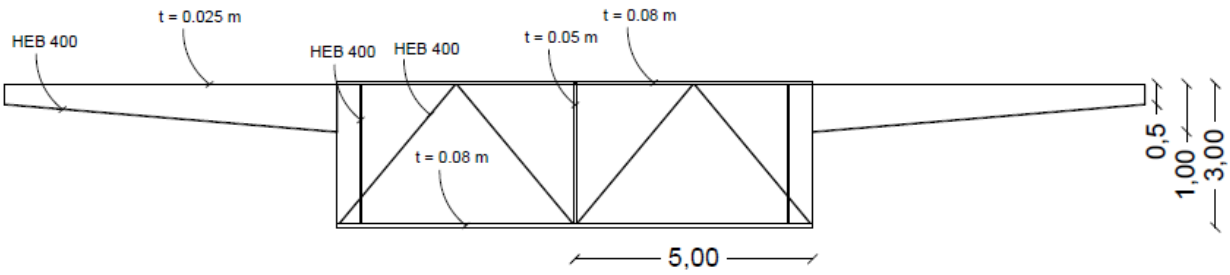

Figure 22: Cross - section nº 1

First of all we will try a similar section to which we have used in 3D Model.

- Section nº 5

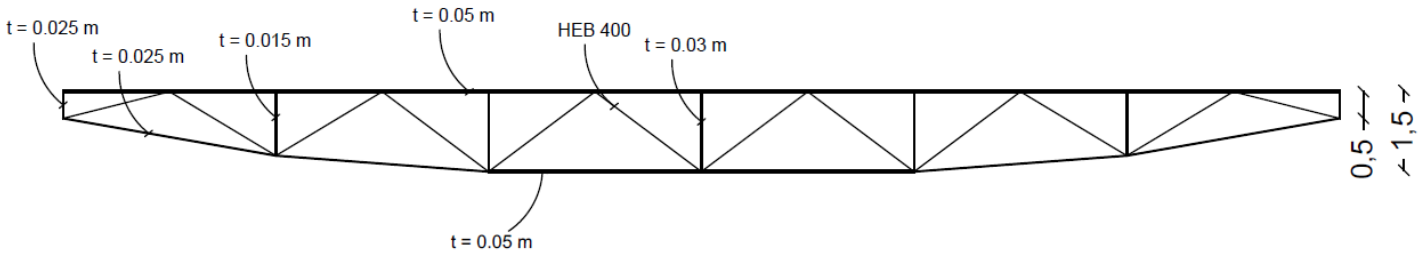

Figure 23: Cross – section nº 5

In this case we will we use almost the same shape but with less stiffeners but with more height.

- Section nº 7

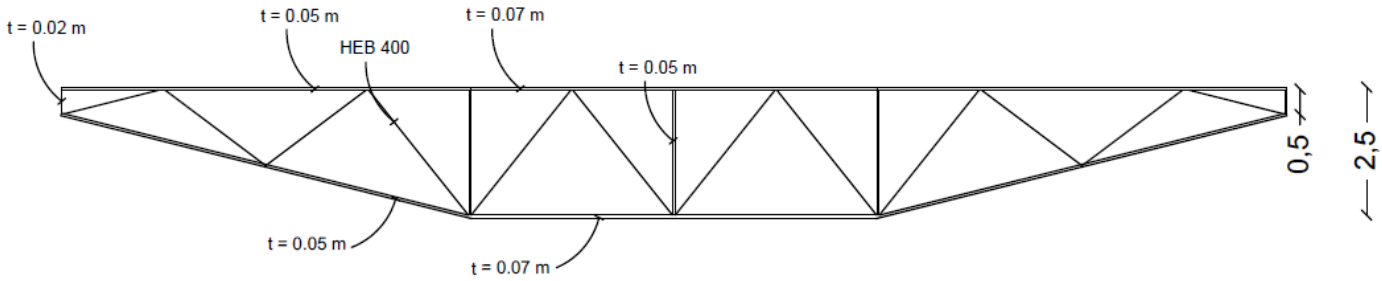

Figure 24: Cross – section nº 7

The aim of this change of cross – section is to decrease the economic costs using less material thanks to the overhangs.

- Section nº 8

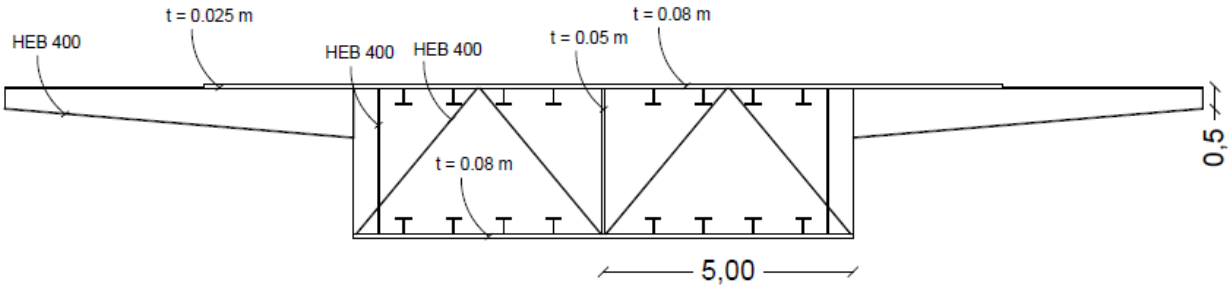

Figure 25: Cross – section nº 8

Finally in this last section so the section we will use there are 16 stiffeners in order to accomplish the requirements.

5.2.5 Design of the cable-stayed structure

5.2.5.1 Cable arrangement

As it has been mentioned before we will only work in one plane so we will only have to decide the cable arrangement in the longitudinal plane. We will use again a semi-harp system.

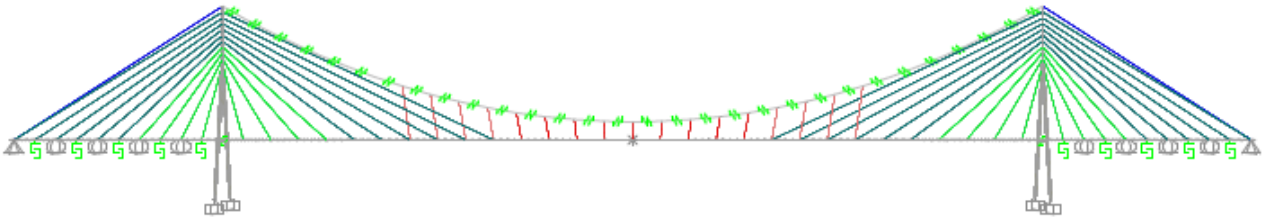

Image 23: Cable arrangement in the longitudinal direction

5.2.5.2 Deck

As it happened with the 3D model we will have two different types of deck depending if we are on the main span or on one of the lateral spans. Therefore, we will use the same geometry in parallel with the same progression of sections that we have used for the suspension part (1-3, 5-4, 8-6). Then, using again concrete RC 35 for the lateral span these are the following cross-sections that we have tried:

- Section nº 3

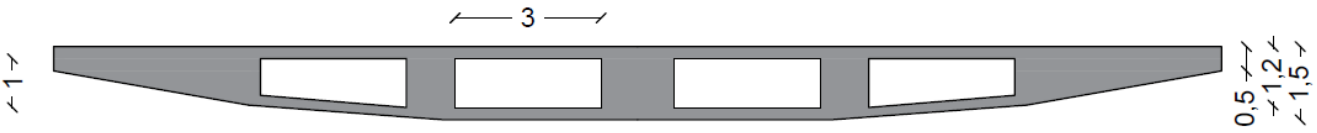

Figure 26: Cross – section nº 3

- Section n º 4

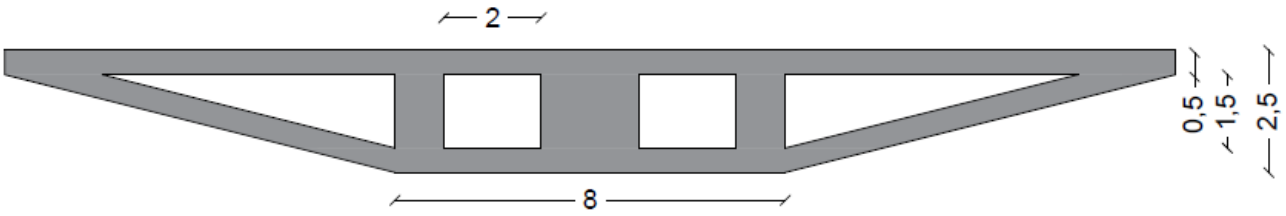

Figure 27: Cross – section nº 4

- Section nº 6

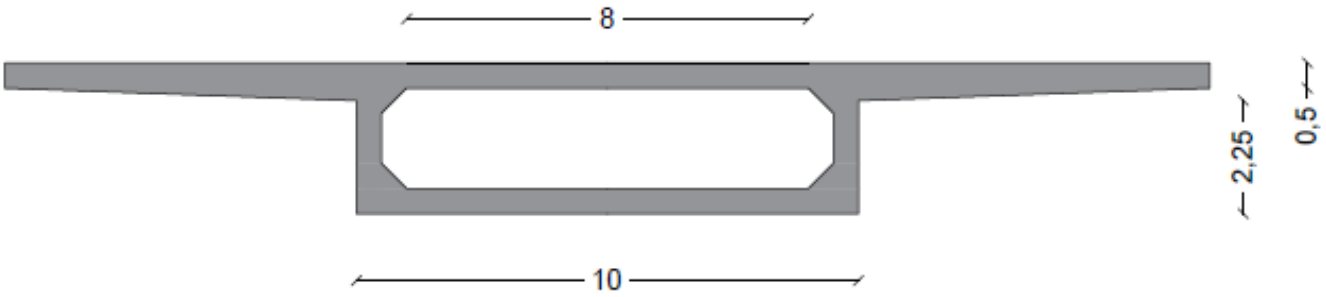

Figure 28: Cross – section nº 6

5.2.5.3 Piles

The piles will be an auxiliary element and we will use a regular rectangular cross-section with RC 30.

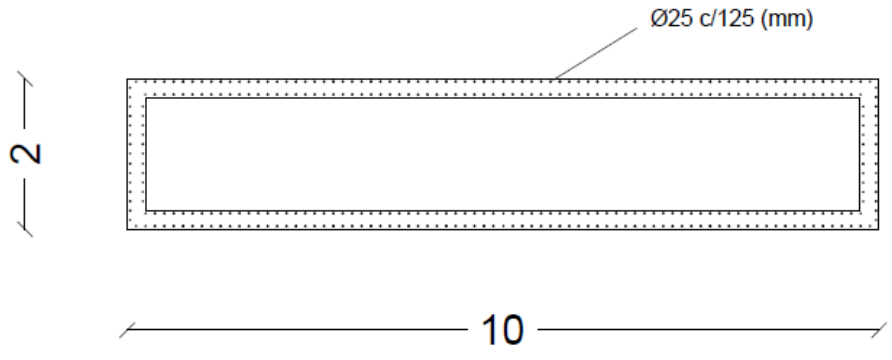

Figure 29: Piles cross – section

5.2.6 Summary

General characteristics	
Main span length	1.416 m
Lateral span length	373 m
Width	24 m
Tower height	330 m
Suspension bridge part	
Cable arrangement	Single cable plane
Cable sag of main cable	179 m
Nº of hangers	15
Hanger length	55– 91 m
Deck	Steel box section
Cable-stayed bridge part	
Cable arrangement	Semi-harp system
Nº of cables	40
Cable length	135-517 m
Deck	Steel box section/Concrete box section

Table 11 Characteristics of the 2D model adopted

6. ACTING LOADS

The loads will be defined according to ***IAP-11***:

6.1 Permanent loads with constant value (g_k)

6.1.1 Own weight

Depending on each cross-section, with specific weights for each material in accordance with the following table:

Material	Weight (T/m^3)
Concrete	2,5
Steel	7,85

Table 12: Weight of the different materials used

6.1.2 Dead loads

According to the detailed platform we will have the following dead loads:

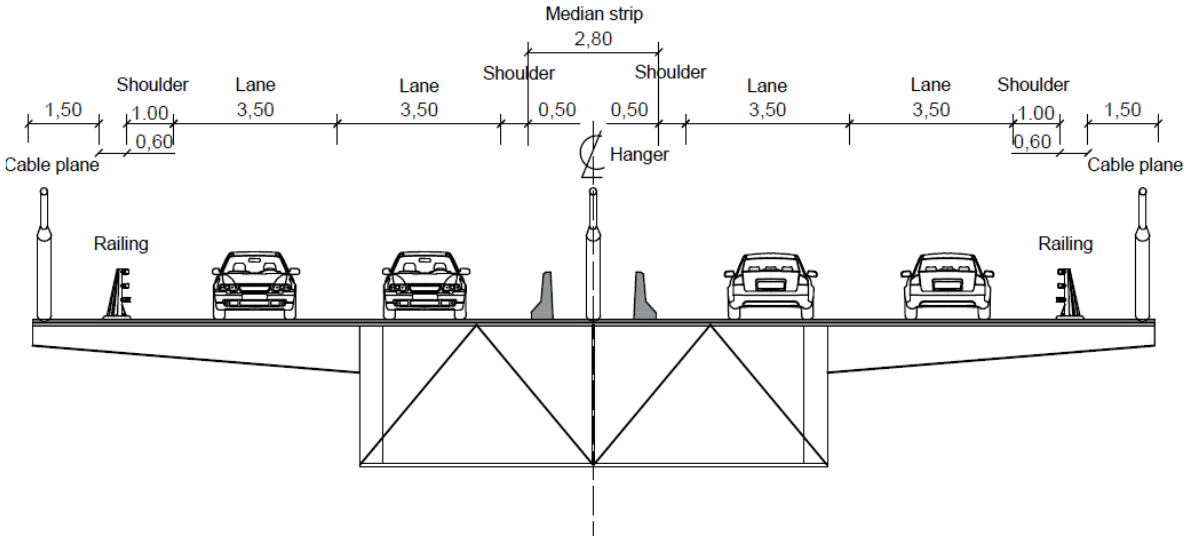

Figure 30: Detailed 2D deck cross-section used

Element	Load
Pavement (0,1 m)	2,3 T/m^2
Railings	2 x 0,6 T/m

Table 13: Weight of the dead loads applied

$$Pavement = 22{,}8 \cdot 0{,}1 \cdot 2{,}3 = 5{,}24\ T/m$$

$$Railings = 1{,}2\ T/m$$

6.2 Variable loads (q_k): live load

6.2.1 Moving load

According to the ***IAP-2011*** will consider the simultaneous action of the following loads:

Width of the platform (w)	Number of virtual lanes (n_l)	Width of the virtual lane (w_l)	Remaining area
w < 5,4 m	n_l = 1	3 m	w – 3 m
5,4 m ≤ w ≤ 6 m	n_l = 2	w/2	0
w ≥ 6 m	n_l = ent (w/3)	3 m	w - 3 n_l

Table 14: Definition of virtual lanes

Location	Heavy vehicle $2Q_{ik}$ (kN)	Live load q_{ik} (kN/m^2)
Virtual lane 1	2 · 300	9,0
Virtual lane 2	2 · 200	2,5
Virtual lane 3	2 · 100	2,5
Remaining area	0	2,5

Table 15: Characteristic values of live load

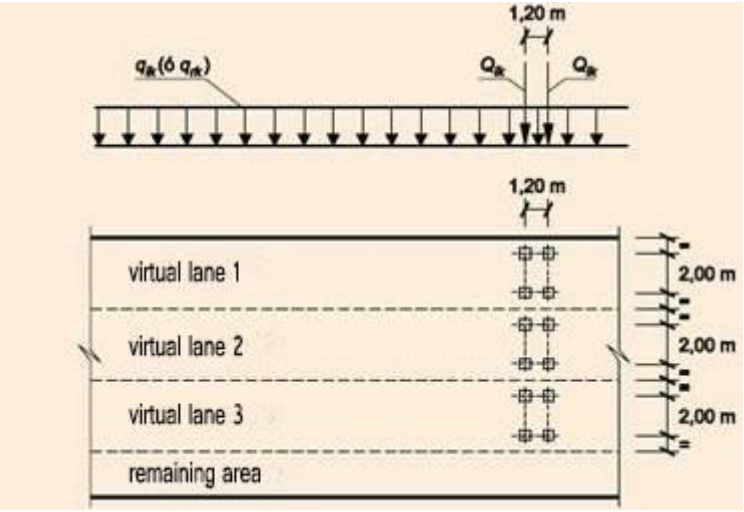

Image 24: distribution of heavy vehicles and uniform load

Since the deck has a width of 24 m with 3 virtual lanes of 3 m and then a remaining area of 13,8 m.

$$q_k = 3 \cdot 0{,}9 + 3 \cdot 2 \cdot 0{,}25 + 13{,}8 \cdot 0{,}25 = 7{,}65\ T/m$$

$$Q_k = \frac{2 \cdot 30 + 2 \cdot 20 + 2 \cdot 10}{2} = 60\ T/m$$

In ***SAP2000*** we will introduce the leading and trailing load as q_k and the sum between q_k and Q_k as the fixed length.

6.2.2 Wind

In this chapter we will simulate the wind load as an equivalent static load. We will consider the Spanish Normative ***IAP-11*** and we will follow all the relevant steps to calculate the effects of the static wind load in the structure.

6.2.2.1 Basic wind speed

The essential basic wind speed $v_{b,0}$ is the average speed over a period of 10 minutes, a return period T of 50 years, at a height of 10 meters above the ground and in a zone with low vegetation and isolated obstacles. In this case, following the normative and supposing that our bridge is in Catalonia $v_{b,0}$ will be 28 Km/h.

Thanks to the essential basic wind speed the basic wind speed will be obtained through the following expression:

$$v_b = C_{dir} \cdot C_{season} \cdot v_{b,0}$$

Where:

- $C_{dir} \rightarrow directional\ wind\ chill, that\ will\ be\ 1{,}00\ in\ this\ case$
- $C_{season} \rightarrow wind\ seasonal\ factor, that\ will\ be\ 1{,}00\ in\ this\ case$

Then:

$$v_{b,0} = 1 \cdot 1 \cdot 28 = 28\ m/s$$

6.2.2.2 Average wind speed

The average wind speed $v_m(z)$ at a height z above the ground will depend on the rugosity of the ground, on the topography and the basic wind speed v_b and it will be determined with the following expression:

$$v_m(z) = C_r(z) \cdot C_0 \cdot v_b(T)$$

Where:

- $v_b(T) \rightarrow basic\ wind\ velocity\ for\ any\ return\ period$

$$v_b(T) = v_b(100) = v_b \cdot C_{prob} = 28 \cdot 1{,}04 = 29{,}12 \frac{m}{s}$$

Being C_{prop} a probability factor that without strict studies can be taken 1,04.

- $C_0 \rightarrow Topography\ factor, that\ in\ this\ case\ will\ be\ 1{,}1$
- $C_r(z) \rightarrow Rugosity\ factor\ obtained\ with\ the\ following\ equation$:

$$C_r(z) = k_r \cdot \ln\left(\frac{z}{z_0}\right)$$

Being:

- $z \rightarrow height\ of\ the\ point\ where\ the\ thrust\ of\ the\ wind\ acts\ respect\ to\ ground.$
- $k_r \rightarrow Ground\ factor$
- $z_0 \rightarrow length\ of\ the\ rugosity$

All these values are taken from specific tables and chapters of IAP-11. In this case, for we will have:

$$C_r(z) = \begin{cases} z = 100\ m \\ z_0 = 0{,}003 \\ K_r = 0{,}156 \end{cases} \rightarrow\ C_r(z) = 0{,}156 \cdot \ln\left(\frac{100}{0{,}003}\right) = 1{,}625$$

Finally:

$$v_m(z) = 1{,}625 \cdot 1{,}1 \cdot 29{,}12 = 52{,}05\ m/s$$

6.2.2.3 Wind thrust

The wind thrust will be calculated separately for the different elements that are part of the bridge since the wind exposure is different for all of them. Anyway, for any element we will count with this expression:

$$F_w = \left(\frac{1}{2} \cdot \rho \cdot v_b(T)^2\right) \cdot C_e(z) \cdot\ C_f \cdot A_{ref}$$

Where:

- $\frac{1}{2} \cdot \rho \cdot v_b(T)^2\ \rightarrow pressure\ of\ the\ basic\ wind\ speed$
- $\rho\ \rightarrow density\ of\ the\ air, that\ will\ be\ 1{,}25 \frac{Kg}{m^3}$
- $C_f \rightarrow\ force\ coefficient\ \ of\ the\ considered\ element$
- $A_{ref} \rightarrow Reference\ area$
- $C_e(z)\ \rightarrow\ exposure\ coefficient\ depending\ on\ the\ height\ z$

$$C_e(z) = {k_r}^2 \left[{C_o}^2 \ln^2(z/z_0) + 7K_I C_0 \ln\left(\frac{z}{z_0}\right)\right]$$

$$C_e(z) = \begin{cases} z = 100\ m \\ z_0 = 0{,}003 \\ K_r = 0{,}156 \rightarrow\ C_e(z) = 5{,}145 \\ K_I = 1{,}00 \\ C_0 = 1{,}1 \end{cases}$$

DECK

In the calculation of the transversal thrust on the deck it will be assumed that the reference area $A_{ref,x}$ is the product between the length of the considered part of the bridge and the equivalent height h_{eq}.

With the absence of experimental data, the force coefficient in x direction will be determined through the following expression:

$$C_{f,x} = 2{,}5 - 0{,}3 \cdot \frac{B}{h_{ef}}$$

Where:

- $B \rightarrow total\ widht\ of\ the\ deck, in\ this\ case\ 24\ m$
- $h_{eq} \rightarrow equivalent\ height\ taking\ into\ account\ or\ not\ the\ overload$

Then:

$$Without\ overload\ \rightarrow\ h_{eq} = h_{beam} + h_{pav.} + 2 \cdot h_{rail.} = 3{,}00 + 0{,}1 + 1{,}80 = 4{,}90\ m$$

$$With\ overload\ \rightarrow\ h_{eq} = h_{beam} + h_{pav.} + 2 \cdot h_{rail.} = 3{,}00 + 0{,}1 + 2{,}00 = 5{,}10\ m$$

And:

$$Without\ overload\ \rightarrow\ C_{f,x} = 2{,}5 - 0{,}3 \cdot \frac{24}{4{,}90} = 1{,}031 < 1{,}30 \rightarrow 1{,}30$$

$$With\ overload\ \rightarrow C_{f,x} = 2{,}5 - 0{,}3 \cdot \frac{24}{5{,}10} = 1{,}088 < 1{,}30\ \rightarrow 1{,}30$$

Finally:

$$Without\ overload\ \rightarrow F_w = \left(\frac{1}{2} \cdot 1{,}25 \cdot 29{,}12^2\right) \cdot 5{,}145 \cdot 1{,}30 \cdot 4{,}9 = 17.369{,}51 \frac{N}{m}$$

$$With\ overload\ \rightarrow F_w = \left(\frac{1}{2} \cdot 1{,}25 \cdot 29{,}12^2\right) \cdot 5{,}145 \cdot 1{,}30 \cdot 5{,}1 = \mathbf{18.078{,}47}\ \boldsymbol{\frac{N}{m}}$$

Since the difference between both values is small we will adopt the value with overload.

$$F_w = 18.078{,}47 \frac{N}{m}$$

TOWERS

The force coefficient in case of towers and piles its determined by the relation B/H. Since we have section nº2:

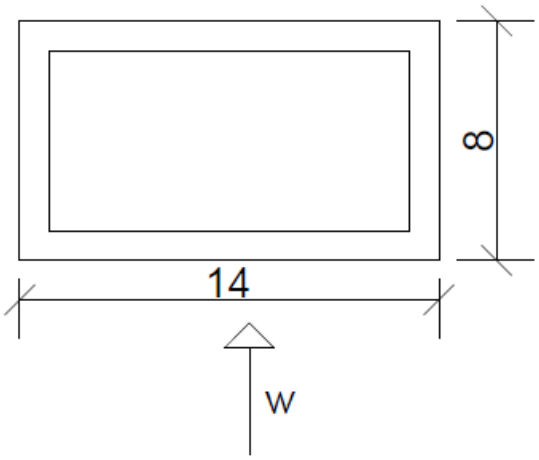

Figure 31: Direction of the incidence wind in section nº 2

$$\frac{B}{h} = 0{,}571 \rightarrow C_f = 2{,}35$$

$$F_w = 8712{,}449 \cdot 2{,}35 \cdot 14 = 286.639 \frac{N}{m}$$

PILES

Since we have section nº10:

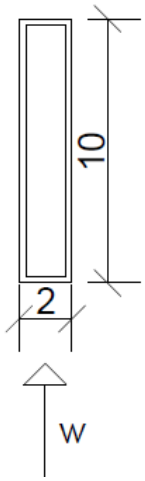

Figure 32: Direction of the incidence wind in section nº 10

$$\frac{B}{h} = 5{,}00 \rightarrow C_f = 1{,}00$$

$$F_w = 17.424\ N/m$$

**Note: The static loads of the wind hasn't been considered in the calculations*

6.3 Combination of loads

For the combination of loads we will work in service limit state (S.L.S) and in ultimate limit state (U.L.S).

6.3.1 Combination for U.L.S

Only in persistent or transient situation:

$$\sum_{j\geq 1} \gamma_{G,j}\, G_{k,j} + \sum_{m\geq 1} \gamma_{G,m} {G^*}_{k,m} + \gamma_{Q,1} Q_{k,1} + \sum_{i\geq 1} \gamma_{Q,i}\, \psi_{0,i} Q_{k,i}$$

Where:

- $G_{k,j} \rightarrow Characteristic\ value\ of\ each\ permanent\ load$
- ${G^*}_{k,m} \rightarrow Characteristic\ value\ of\ each\ permanent\ load\ with\ not\ constant\ value$
- $Q_{k,1} \rightarrow Characteristic\ value\ of\ the\ dominant\ variable\ load$
- $\gamma_{Q,j} Q_{k,i} \rightarrow Value\ of\ the\ variable\ load\ combination\ with\ the\ dominant\ load$
- $\gamma_G, \gamma_Q \rightarrow Partial\ coefficients$

6.3.2 Combination for S.L.S

Characteristic combination:

$$\sum_{j\geq 1} \gamma_{G,j}\, G_{k,j} + \sum_{m\geq 1} \gamma_{G,m} {G^*}_{k,m} + \gamma_{Q,1} Q_{k,1} + \sum_{i\geq 1} \gamma_{Q,i}\, \psi_{0,i} Q_{k,i}$$

Frequent combination:

$$\sum_{j\geq 1} \gamma_{G,j}\, G_{k,j} + \sum_{m\geq 1} \gamma_{G,m} {G^*}_{k,m} + \gamma_{Q,1} \psi_{1,1} Q_{k,1} + \sum_{i\geq 1} \gamma_{Q,i}\, \psi_{2,i} Q_{k,i}$$

6.3.3 Combinations used

- COMB 1 – Corresponds to phase 4.
- COMB 2 – Corresponds to COMB 1 + Moving load.
- COMB 31 – Equal to COMB 2.
- COMB 41 - Corresponds to phase 4 but in U.L.S.
- COMB 42 - Corresponds to COMB 1 + Moving load but in U.L.S.
- COMB 71 - Equal to COMB 42.

7. CALCULATION OF PHASES

7.1 Phase 1

This phase requires the calculation of the necessary installation force in the cables. Historically there have been various methods for measuring the force required to be supported by each one of the cables. Thus it exists 4 deployment methods which are:

- Method of the articulated deck in all the cables.
- Annulment of displacement method.
- Method of cancellation of the reactions on fictitious support.
- Method of cancellation of displacements throughout the construction process.

The methods are closely linked to the process of building and designer preferences so it has decided to use the **annulment of displacement** method in the first instance. As its name indicates the ultimate goal of this method consist on cancelling the vertical displacements of the board when it is subjected to its own weight and the permanent loads corresponding to the pavement and railings.

Generation matrix method is proposed to raise the problem of obtaining prestressing forces. We consider the "m" cable structure and "n" nodes of the board where we want the final movement is equal to 0.

We will call **P** to the column vector containing the prestressing forces on each cable, this being the unknown of our problem while we will call **δ** to the column vector containing the sags of the nodes for our hypothesis load. In particular $\boldsymbol{\delta_{pp}}$ is the deformed because of the weight and the permanent loads mentioned above.

The deformed of the deck **δ** corresponding to any combination of prestressing forces **P** applied to the cables **P** and those forces are related through a matrix we will call **F**.

$$\delta = F \cdot P$$

This matrix is obtained by calculating "m" simple loading stages that consists to apply a prestressing force to each wire unit separately. For each single load stage we will get the deformed of the "n" selected nodes. Sorting by columns the "n" elements of the deformed for these load cases the matrix F is obtained:

$$\begin{pmatrix} \emptyset_{11} & \emptyset_{12} & \emptyset_{1m} \\ \emptyset_{21} & \emptyset_{22} & \emptyset_{2m} \\ \emptyset_{i1} & \emptyset_{i2} \cdots & \emptyset_{im} \\ \cdots & \cdots & \cdots \\ \emptyset_{n1} & \emptyset_{n2} & \emptyset_{nm} \end{pmatrix} \cdot \begin{pmatrix} P_1 \\ P_2 \\ P_j \\ \cdots \\ P_m \end{pmatrix} = \begin{pmatrix} \delta_1 \\ \delta_2 \\ \delta_i \\ \cdots \\ \delta_n \end{pmatrix}$$

To summarize, each element Øij of the matrix F represents the displacement of the node i when we prestress with 1 ut. of force the cable j.

The deformed corresponding to the combination of permanent loads plus the prestressing force is as follows:

$$\delta = F \cdot P + \delta_{pp} = 0$$

Anyway to represent the unit force by ***SAP2000*** program it will be decided to apply negative temperatures simulating the behavior of prestressing cables. In this case a unit temperature of -100 ° C will be adopted for the purpose of getting more reasonable results be adopted.

By using tools such as ***Microsoft Excel*** and ***VBA*** programmer we will get the system of equations we want and therefore we will find the matrix **F** of 20 x 20 and the column vector $\boldsymbol{\delta_{pp}}$. At this point we must solve the system and the ***Matlab*** program will be selected to finally get the prestressing forces to be applied in each cable. We have to realize that we have more than 20 points where the cables are connected to the structure, so we will discard first the points in the deck that are modeled as joints (5 points) and we will select with certain logic the remaining 5 points in the tower.

The following image shows which are the selected points where we have imposed a null value and the numeration of each one.

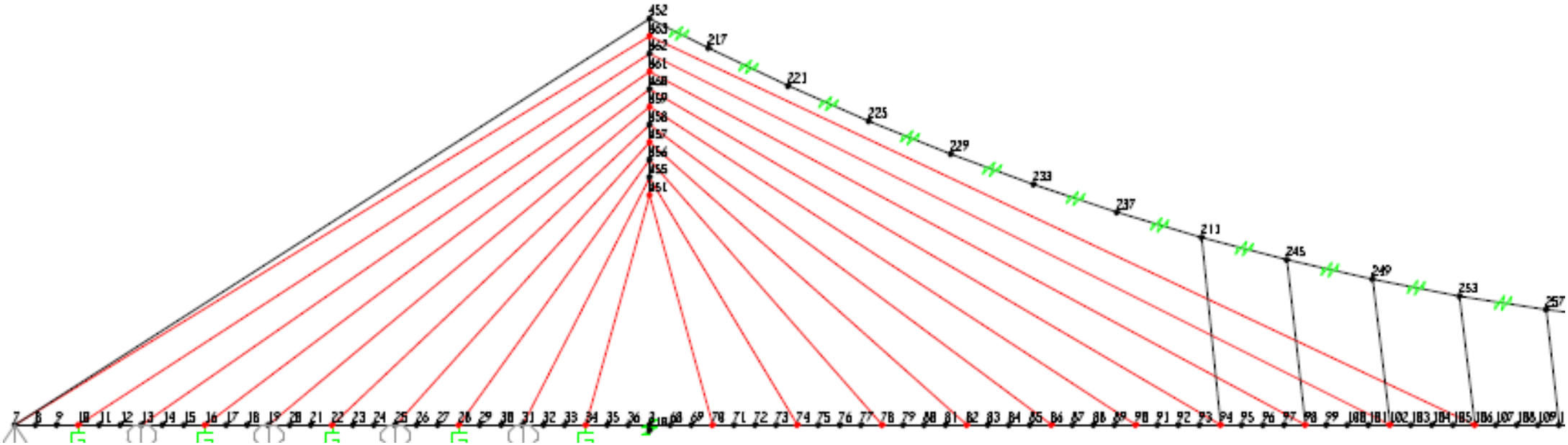

Image 25: Selected points with a null value of deflection

Knowing all of this we will finally have the matrix **F** on the one hand and column vector $\boldsymbol{\delta_{pp}}$ on the other hand. Thus we will be able to solve the system and obtain the necessary prestressing force **P**.

	T1	T2	T3	T4	T5	T6	T7	T8	T9	T10	T11	T12	T13	T14	T15	T16	T17	T18	T19	T20
10	-0,000262	0,000026	-0,00132	4,492E-06	-0,00266	-2,562E-06	-0,00255	-3,19E-06	0,000939	-5,568E-06	-0,00464	-0,000014	-0,023	-0,000023	-0,00638	-0,00001	0,051582	0,000023	-0,008166	0,000051
16	-0,001006	0,000157	-0,00092	0,000066	0,001907	0,000003878	-0,00157	-0,000011	-0,01728	-0,000013	-0,00254	1,621E-06	0,046693	0,000021	-0,003	0,000007903	-0,01898	-6,891E-06	-0,003292	-1,3E-05
22	0,002138	-0,00037	-0,0018	-0,000175	-0,01513	-0,000022	-0,00288	0,000017	0,048797	0,000032	-0,00418	0,000013	-0,01753	1,288E-07	-0,00446	-9,97E-07	-0,00077	-6,144E-06	-0,004657	-2,6E-05
28	-0,013586	0,002229	-0,0018	0,000993	0,045231	0,000094	-0,00258	-0,000096	-0,01633	-0,000084	-0,00329	-0,000026	-0,00039	0,000004001	-0,00318	0,000011	-0,00365	-1,038E-06	-0,002943	-3,6E-05
34	0,05058	-0,00967	-0,00244	-0,004747	-0,01348	-0,000518	-0,00308	0,000432	-0,00105	0,000386	-0,00366	0,000143	-0,00385	0,000022	-0,00321	-0,000015	-0,00266	-0,000031	-0,002633	-7,1E-05
70	-0,007624	0,07633	0,005899	0,041852	0,008574	0,005628	0,008385	-0,003312	0,009382	-0,003276	0,01052	-0,001282	0,009951	-0,000206	0,009746	0,000146	0,008706	0,000218	0,008523	0,000293
74	-0,000026	0,04608	0,014441	0,12419	0,017523	0,063101	0,020627	0,011775	0,02404	-0,004625	0,026312	-0,005622	0,024997	-0,00301	0,024969	-0,00098	0,02269	0,000179	0,022592	0,001066
78	0,007361	0,005643	0,02155	0,071642	0,025193	0,153118	0,031604	0,087419	0,037682	0,027373	0,041587	-0,00319	0,040128	-0,008318	0,040903	-0,0057	0,037955	-0,002104	0,03871	0,001229
82	0,010659	-0,00674	0,027027	0,014617	0,03184	0,098799	0,040983	0,18124	0,049904	0,131277	0,056174	0,039826	0,055336	-0,000578	0,057647	-0,010201	0,054709	-0,008195	0,057236	-0,00339
86	0,011944	-0,00648	0,031085	-0,006099	0,037265	0,028405	0,048823	0,120332	0,060822	0,242011	0,070169	0,1561	0,070796	0,057696	0,075507	0,006644	0,073338	-0,011921	0,078669	-0,01794
90	0,012537	-0,0041	0,033936	-0,00791	0,041448	-0,00348	0,055268	0,040148	0,070449	0,170997	0,083463	0,276353	0,086457	0,19316	0,094548	0,082468	0,094017	0,00994	0,103312	-0,0369
94	0,012843	-0,00259	0,035768	-0,004811	0,044531	-0,010003	0,060512	-0,00033	0,078905	0,06847	0,095926	0,208749	0,102113	0,321209	0,114595	0,233533	0,116669	0,096715	0,131199	-0,02258
98	0,012938	-0,002	0,036788	-0,002047	0,046736	-0,007286	0,064803	-0,011518	0,086418	0,008674	0,107653	0,095349	0,117589	0,24958	0,135317	0,364144	0,140963	0,267782	0,161996	0,105432
102	0,012864	-0,00189	0,037253	-0,000424	0,048348	-0,002942	0,06845	-0,009966	0,093296	-0,015862	0,118881	0,012237	0,132895	0,1095	0,156374	0,283605	0,166351	0,443156	0,194936	0,438599
106	0,012699	-0,00191	0,037451	0,000592	0,049678	0,001141	0,071791	-0,004905	0,09988	-0,025745	0,129882	-0,047657	0,148121	-0,026853	0,177563	0,117448	0,192214	0,461054	0,228939	0,974707
451	-0,009303	0,00168	-0,02377	0,00062	-0,02685	0,000044	-0,03293	-0,000055	-0,03843	-0,000033	-0,04147	0,000023	-0,03913	0,000079	-0,03895	0,000084	-0,03522	-0,000084	-0,034843	-0,0006
457	-0,008596	0,001432	-0,02291	0,000466	-0,02733	0,000009088	-0,03545	0,00005	-0,04347	0,000028	-0,04943	0,000037	-0,04925	0,000059	-0,05191	0,000049	-0,04987	-0,000079	-0,05289	-0,00044
459	-0,007635	0,001243	-0,02092	0,000392	-0,0259	-0,000035	-0,03497	-0,000093	-0,04516	-0,000014	-0,05422	0,000176	-0,05661	0,000092	-0,06242	0,000021	-0,06259	-0,000069	-0,069375	-0,00023
461	-0,006535	0,001031	-0,01853	0,000312	-0,02395	-0,00003	-0,03374	-0,000089	-0,04562	-0,000103	-0,05752	-0,000082	-0,0635	-7,986E-06	-0,07377	0,000148	-0,07718	0,000056	-0,089076	0,000119
463	-0,005402	0,000814	-0,01605	0,000227	-0,02187	-0,000028	-0,03233	-0,000066	-0,04581	-0,000103	-0,06047	-0,000179	-0,06978	-0,000278	-0,08447	-0,000267	-0,09225	0,000089	-0,110889	0,00103

Table 16: Matrix F

	10	16	22	28	34	70	74	78	82	86	90	94	98	102	106	451	457	459	461	463
δ_{pp}	-0,059026	-0,007801	-0,007269	-0,008958	-0,030636	-0,280455	-0,645864	-1,023469	-1,422565	-1,854157	-2,358801	-2,906549	-3,399079	-3,708612	-3,777948	0,493396	0,603687	0,680058	0,756847	0,8332

Table 17: Transposed column vector δ_{pp}

Then, our prestressing column vector **P** in terms of temperature will be the following one:

	1	2	3	4	5	6	7	8	9	10	11	12	13	14	15	16	17	18	19	20
P	-218,91	-159,76	-30,6	-133,96	-196,71	-166,01	-137,09	-177,32	-186,23	-164,44	-122,8	-174,44	-212,74	-185,22	-129,54	-188,04	-261,83	-222,67	-64,29	-96,28

Table 18: Prestressing column vector P

Once we have our results in terms of temperature we can know the axial force we will need and therefore the "real" prestressing force. The ***image 26*** shows the axial force diagram in **phase 1** whereas the diagram for **phase 4** will have the same shape.

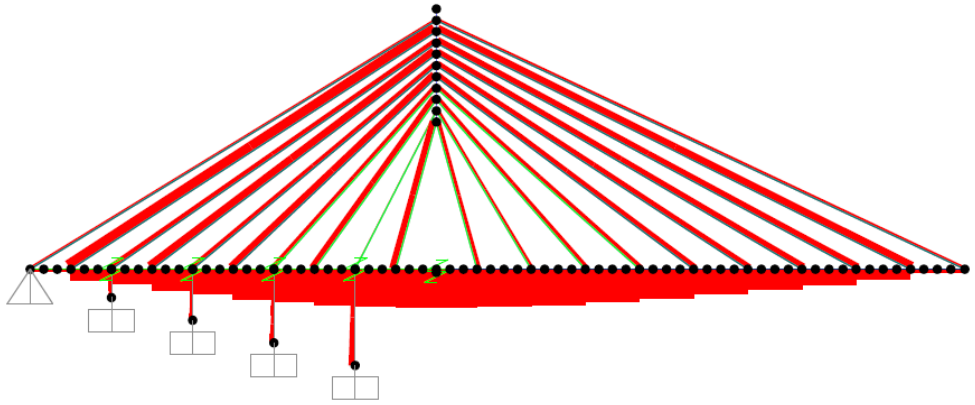

Image 26: Axial force diagram in Phase 1

The following tables display the results in both phases for each cable[4]:

Phase 1			
nº	T(N)	nº	T(N)
1	28.800.535,0	2	18.107.163,1
3	3.214.311,8	4	13.799.171,3
5	26.645.153,4	6	18.183.114,0
7	18.402.197,0	8	19.921.171,5
9	30.669.383,2	10	22.307.183,4
11	19.923.304,9	12	24.326.983,9
13	35.155.497,9	14	26.490.884,7
15	21.093.632,7	16	27.305.413,7
17	43.546.660,6	18	33.510.845,2
19	10.169.848,1	20	12.442.968,9

Table 19: Axial forces in phase 1

Phase 4			
nº	T(N)	nº	T(N)
1	31.799.236,0	2	17.521.508,2
3	11.578.955,8	4	13.701.683,8
5	36.839.240,8	6	18.205.735,4
7	31.802.705,2	8	19.945.752,8
9	47.638.198,9	10	22.340.462,2
11	40.094.037,3	12	24.387.284,3
13	56.306.255,7	14	26.991.793,1
15	44.536.051,0	16	28.792.517,6
17	67.183.972,5	18	36.359.570,0
19	36.519.320,7	20	16.347.248,7

Table 20: Axial forces in phase 4

Since we are working on a staged construction process the prestressing force obtained is not what we really would have to impose since the construction in phases produces a redistribution of internal forces of the structure. At this point we will use the method for annulment of displacements throughout the construction process that overrides the displacements in the last segment in every phase of construction.

As we have seen the method of successive segments consists of the assembly of modules next to the towers being these formed by the part of the table with their respective cables.

Generally, these partial structures being mounted are more flexible than the final structure and are subject to construction loads that are different from the stresses of the bridge in the final

[4] In fact we are only interested in phase 1 results here

stage. Arises the difficulty of projecting a constructive process to ensure that there are very high stresses in any of the partial structures in the sequence.

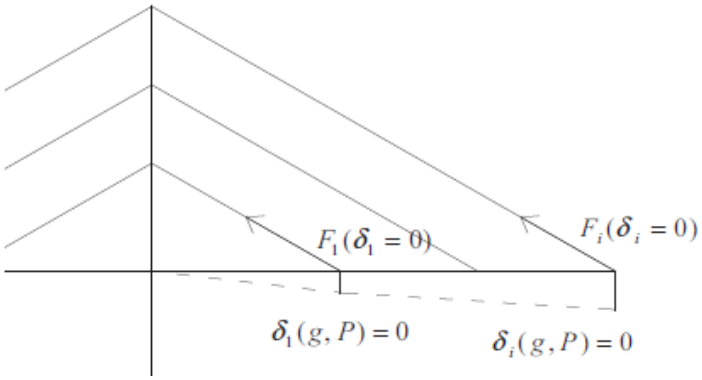

Figure 33: Diagram force of each cable i in the construction stage

For each construction stage (i) is obtained the final displacement in the last segment due to it own weight $\boldsymbol{\delta_i\ (g_i)}$**.** Then, the $\mathbf{P_i}$ force to be applied to cancel this type of displacement is calculated, so:

$$\delta_i(g_i) + \delta_i(P_i) = 0$$

This is the process to calculate these forces in each construction stage of the bridge. However, we know that the **SAP2000** program allows us to work in phases thanks to the option "non-linear staged construction" so we will define as many phases as cables have in the structure. We can see the process in the ***image 27***.

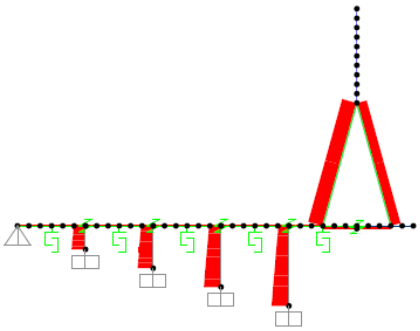

Stage 1

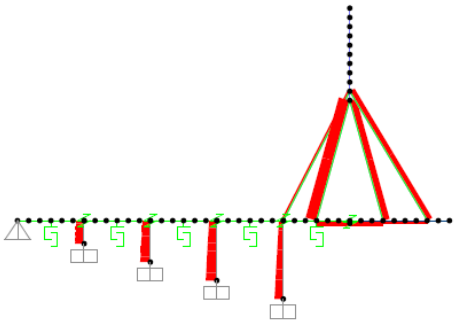

Stage 2

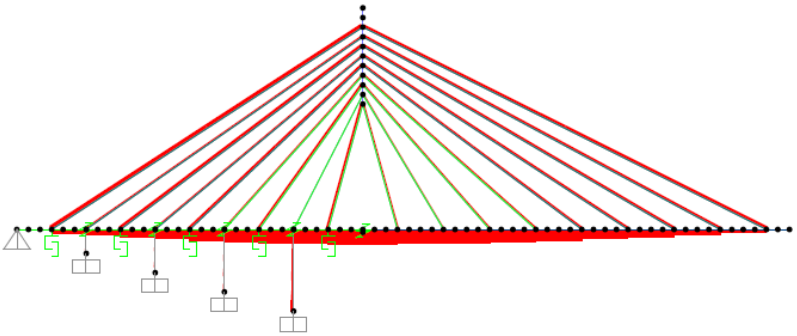

Penultimate Stage

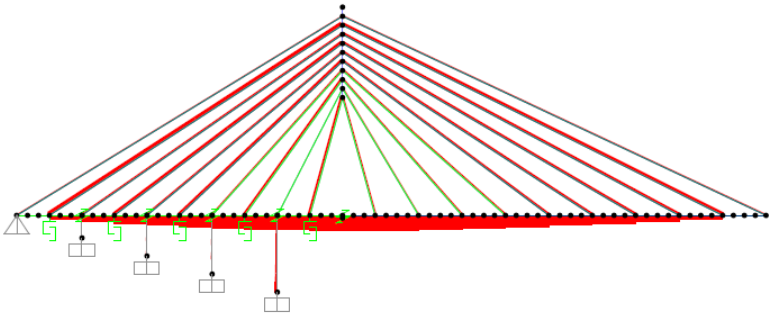

Image 27: Process of the non-linear staged construction

Following the process we can see above we can obtain the definitive axial force to prestress each cable. We have to note that some compressions could appear and that can't happen so we will fix the compression limit with the program.

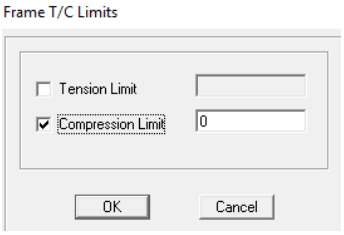

Image 28: Compression limit in SAP2000

The following table show us the final axial forces:

Evolutive construction			
nº	T(N)	nº	T(N)
1	22.252.272,0	2	17.612.462,0
3	0,0	4	14.802.802,0
5	17.153.822,0	6	18.612.846,0
7	11.656.904,0	8	20.512.576,0
9	21.425.544,0	10	22.872.220,0
11	13.948.830,0	12	24.920.322,0
13	27.909.126,0	14	26.935.202,0
15	16.284.954,0	16	28.355.614,0
17	36.312.822,0	18	31.715.642,0
19	7.314.622,0	20	12.442.962,0

Table 21: Final axial forces

7.2 Phase 2

This phase we will have vertical movements in the cable, hangers and segments, such that the level of the deck in **phase 1** will not coincide with the level of the deck in **phase 2**. To show the results of the vertical movements of **phase 2** previously we have to determine the numeration of the nodes:

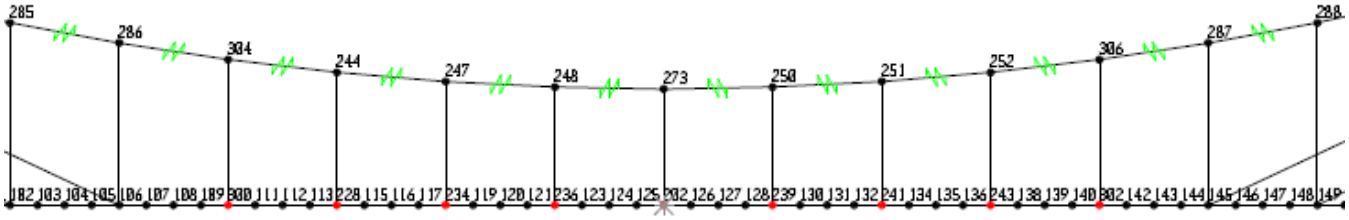

Image 29: Numeration of the nodes corresponding to phase 2

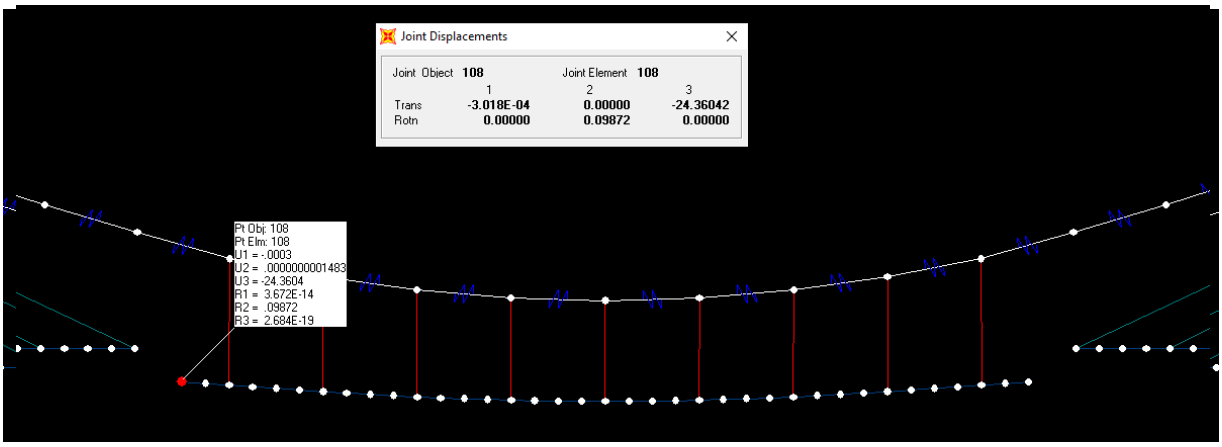

Image 30: Deflection of the turning point corresponding to the suspended deck

In the next images we will see the deflection in the most important points of this phase.

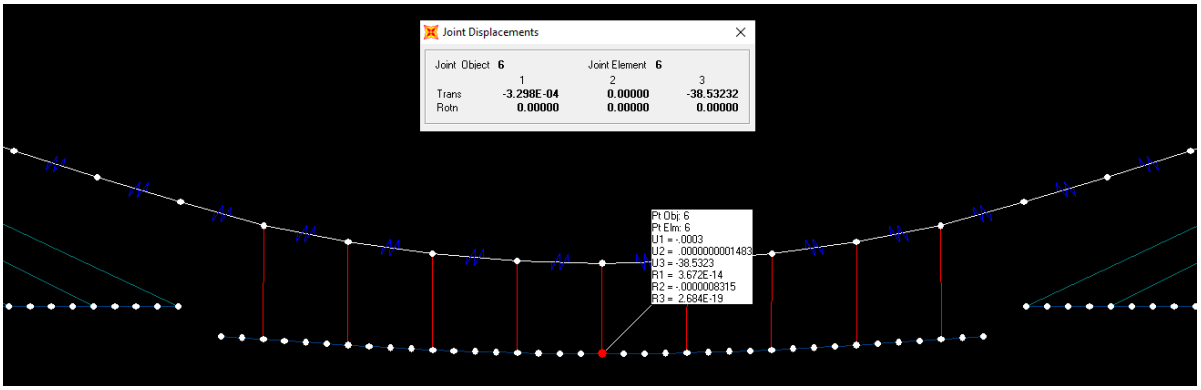

Image 31: Deflection of the centre of the main span

Anyway, we can obtain the movements of all the nodes so:

PHASE 2	
Node	V.movement (m)
6	-38,532322
118	-31,383654
137	-35,21498
202	-37,684663
227	-37,684589
234	-35,214864
236	-31,383516
239	-26,730752
241	-26,730603

Table 22: Vertical movements in phase 2

7.3 Phase 3

The aim in this phase is to know which is the value of the deformations we have to impose. The first idea is to proceed as we have done in the first phase but we won't achieve the best possible results since the hangers have a non-linear behavior. In spite of this, we will check these results using the same methodology of the first phase in order to have approximate results.

Then the process will consist in imposing what we will call unitary deformation in each hanger (we count with 9 hangers but because of the symmetry we can only impose the deformation in 5 of them) and besides it will be **-20 meters**. So will obtain the following matrix:

	PHASE 3				
Node	P1 (m)	P2 (m)	P3 (m)	P4 (m)	P5 (m)
6	-33,17234	-31,184419	-33,90128	-35,119439	-37,644071
118	-30,518074	-29,348411	-28,039318	-26,354341	-22,312485
137	-33,34298	-30,707892	-29,106126	-30,674979	-31,213771
202	-34,105993	-30,309439	-32,428716	-34,007138	-36,09033
227	-34,105246	-30,309525	-32,428644	-34,007057	-36,090226
234	-33,34175	-30,707991	-29,106017	-30,674854	-31,21361
236	-30,516548	-29,348558	-28,039187	-26,3542	-22,312302
239	-26,570816	-26,453948	-26,347382	-25,537173	-9,187744
241	-26,569073	-26,454173	-26,347236	-25,537022	-9,187557

Table 23: Vertical movements in phase 3 with a unitary deformation

The difference of the movements between **phase 2** and **phase 3** (applying -20 meters) will give as the matrix we need to solve the system and we will call it **A**:

$$B = A * x$$

Where:

	A				
Node	P1 (m)	P2 (m)	P3 (m)	P4 (m)	P5 (m)
6	5,359982	7,347903	4,631042	3,412883	0,888251
118	0,86558	2,035243	3,344336	5,029313	9,071169
137	1,872	4,507088	6,108854	4,540001	4,001209
202	3,57867	7,375224	5,255947	3,677525	1,594333
227	3,579343	7,375064	5,255945	3,677532	1,594363
234	1,873114	4,506873	6,108847	4,54001	4,001254
236	0,866968	2,034958	3,344329	5,029316	9,071214
239	0,159936	0,276804	0,38337	1,193579	17,543008
241	0,16153	0,27643	0,383367	1,193581	17,543046

Table 24: Matrix A

B (m)
38,479122
31,330454
35,16178
37,631463
37,631389
35,161664
31,330316
26,677552
26,677403

Table 25: Matrix B

B corresponds to the unitary vector and it's the difference between the level of the suspended deck and the level we want to reach (level of the cable stayed bridge) that in this case is **-0.05299 m**.

Solving this system we will obtain **x** which is the relation we will have to multiply by our unitary deformation.

Hanger	x	Imposed deformation (m)
P1	1,8838	-37,676
P2	1,8554	-37,108
P3	1,7574	-35,148
P4	1,5913	-31,826
P5	1,3275	-26,55

Table 26: Final imposed deformation given by the system

As already assumed the results have not given us the exact deflections we need we know that these are a good starting point, so we will iterate trying different values for each hanger until we reach the same level in both decks.

Hanger	Imposed deformation (m)
P1	-35,925
P2	-34,928
P3	-31,905
P4	-26,840
P5	-20,088

Table 27: Imposed deformation we will need

We will add the rest of permanent load adding another imposed deformation which in this case will be much reduced.

It has explained previously that once we add the rest of permanent load we will need to impose another deformation too. In this case we will have to add **-5,4919 meters**.

Hanger	Imposed deformation (m)
P1	-41,413
P2	-40,415
P3	-37,393
P4	-32,328
P5	-25,575

Table 28: Final imposed deformation we will need

Finally with these deformations we will obtain the value shown in the ***image 32*** corresponding to **-0,0532 m** which can be considered that is optimal.

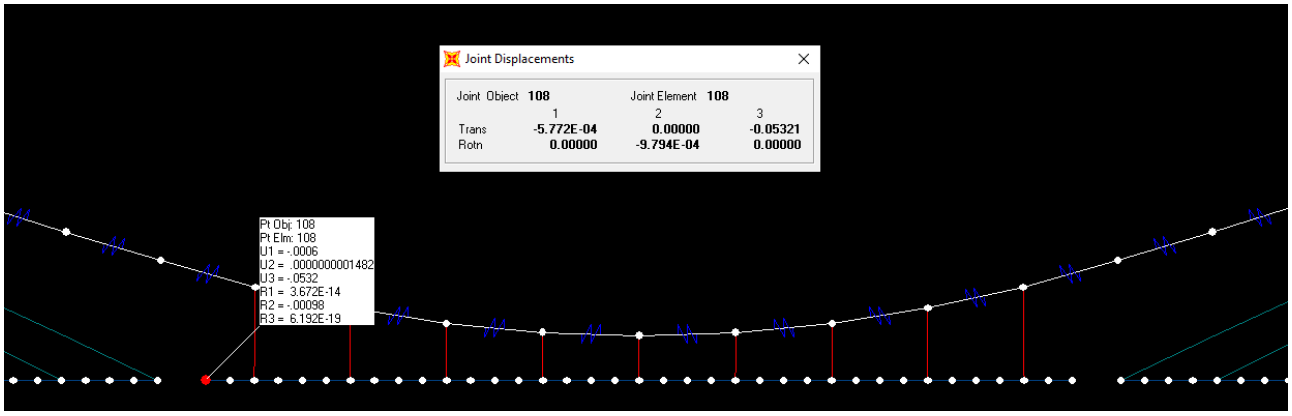

Image 32: Final deflection of the deck after the imposed deformations in phase 3

8. MODELING SADDLES

8.1 Classical theory

The saddle element in the coronation of the pile is modeled reproducing the formulation of the cable rolled into a circle sector, always considering that we are in limit state.

The cable being supported on a rough surface has tangential forces due to friction, thus complicating the problem considerably. Thus we assimilate the problem to a particular important case such as on a rough winding drum. The following hypotheses are then considered:

1. There are no external loads applied to the cable.

2. The drum has a convex cross section (no need to require that it be circular).

3. The cable is wound along a straight section of the drum.

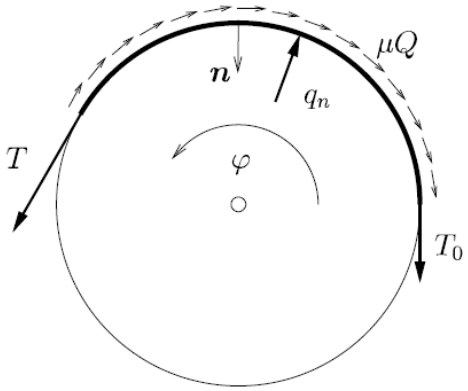

Figure 34: Cable wound on a rugged drum, in which it is stretched with a tension T in position of strict balance

To find the relation between stresses at both sides of the drum we will be in the limit boundary equilibrium. If we pull one end of the cable more than the other the cable will slip on the drum to by its inherent condition of extensibility. Assuming we are pulling tension which we shall call T on one side and to a lower stress at which call T_0, friction is mobilized in the opposite direction T as shown in ***figure 34***.

Planteando las ecuaciones de equilibrio siendo q_n la reacción normal al tambor tendremos:

Raising the equilibrium equations being q_n the drum normal reaction we will have

· According to the tangent direction:

$$\frac{dT}{dS} - \mu q_n = 0 \quad (1)$$

· According to the normal direction:

$$\frac{T}{R} - q_n = 0 \quad (2)$$

As clarification, the negative sign of q_n is from considering the positive direction opposite to the normal n, i.e. towards the convex side of the drum.

From equation nº 2 we obtain that $q_n = T/R$, so that from equation nº 1 we deduce,

$$\frac{dT}{dS} = \mu \frac{ds}{R} = \mu \, d\varphi$$

Integrating between two points, the origin $\varphi = 0$ where we assume that the tension T is equal to T_0 and $\varphi = \varphi$ where the tension T is equal to T. Thus we get:

$$T = T_o e^{\mu\varphi}$$

This formula indicates the increased tension produced by friction, from a point in $\varphi = 0$ with the stress T_0 to a point where the cable is wound an angle φ , from which it is pulled by tension $T > T_0$.

8.2 Modelling with SAP2000

In the studied case the parameters adopted for modeling of the saddle are:

· Friction coefficient: $\mu = 0{,}3$

· Opening angle: $\varphi = 30$ º

According to the implementation of the program ***SAP2000*** the model adopted that reproduces approximately the formulation mentioned above, can be seen in the following figure:

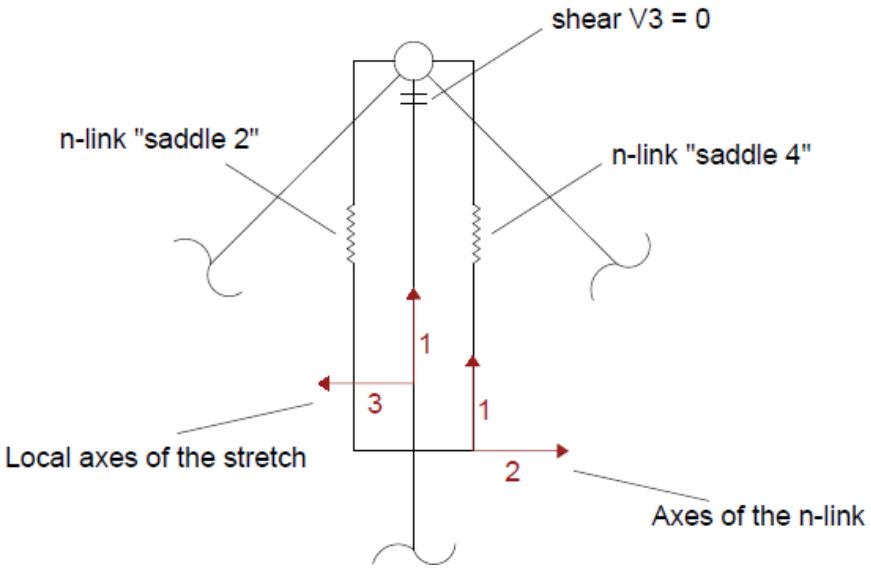

Figure 35: General detail of the auxiliary section

We see in the last stretch of the coronation of the pile, always according to the application, it's is assigned ShearForce 3 = 0. With this we freed the shear stress at that point and we prevent bending stresses occur. It is to be noted that coronation of the pile has the rotation released as is connected to two elements of the cable and that have the ability to absorb stresses.

During this study, two n-links which we will call "saddle 2" (referring to **phase 2**) and "saddle 4" (referring to the completion of **phase 4**) of **multilinear elastic** type will be added. This choice is because we are in a position to limit state and therefore the behavior of the saddle becomes rigid- plastic.

The n-link "Saddle 2" is intended to reproduce the additional rigidity that involves the presence of the saddle while the n-link "saddle 4" reproduces the additional rigidity that may occur in the presence of live loads.

Before we place ourselves in **phase 2** previously we will check that, without n-links and real rigidity of pile $T > T_o e^{\mu\varphi}$ friction happens to mobilize.

Once justified the friction is mobilized, the procedure is based on starting a process of iteration until it meets $T = T_o e^{\mu\varphi}$. In this iteration process we have to go by varying the shear force provided by the spring until we get the balance of forces in the node and always fulfilling the foregoing. The force obtained will have a value of 4,250 Tn and its rigid - plastic behavior will be reflected as follows:

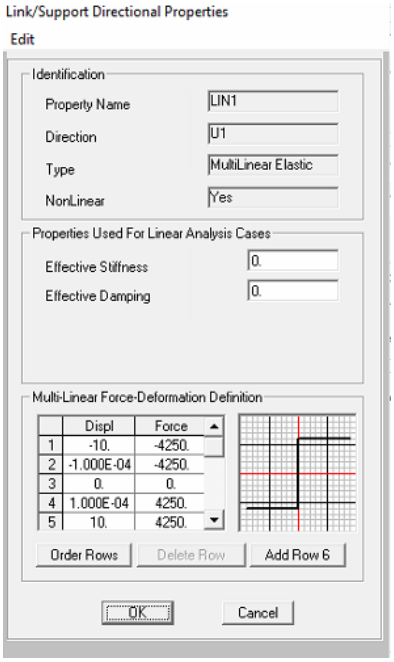

Image 33: Characteristics of the n-link represented with SAP2000 program

The definition of the property of n-link complying approximately limit state formulation is given by the U2 component while the remaining components have no impact being U1 = U3 = R1 = R2 = R3 = 0.

Here are the comparative results of **phase 2** extended until **phase 4** taking into account the load case PP + CP with the following models:

- Model with pile and its actual stiffness.
- Model with pile and with the shear force equal to 0 in coronation.
- Model with saddle and friction.

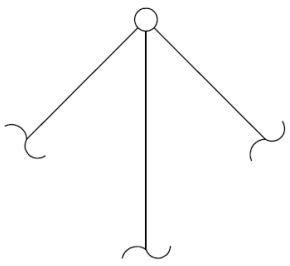

Figure 36: Model with pile and its actual stiffness.

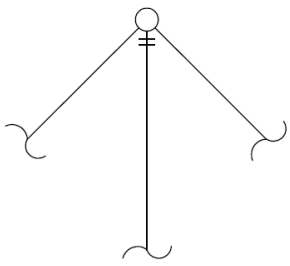

Figure 37: Model with pile and with the shear force equal to 0 in coronation

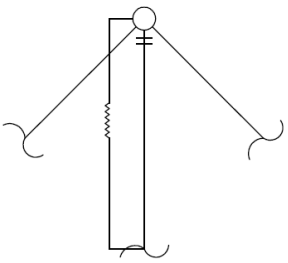

Figure 38: Model with saddle and friction

Moreover the results being compared are:

- Force T_o of the Holding cable
- Force T of the Central suspension cable T
- Movement of the cable to the center of the U3 overture

Phase 4 PP+CP	Model with pile and its actual stiffness	Model with pile and with the shear force equal to 0 in coronation.	Model with saddle and friction
T_o (Tn)	11.038	22.695	18.100
T (T)	21.397	21.100	21.300
U_3 (m)	-38,04	-41,60	- 39,39

Table 29: Comparison of the force in the main cable and the movement in the center of the U3 overture in phase 4

The results obtained are consistent observing that in the **"Model with saddle and friction"** are intermediate values between the two remaining cases

Another important aspect to consider is the strength of the suspension central cable. Its shown virtually unchanged from the constraints imposed both on the pile as in the saddle. Given this fact, the module adopted can be strengthened imposing on the hold cable and in the case of **"Model with saddle and friction"** a lower stress limit of 18,100 Tn.

In addition to these three models it has made an additional model replacing the n-links by plastic hinges (Hinges tool SAP) at the coronation of the pile. In this case only solution is considered assuming a limit value V3 when the friction tends to infinity for the patella, which means that modeling is not applicable.

In **phase 4**, with the situation of the entire structure and the load case PP + CP, n-link "saddle 4" to the existing "saddle 2" is added. Prior to initiating a process of iteration, cable forces are calculated by integrating a n-link "saddle 4" infinitely rigid to shear forces in order to compare whether an additional friction with the Moving Load application is mobilized.

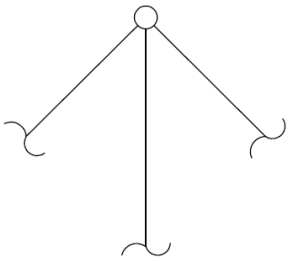

Figure 39: Model with pile and its actual stiffness.

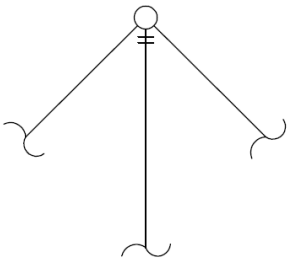

Figure 40: Model with pile and with the shear force equal to 0 in coronation

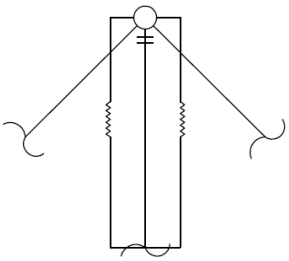

Figure 41: Model with saddle and friction (n-link 2 and n-link 4))

Los resultados obtenidos indican que en este caso $T < T_o e^{\mu\varphi}$, es decir, no se moviliza el rozamiento. Con el mismo proceso iterativo utilizado anteriormente no se llegan a igualar ambas tensiones incluso para fuerzas de cortante en el muelle de hasta. A continuación se presentan los resultados comparativos de la COMB 31 (recordemos que esta combinación está compuesta por el PP+CP+Moving Load).

The results indicate that in this case $T < T_o e^{\mu\varphi}$, ie not mobilize friction. With the same iterative process used previously we don't come to equalize both stresses even for shear forces in the spring of up to 10^6 Tn. Here are the comparative results of the COMB 31 (remember that this combination is composed of the PP + CP + Moving Load) are presented.

COMB 31 PP+CP+ML	Model with pile and its actual stiffness	Model with pile and with the shear force equal to 0 in coronation.	Model with saddle and friction
T_o (Tn)	15.012	26.659	22.500
T (T)	25.067	24.760	25.000
U_3 (m)	-46,09	-49,74	-47,38

Table 30: Comparison of the force in the main cable and the movement in the center of the U3 overture in comb 31

Finally it reproduces the same as has been contemplated in phase 2, so we put a limit stress with a value T = 25.000 Tn, and giving similar to those obtained, ie values can't be met $T = T_o e^{\mu\varphi}$ and therefore friction is not mobilized.

8.3 Conclusion

The final conclusion is to consider the saddle model with friction has little impact with respect to the other two options mentioned above:

- Model with pile and its actual stiffness.
- Model with pile and with the shear force equal to 0 in coronation.

Consequently, the implementation of a saddle with rollers that provide a shear stress V3 equal to 0 at the coronation of the pile in order to minimize the efforts on this and turn on the foundations is considered as the best option. Likewise, it is considered to be structurally correct that the cable has the minimum interference coronation and further efforts are as equal as possible on both sides of the saddle.

9. LIMIT STATE VERIFICATION

9.1 S.L.S

9.1.1 Verification of deflections

In this chapter recourse to the Spanish regulation, in particular to ***"IAP-11: Instrucción sobre las acciones a considerer en el Proyecto de puentes de carretera"***. We will have to verify that the maximum vertical deflection corresponding to the frequent value of the live load does not exceed the following values:

- L/1000 in road bridges.
- L/1200 in walkways.
  Being L the length of the span.

First of all we are dealing with road bridges and secondly IAP-11 tells us that in cable-stayed and suspension bridges we can take L as the distance between turning points of the deformed shape for the hypothesis of load case considered.

We can see clearly where the turning points in the ***figure 42*** are.

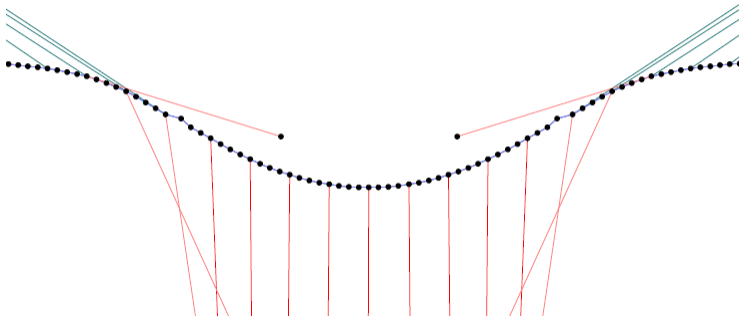

Figure 42: Turning points of the structure

In our case we will have the layout shown in the ***figure 43***.

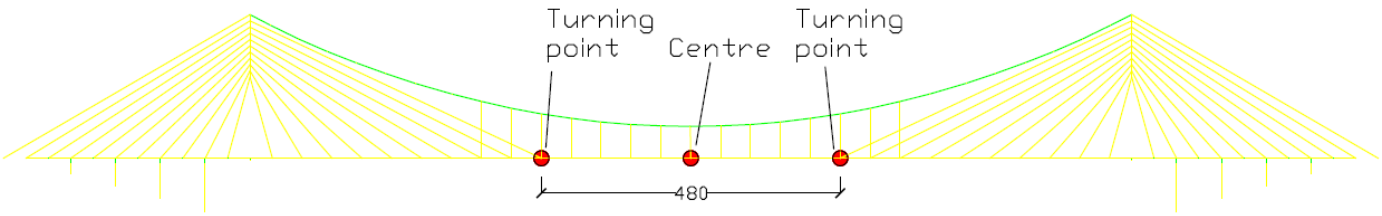

Figure 43: Layout with the three important deflection points

As we are talking about the effect of the live load in the frequent combination we will have to see the difference between the deflection in **phase 4** and in **phase 31** (frequent case). We will

have to study the turning points and the point corresponding to the center of the largest span. The cross-section we will use for the deck it will be the section nº 8 with a height of 3 m.

Centre of the span		Turning points	
U_3 Phase 4 (m)	-0,21979	U_3 Phase 4 (m)	-0,50704
U_3 Comb 31 freq. (m)	-3,3477	U_3 Comb 31 freq. (m)	-1,57651

Table 31: Deflection for phase 4 and comb 31 in the three important points

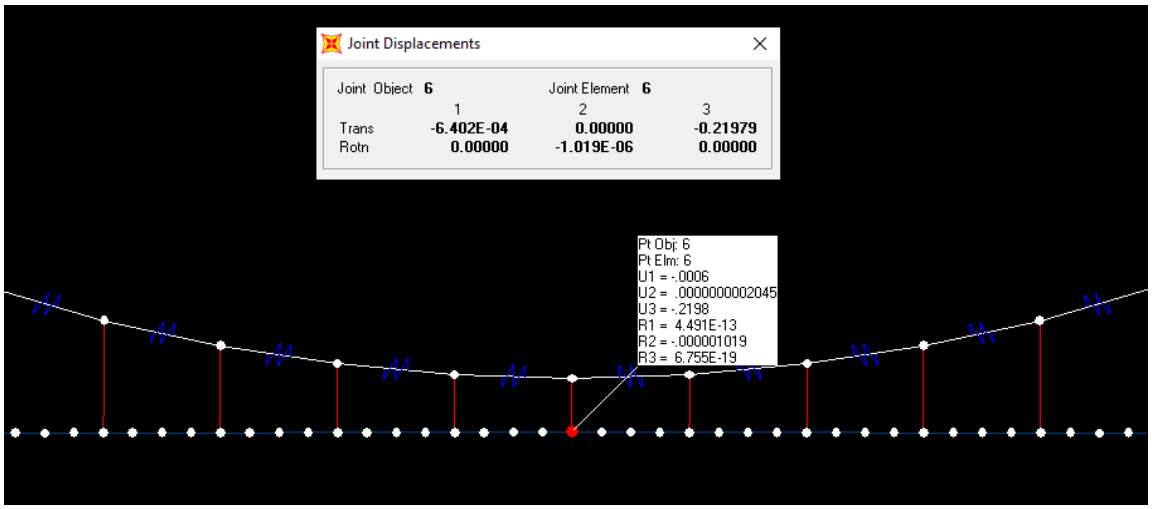

Image 34: Deflection in the centre of the span corresponding to phase 4

As an example and a proof of this results we can see in the following images the results given by **SAP2000** in the centre of the span. The procedure will be the same in the turning points.

Then, the deflection in the centre of the span due to live load will be:

$$Centre\ of\ the\ span \rightarrow U_3 = 3{,}3477 - 0{,}21979 = 3{,}128\ m$$

$$Turning\ points \rightarrow U_3 = 1{,}57651 - 0{,}50704 = 1{,}07\ m$$

And:

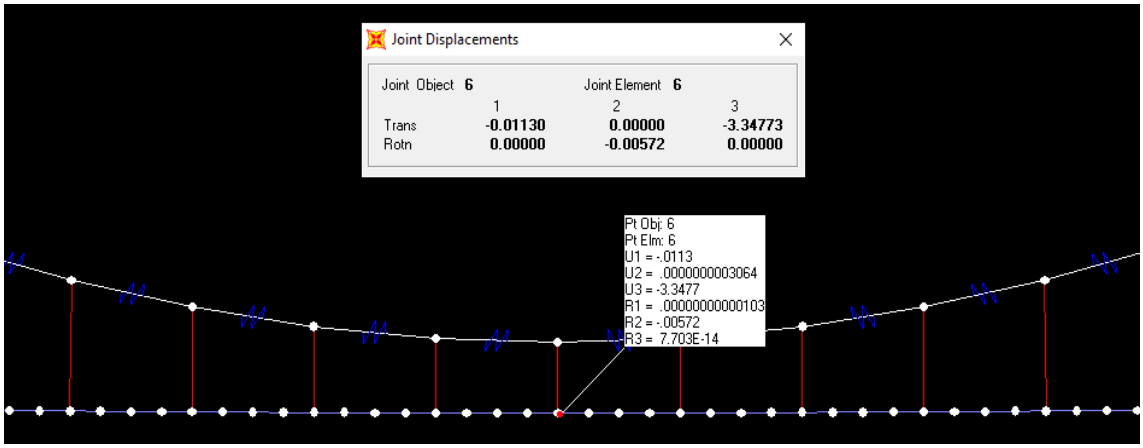

Image 35: Deflection in the centre of the span corresponding to COMB31 freq.

$$Relative\ deflection \rightarrow\ U_3 = 3{,}128 - 1{,}071 = 2{,}057\ m$$

If we go to ***IAP-11***:

$$\frac{L}{1000} = \frac{480}{1000} = 0{,}48 < 2{,}057\ m$$

As we can see this value doesn't accomplish the Spanish legislation so we will try another section with more height, particularly with 4 m (section nº 10). Working in the same way we have done before we will have these results:

$$Centre\ of\ the\ span \rightarrow U_3 = 2{,}576 + 0{,}29437 = 2{,}87\ m$$

$$Turning\ points \rightarrow U_3 = 1{,}402 - 0{,}319 = 1{,}083\ m$$

And:

$$Relative\ deflection \rightarrow\ U_3 = 2{,}870 - 1{,}083 = 1{,}787\ m$$

If we go to ***IAP-11***:

$$\frac{L}{1000} = \frac{480}{1000} = 0{,}48 < 1{,}787\ m$$

Even though we have increased our section in 1 meter we haven't achieved a significant decrease in the deflection.

We have to note that the deflection of a cable is the sum of:

- Deflection generated by the non-linear analysis, which is the most important one. This is basically a cinematic phenomenon rather than structural.

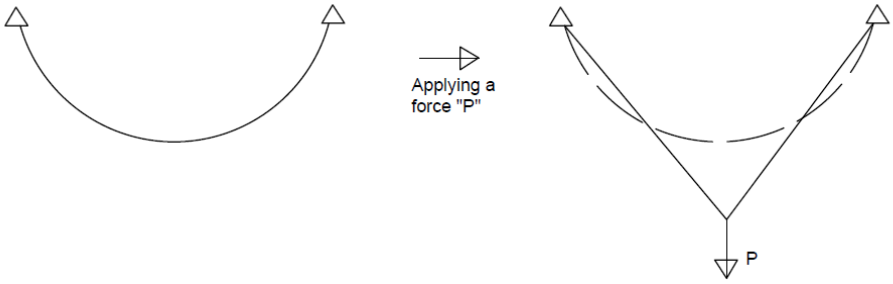

Figure 44: Deflection generated by the non-linear analysis

- Deflection generated by the linear analysis corresponding to the mechanical analysis. It follows hook's law, i.e. **σ = E*ε** but is irrelevant regarding the non-linear.

That's the reason why we can't choose to increase the section of the cable as a solution because it won't have a major impact.

Another solution we could think that is would worth is to increase the stiffness of the deck but it have been proved and we don't have great improvements.

9.1.2 Verification of the tensional state

We will stablish two different alternatives that will evaluate the values of the stresses: medium stress and maximum stress. The medium stress, σ_{med}, is obtained as the relation between the force sustained by the cable and its cross-section. The maximum stress, σ_{max}, is obtained adding the increment of tension produced by flexion to the previous value.

The verification of the maximum stress is only obligatory for very large cables (more than 150 m of length) or when significant effects are foreseeable because of the cable bend. This verification will prevail among the verification of medium stress for all purposes. However, these verifications may be questionable and if they still remain is because they are useful for the designer and because they are a first approach to the problem of fatigue.

For the characteristic load combination the limit values for the stresses are:

$$\sigma_{ELS\ med} \leq 0{,}45\ f_u = 0{,}45 * 186.000 = 83.700 \frac{T}{m^2}$$

$$\sigma_{ELS\ max} \leq 0{,}50\ f_u = 0{,}5 * 186.000 = 93.000 \frac{T}{m^2}$$

Where f_u is the ultimate tensile strength that in this case is **186.000 T/m²** since we have Y1860 S7.

9.1.2.1 Suspension bridge - main cable

The main cable has more than 150 meters so we will have to check both verifications. First of all, we will label the segments of the cable because the tensional state won't be the same along the cable.

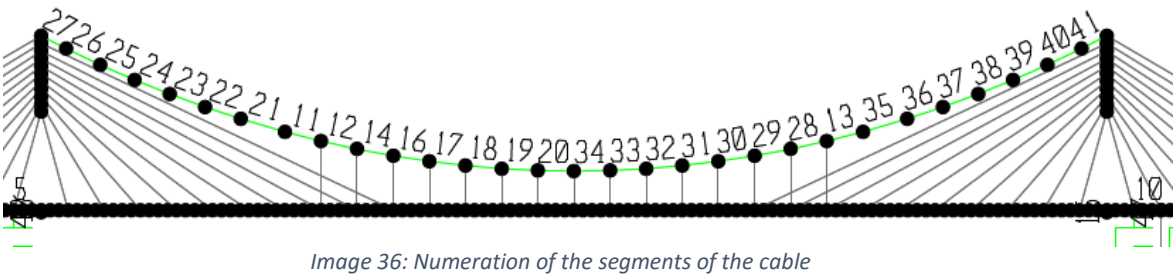

Image 36: Numeration of the segments of the cable

The program gives us the results in **COMB31** about force supported in each segment as we can see in the following table:

Link	StepType	P	Link	StepType	P	Link	StepType	P
11	Max	24199,3879	22	Max	24379,963	32	Max	23185,137
11	Min	20361,8293	22	Min	20521,1399	32	Min	19508,7756
12	Max	24082,7677	23	Max	24434,4585	33	Max	22989,3111
12	Min	20261,646	23	Min	20572,456	33	Min	19349,8021
13	Max	24199,3439	24	Max	24472,062	34	Max	22888,6869
13	Min	20361,8135	24	Min	20610,5621	34	Min	19269,4051
14	Max	23945,3361	25	Max	24494,0088	35	Max	24297,5994
14	Min	20145,1259	25	Min	20636,4569	35	Min	20447,6504
16	Max	23790,1529	26	Max	24501,6134	36	Max	24379,9311
16	Min	20021,7173	26	Min	20651,1842	36	Min	20521,123
17	Max	23448,9689	27	Max	24503,7301	37	Max	24434,426
17	Min	19726,2163	27	Min	20661,9349	37	Min	20572,4387
18	Max	23185,1834	28	Max	24082,7246	38	Max	24472,018
18	Min	19508,8022	28	Min	20261,6307	38	Min	20610,5444
19	Max	22989,4039	29	Max	23945,2937	39	Max	24493,9642
19	Min	19349,8763	29	Min	20145,1112	39	Min	20636,4388
20	Max	22888,8225	30	Max	23790,1923	40	Max	24501,5684
20	Min	19269,5212	30	Min	20021,7275	40	Min	20651,1657
21	Max	24297,6441	31	Max	23448,9603	41	Max	24503,6849
21	Min	20447,6667	31	Min	19726,2439			

Table 32: Force supported in each segment in COMB 31

Knowing the force and the cross-section area of the main cable, that is **0,2827 m²**, we can get the maximum stress that does not exceed the limit value.

P	σ_{med}	P	σ_{med}
24434,4585	86432,4673	24434,426	86432,3523
24472,062	86565,4828	24472,018	86565,3272
24494,0088	86643,1157	24493,9642	86642,9579
24501,6134	86670,0156	24501,5684	86669,8564
24503,7301	86677,503	24503,6849	86677,3431

Table 33: Maximum stresses

9.1.2.2 Suspension bridge – hangers

Working in the same way than the other chapter we will label the hangers. We have to remember we have two types of hangers and then two different areas. So firstly we have:

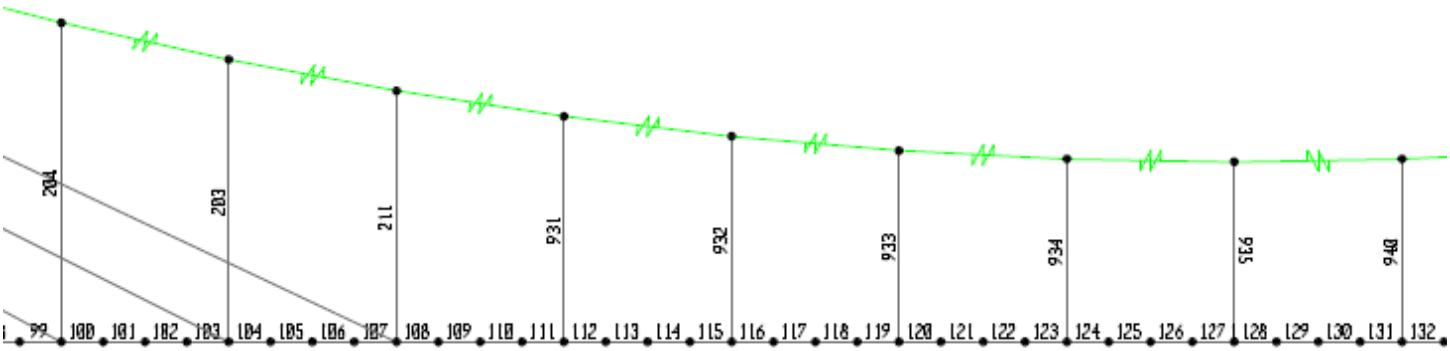

Image 36: Numeration of the hangers

So firstly we have:

$$Hanger\ 1\ \rightarrow Area = 0{,}159\ m^2$$

Frame	StepType	P	Frame	StepType	P
931	Max	1678,2502	935	Min	1357,3451
931	Min	1394,4395	940	Max	1711,6314
932	Max	1572,084	940	Min	1350,3793
932	Min	1260,8793	944	Max	1723,0383
933	Max	1722,8778	944	Min	1376,2876
933	Min	1376,1231	945	Max	1572,2005
934	Max	1711,459	945	Min	1261,008
934	Min	1350,218	946	Max	1677,7937
935	Max	1726,4299	946	Min	1394,0217

Table 34: Stresses in type 1 hangers

The maximum stress will be:

$$\sigma_{max} = \frac{P}{A} = \frac{1.726{,}43}{0{,}159} = 10.858{,}05\frac{T}{m^2} \leq 93.000\frac{T}{m^2}$$

And secondly we have:

$$Hanger\ 2\ \rightarrow Area = 0{,}0314\ m^2$$

Frame	StepType	P
203	Max	0,0008526
203	Min	-0,0006036
204	Max	0,0015
204	Min	-0,0006824
211	Max	213,647
211	Min	-154,7351

Table 35: Stresses in type 2 hangers

The maximum stress will be:

$$\sigma_{max} = \frac{P}{A} = \frac{213{,}657}{0{,}0314} = 6.804{,}36\frac{T}{m^2} \leq 93.000\frac{T}{m^2}$$

In both cases we are not exceeding the limit value so we are fulfilling the requirements.

9.1.2.3 Cable-stayed bridge – cables

We already know that the cables are grouped depending on the cross – section so we will differentiate them in order to calculate the final tensional state. Firstly we have:

$$T1\ to\ T8 \rightarrow 0{,}0594\ m^2$$

Frame	Construction nº	StepType	P
528	3	Max	1005,0093
528	3	Min	250,9631
529	5	Max	3552,724
529	5	Min	2619,3218
530	7	Max	2804,1229
530	7	Min	1833,9151
537	1	Max	3311,2216
537	1	Min	2823,3366
591	2	Max	2179,5628
591	2	Min	1728,635
592	4	Max	1963,8361
592	4	Min	1354,9114
593	6	Max	2482,346
593	6	Min	1813,2915
594	8	Max	2676,9593
594	8	Min	1975,9216

Table 36: Stresses in T1 to T8 cables

The maximum stress will be:

$$\sigma_{max} = \frac{P}{A} = \frac{3.552{,}724}{0{,}0594} = 59.810{,}17\frac{T}{m^2} \leq 93.000\frac{T}{m^2}$$

And secondly we have:

$$T9\ to\ T20\ \rightarrow 0{,}0962\ m^2$$

Frame	Construction nº	StepType	P	Frame	Construction nº	StepType	P
531	9	Max	4268,4247	595	10	Max	3063,6536
531	9	Min	3061,3262	595	10	Min	2140,3005
532	11	Max	3231,4411	596	12	Max	3304,3161
532	11	Min	2002,2854	596	12	Min	2252,9996
533	13	Max	4801,4404	925	14	Max	3580,0207
533	13	Min	3532,3827	925	14	Min	2455,6092
534	15	Max	3377,7882	926	16	Max	3829,2888
534	15	Min	2133,7209	926	16	Min	2655,3129
535	17	Max	5650,3081	927	18	Max	5068,8277
535	17	Min	4419,8373	927	18	Min	3351,8798
536	19	Max	2279,5979	928	20	Max	4040,5434
536	19	Min	1025,3543	928	20	Min	1164,3608

Table 37: Stresses in T9 to T20 cables

The maximum stress will be:

$$\sigma_{max} = \frac{P}{A} = \frac{5.650{,}31}{0{,}0962} = 58.735{,}03\frac{T}{m^2} \leq 93.000\frac{T}{m^2}$$

And finally we are fulfilling the normative.

9.1.3 Verification of local plastifications

In this part we will only verify the deck corresponding to the main span part (metallic deck). The study of the concrete deck beyond our reach because of the mechanical characteristics and problems that this type of material can have.

In terms of service, it must perform tensional verifications with the following objectives:

- Ensuring a quasi-linear behavior of the bridge against the service loads to verify the calculation models usually adopted to control the remaining service limit states.

- Delimit the possible signs of accumulation of plastic remaining deformations against repetitive live loads.
- Avoid the phenomena of oligocyclic fatigue (low number of cycles), not included in the verification models of the limit fatigue state included in RPM-95.

The resulting comparison tension in steel σ_{co} should not exceed the following value:

$$Characteristic\ combination\ \rightarrow 0{,}9 * f_y = 0{,}9 * 31.500 = 28.350 \frac{T}{m^2}$$

In this case the value will be extracted from the **table 3.2.1.6.** *"CARACTERISTICAS MECANICAS DE ACEROS INCLUIDOS EN NORMA UNE 36-080"* in the normative ***"RPM-95"***. For **S 355 J2G3** and a thickness of **80 mm** in the top of the section $\mathbf{f_y}$ will be **315 N/mm^2.**

According to this information the calculation of this comparison tension will be carried out by "PRONTUARIO INFORMÁTICO DE ESTRUCTURAS METÁLICAS Y MIXTAS (PIEM)" and the program ***SAP2000***.

We will verify two sections: the centre of the span with the maximum positive momentum and the corresponding area below the last cable with the maximum negative momentum. For both we will count with a section of 3 meters of height.

9.1.3.1 PIEM

This program allow us to calculate the tensional state of the deck but previously we have to comment some different important aspects. On the one hand the program carries out the reduction due to the longitudinal shear of the top/bottom flange of the beam following the "*Eurocode 3"* and therefore the reduction is made for continuous beams so we will have to approximate this to our case. On the other hand the program gives us the reduction whether we are working with a section of 2 webs but not 3, so we will adapt the hypothetical reduction of the case with 2 webs into our case (with 3 webs).

The verification will be carried out for the two sections we have commented previously and the program needs the existing moment and axial force in both sections to do all the relevant calculations. Then we will put:

$$Central\ section \begin{Bmatrix} M = 333.214{,}5\ KN \cdot m \\ N = 38.830{,}4\ KN \end{Bmatrix}$$

$$Section\ below\ the\ cable \begin{Bmatrix} M = -410.576{,}1\ KN \cdot m \\ N = -62.825{,}44\ KN \end{Bmatrix}$$

Central section

The following table shows the calculation in different parts: 1 corresponding to the top flange, 2 to the bottom flange and the rest (3, 4, 5) are the webs of the beam. In this section the maximum momentum is positive so the compressed flange will be the top one

1/r [km-1]	x [cm]	N [kN]	M [kNm]
0.559	**116.98**	37813.40	333214.50

Parte	zmin [cm]	zmax [cm]	¿Pos. Aboll.?	b,eff [mm]	b,eff/b	c1,eff/c1	b1,eff/b1	c2,eff/c2
1	-139.22	-131.22	Si	8700.00	1.00	-	1.00	-
2	160.76	168.76	Si	6920.00	1.00	-	1.00	-
3	-139.24	160.76	Si	3000.00	1.00	-	1.00	-

Parte	eps,sup [mm/m]	eps,inf [mm/m]	sigma,sup [MPa]	sigma,inf [MPa]	Material	Clase (EN 1993)	¿Parte Activa?
1	-0.654	-0.609	-130.70	-121.76	S-355.mat	1	Si
2	1.023	1.067	204.54	213.48	S-355.mat	1	Si
3	-0.654	1.023	-130.73	204.54	S-355.mat	1	Si

Parte	zmin [cm]	zmax [cm]	¿Pos. Aboll.?	b,eff [mm]	b,eff/b	c1,eff/c1	b1,eff/b1	c2,eff/c2
3	-139.24	160.76	Si	3000.00	1.00	-	1.00	-
4	-139.24	160.76	Si	3000.00	1.00	-	1.00	-
5	-139.24	160.76	Si	3000.00	1.00	-	1.00	-

Parte	eps,sup [mm/m]	eps,inf [mm/m]	sigma,sup [MPa]	sigma,inf [MPa]	Material	Clase (EN 1993)	¿Parte Activa?
3	-0.654	1.023	-130.73	204.54	S-355.mat	1	Si
4	-0.654	1.023	-130.73	204.54	S-355.mat	1	Si
5	-0.654	1.023	-130.73	204.54	S-355.mat	1	Si

Image 37: PIEM data and tensional results for the central cross - section

.

As we can see the tensional values does not exceed the limit value:

$$\sigma = 21.348 < \sigma_{co} = 28.350 \rightarrow OK$$

Section below the cable

In this section the maximum negative momentum is negative so the compressed flange will be the bottom one.

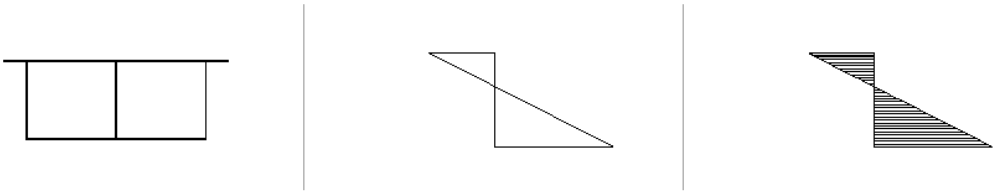

Image 38: Stress diagram of the cross - section below the cable

As we can see the tensional values does not exceed the limit value:

	Parte	zmin [cm]	zmax [cm]	¿Pos. Aboll.?	b,eff [mm]	b,eff/b	c1,eff/c1	b1,eff/b1	c2,eff/c2
	3	-139.24	160.76	Si	3000.00	1.00	-	1.00	-
	4	-139.24	160.76	Si	3000.00	1.00	-	1.00	-
▶	5	-139.24	160.76	Si	3000.00	1.00	-	1.00	-

	Parte	eps,sup [mm/m]	eps,inf [mm/m]	sigma,sup [MPa]	sigma,inf [MPa]	Material	Clase (EN 1993)	¿Parte Activa?
	3	0.752	-1.314	150.39	-262.71	S-355.mat	1	Si
	4	0.752	-1.314	150.39	-262.71	S-355.mat	1	Si
▶	5	0.752	-1.314	150.39	-262.71	S-355.mat	1	Si

Image 39: PIEM data and tensional results for the cross - section below the cable

$$27.372\frac{T}{m^2} < 28.350\frac{T}{m^2} \rightarrow OK$$

9.1.3.2 SAP2000

In this case we will evaluate the two same sections as we have done before and we will apply the reduction of the width both on the top and the bottom flange. We have to note that the sections drawn are upside down because a sign criteria.

Central section

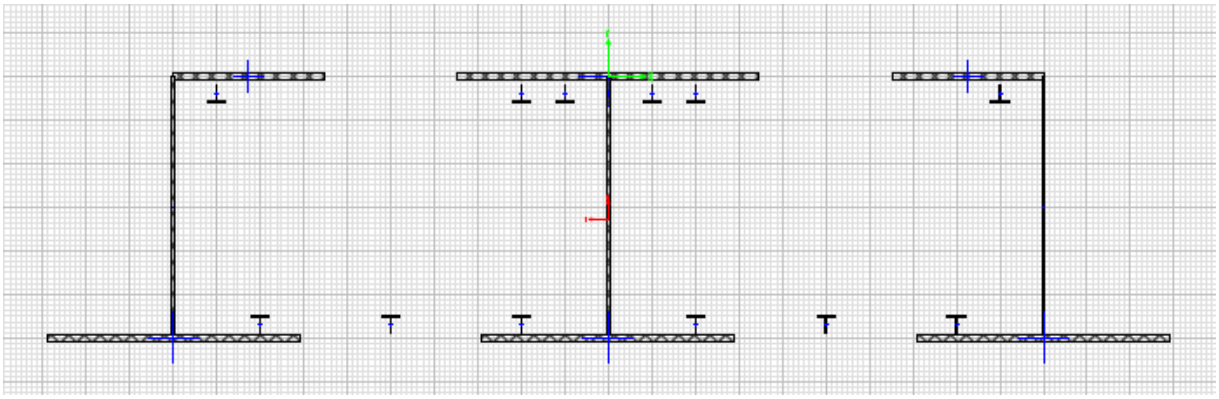

Image 40: Reduced inverted central cross - section

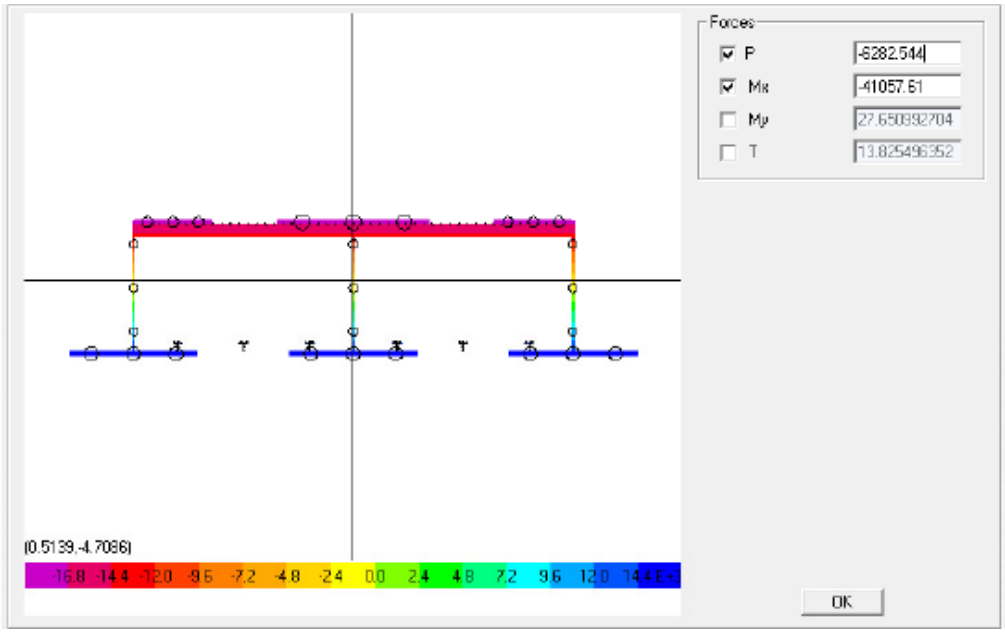

Image 41: Graph of stresses of the central cross – section

As we can see in the following image the tensions varies from -16.800 T/m^2 in the bottom until 14.400 T/m^2 in the top so we won't exceed the limit value.

Section below the cable

In this case the negative moment is really high in U.L.S and the section will very required so we will need to put a reinforced concrete layer having then a mixed section. This layer will have 30 cm of thickness reinforced with 1 Ø 20/25 cm in both flanges.

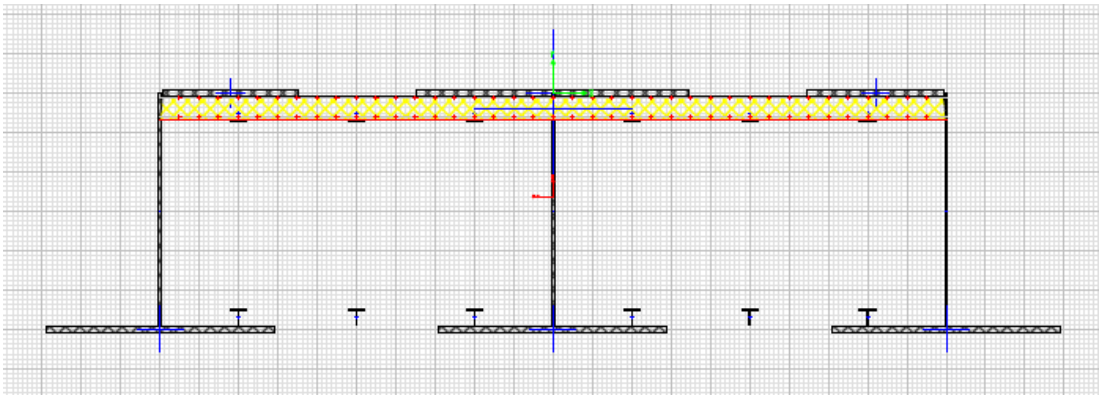

Image 42: Reduced inverted cross – section below the cable

As we can see in the following image the tensions varies from -12.000 T/m^2 in the bottom until 19.200 T/m^2 in the top so we won't exceed the limit value.

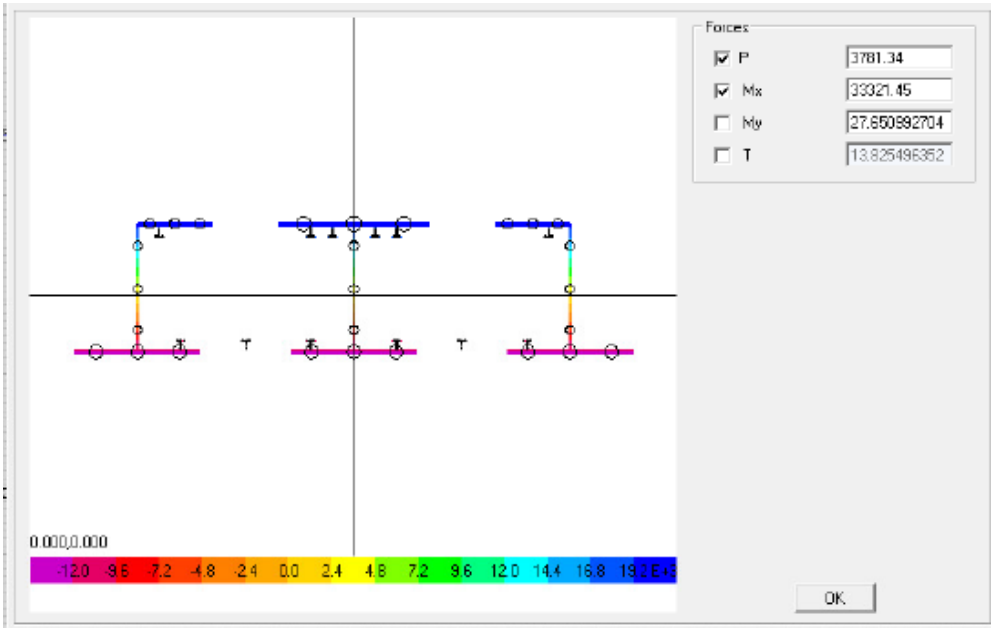

Image 43: Graph of stresses of the cross – section below the cable

9.2 U.L.S

The security of the structure will be considered verified if the following condition is accomplished:

$$S_d \leq R_d$$

Being:

$$S_d: value\ of\ the\ stress\ acting\ on\ each\ section$$

$$R_{d:}\ resistance\ value\ of\ each\ section$$

This verification is done in the final state and at all stages of the construction process for the design values of the corresponding actions for each situation and for the structural scheme corresponding to each one of the possible scenarios.

For the determination of ultimate bending moments and axial forces we will use the following two alternative methods:

- Fixed elastic method (EC) and plastic (P)
- Elastic-plastic method (EP)

9.2.1 PIEM

The program will work in the same way as it does in the Service Limit State so we will follow the same process adding the existing shear force too:

$$Central\ section \begin{Bmatrix} M = 468.768{,}71\ KN \cdot m \\ V = 14.530{,}45\ KN \\ N = 51.100{,}25\ KN \end{Bmatrix}$$

$$Section\ below\ the\ cable \begin{Bmatrix} M = -554.277{,}6\ KN \cdot m \\ V = 16.787{,}5\ KN \\ N = -84.814{,}35\ KN \end{Bmatrix}$$

Anyway, we have to note that in U.L.S is not usual to make the reduction for both flanges since the section is already yielded. However the program doesn't allow us to choose in what flange we want to do the reduction so the reduction will be made for both.

9.2.1.1 Ultimate bending moment

In this chapter the calculation of the ultimate bending moment will be made according to the elastic-plastic method and it will be necessary to follow an iterative process. This process will be made by the PIEM and SAP2000 too in absence of shear and axial forces.

Central section

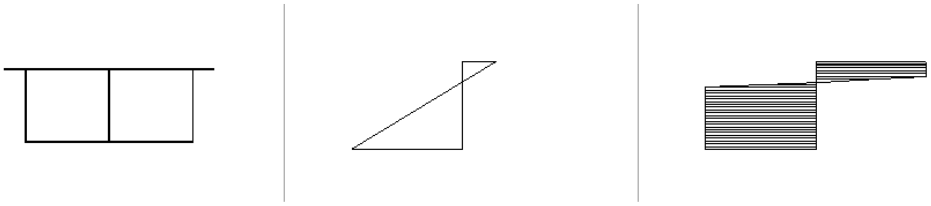

Image 44: Stress diagram of the central cross – section in U.L.S

Finally:

My,Rd(+) [kNm]	1/r [km-1]	x [cm]	Mz [kNm]	lLT [m]	Mcr [kNm]	alphaLT	ksiLT
649852.92	8.428	70.92	619.00	1.00	27045930757.97	0.49	1.00

Parte	zmin [cm]	zmax [cm]	¿Pos. Aboll.?	b,eff [mm]	b,eff/b	c1,eff/c1	b1,eff/b1	c2,eff/c2
1	-139.22	-131.22	Si	8700.00	1.00	-	1.00	-
2	160.76	168.76	Si	6920.00	1.00	-	1.00	-
3	-139.24	160.76	Si	3000.00	1.00	-	1.00	-

Parte	eps,sup [mm/m]	eps,inf [mm/m]	sigma,sup [MPa]	sigma,inf [MPa]	Material	Clase (EN 1993)	¿Parte Activa?
3	-5.977	19.306	-322.73	322.73	S-355.mat	1	Si
4	-5.977	19.306	-322.73	322.73	S-355.mat	1	Si
5	-5.977	19.306	-322.73	322.73	S-355.mat	1	Si

Image 45: PIEM data and tensional results for the central cross – section in U.L.S

$$M_{y,rd} = 64.985{,}29 \frac{\mathrm{T}}{\mathrm{m}^2} > \mathrm{M}_{sd} = 46.876{,}8 \rightarrow \mathrm{OK}$$

Section below the cable

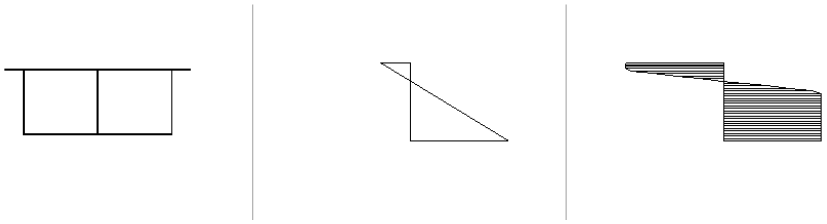

Image 46: Stress diagram of the cross – section below the cable in U.L.S

My,Rd(-) [kNm]	1/r [km-1]	x [cm]	Mz [kNm]	lLT [m]	Mcr [kNm]	alphaLT	ksiLT
-648403.85	-3.738	70.82	-619.69	1.00	15018601559.17	0.49	1.00

Parte	zmin [cm]	zmax [cm]	¿Pos. Aboll.?	b,eff [mm]	b,eff/b	c1,eff/c1	b1,eff/b1	c2,eff/c2
1	-139.22	-131.22	Si	8700.00	1.00	-	1.00	-
2	160.76	168.76	Si	6920.00	1.00	-	1.00	-
3	-139.24	160.76	Si	3000.00	1.00	-	1.00	-

Parte	eps,sup [mm/m]	eps,inf [mm/m]	sigma,sup [MPa]	sigma,inf [MPa]	Material	Clase (EN 1993)	¿Parte Activa?
3	2.648	-8.567	322.73	-322.73	S-355.mat	1	Si
4	2.648	-8.567	322.73	-322.73	S-355.mat	1	Si
5	2.648	-8.567	322.73	-322.73	S-355.mat	1	Si

Image 47: PIEM data and tensional results for the cross – section below the cable in U.L.S

$$M_{y,rd} = -64.840{,}3\frac{\mathrm{T}}{\mathrm{m}^2} > \mathrm{M}_{sd} = -55.427\frac{\mathrm{T}}{\mathrm{m}^2} \rightarrow \mathrm{OK}$$

9.2.1.2 Ultimate shear strength

The ultimate shear strength V_{rd} is determined as the sum of the corresponding to each of the webs of the box section in absence of Bending moment and axial forces.

Vb,Rd [kN]	Vbw,Rd [kN]	Vbf,Rd [kN]	Mf,Rd [kNm]	MEd [kNm]	NEd [kN]	a [m]	ksiy	ksiz	kyy	kzy
29026.74	29026.74	0.00	0.00	0.00	0.00	10	1.000	1.000	1.000->1	0.523->1

Parte	Tipo	hw [mm]	tw [mm]	bf [mm]	tf [mm]	ksi,W	Material	η	Av [mm2]
1	Alma	8700.0	80.0	-	-	0.672	S-355	1.20	696000.0
2	Alma	6920.0	80.0	-	-	0.787	S-355	1.20	553600.0
3	Alma	3000.0	30.0	-	-	0.603	S-355	1.20	90000.0
4	Alma	3000.0	30.0	-	-	0.603	S-355	1.20	90000.0
5	Alma	3000.0	30.0	-	-	0.603	S-355	1.20	90000.0

Image 48: PIEM data and shear force results for the cross – section below the cable in U.L.S

$$V_{pl,rd} = 29.026{,}74\ \mathrm{KN} > \mathrm{V}_{sd} = 14.530{,}45\ \mathrm{KN} \rightarrow \mathrm{OK}$$

9.2.1.3 Interaction bending moment and shear strength

In this case the program will give us the interaction diagram which is divided in 3 zones: the first one comprises between a moment with a value of 0 and the ultimate moment that the flanges can resist; the second one comprises between this last point of the first zone and the point

where we arrive at $0{,}5 \cdot V_{pl,rd}$ and the third zone goes from this last point until a null value of the shear strength.

Central section

In this section we will be inside the domain knowing then that it resists the stresses. Particularly the section will be located in the first zone of the domain (almost the second one).

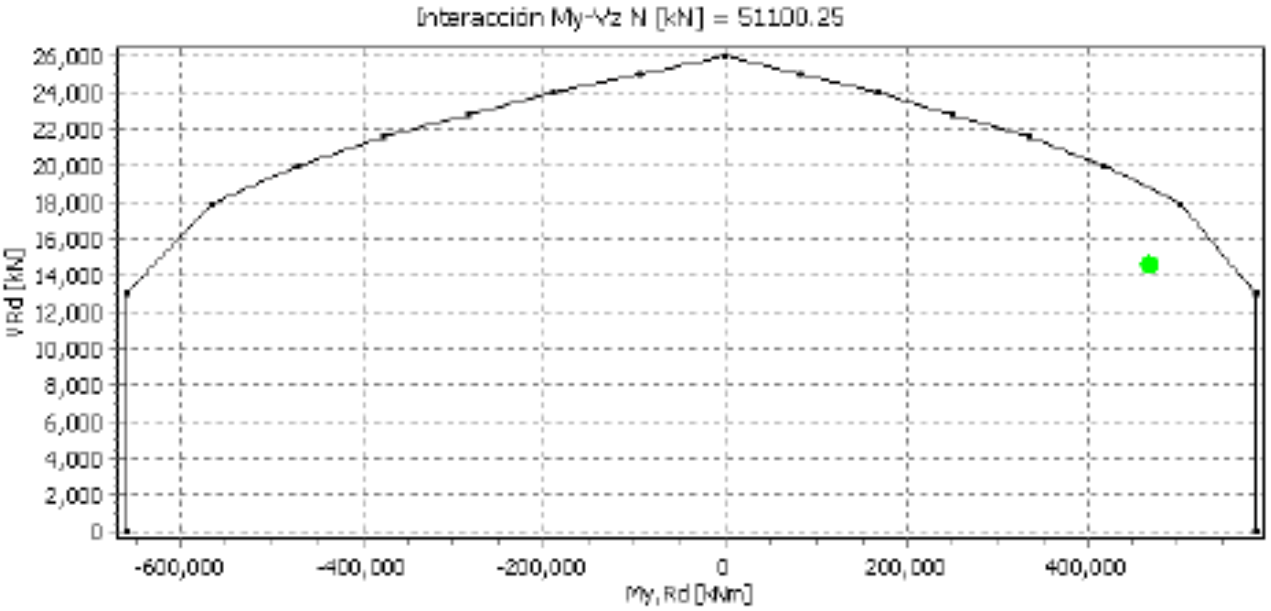

Image 49: Interaction bending moment and shear force graph corresponding to the central cross - section

Finally the diagram also gives us (graphically) the ultimate moment corresponding to the interaction:

Vb,Rd [kN]	Vbw,Rd [kN]	Vbf,Rd [kN]	Mf,Rd [kNm]	MEd [kNm]	NEd [kN]	a [m]	ksiy	ksiz	kyy	kzy
19431.91	19431.91	0.00	0.00	468768.71	51100.25	10	1.000	1.000	1.000->1	0.525->1

Parte	Tipo	hw [mm]	tw [mm]	bf [mm]	tf [mm]	ksi,W	Material	η	Av [mm2]
1	Alma	11600.0	80.0	-	-	0.583	S-355	1.20	928000.0
2	Alma	6920.0	80.0	-	-	0.787	S-355	1.20	553600.0
3	Alma	3000.0	30.0	-	-	0.603	S-355	1.20	90000.0
4	Alma	3000.0	30.0	-	-	0.603	S-355	1.20	90000.0
5	Alma	3000.0	30.0	-	-	0.603	S-355	1.20	90000.0

Image 50: PIEM Ultimate shear force in the central cross - section

$$M_u = 55.000\, T \cdot m$$

Section below the cable

In this section we will be outside the domain so we will have to reconsider it. It's important to remember that in PIEM we don't have the reinforced section and that's why we are not inside the domain.

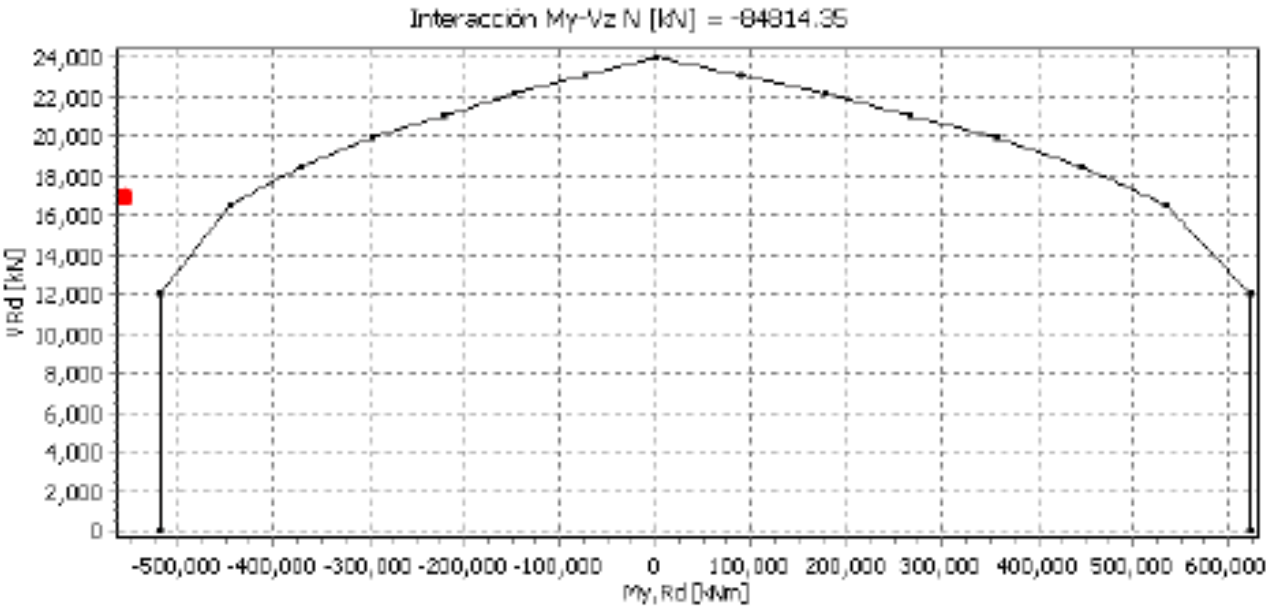

Image 51: Interaction bending moment and shear force graph corresponding to the cross - section below the cable

Vb,Rd [kN]	Vbw,Rd [kN]	Vbf,Rd [kN]	Mf,Rd [kNm]	MEd [kNm]	NEd [kN]	a [m]	ksiy	ksiz	kyy	kzy
iEd>Rd!	-	-	-	-554277.86	-84814.35	10	1.000	1.000	1.000->1	0.523->1

Parte	Tipo	hw [mm]	tw [mm]	bf [mm]	tf [mm]	ksi,W	Material	η	Av [mm2]
1	Alma	8700.0	80.0	-	-	0.672	S-355	1.20	696000.0
2	Alma	6920.0	80.0	-	-	0.787	S-355	1.20	553600.0
3	Alma	3000.0	30.0	-	-	0.603	S-355	1.20	90000.0
4	Alma	3000.0	30.0	-	-	0.603	S-355	1.20	90000.0
5	Alma	3000.0	30.0	-	-	0.603	S-355	1.20	90000.0

Image 52: PIEM Ultimate shear force in the cross – section below the cable

And as before:

$$M_u = -51.000\ T \cdot m$$

9.2.1.4 Interaction bending moment and axial force

Knowing the generality of the methods in this case the program will apply the elastoplastic method (EP) with which is possible to obtain directly the interaction diagram M_{rd} - N_{rd}. In this case we won't take into account the values of the ultimate moment because the ones for the bending moment and shear strength interaction are more restrictive.

Central section

As it happens with the previous interaction this section will accomplish the requirements.

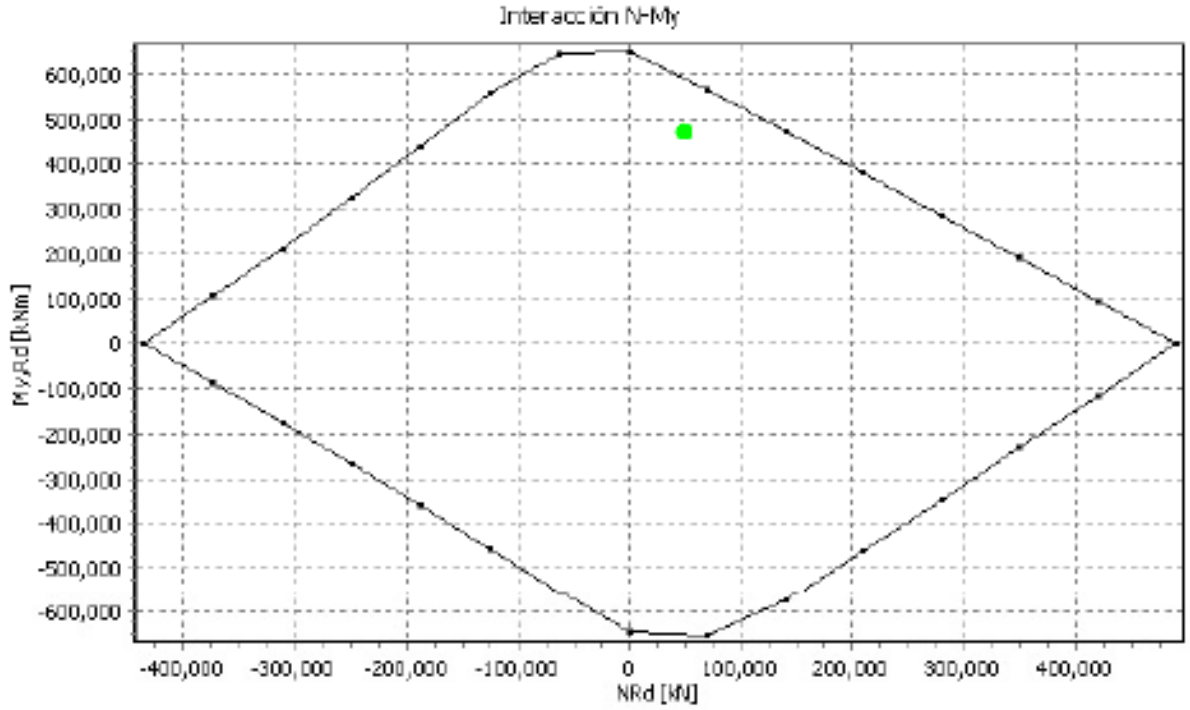

Image 53: Interaction bending moment and axial force graph corresponding to the central cross - section

Section below the cable

Again we will have to reconsider the section.

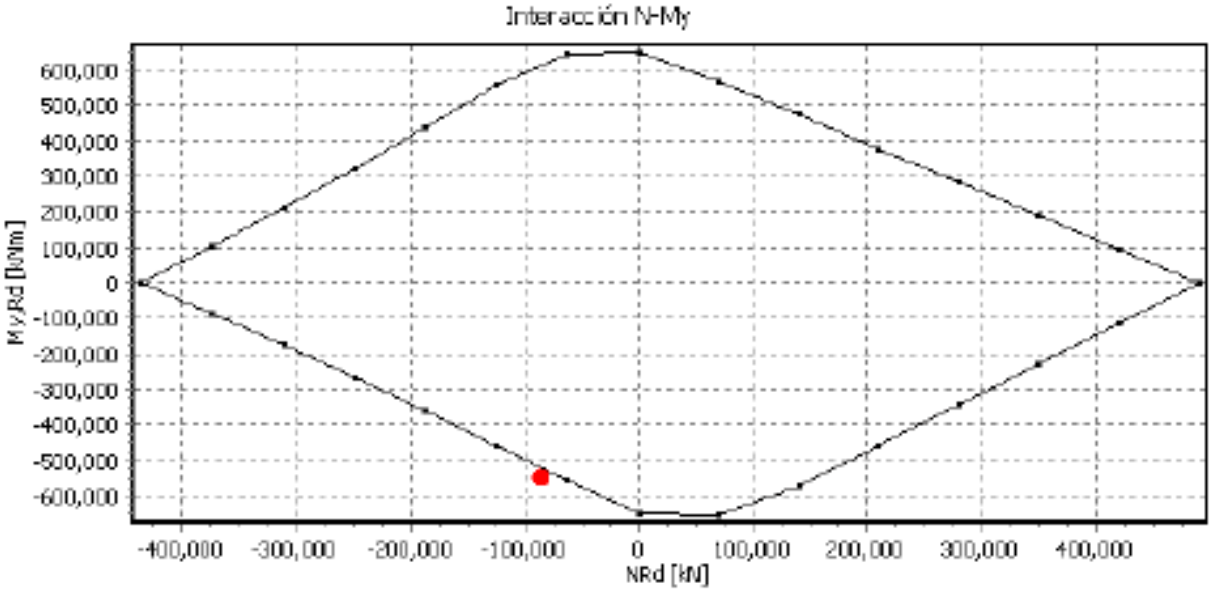

Image 54: Interaction bending moment and axial force graph corresponding to the cross - section below the cable

9.2.1.5 Interaction bending moment, shear strength and axial force

Here it will be used the fixed elastic method and the plastic method (P). For compact sections it is recommended to use specialized texts, and use formulas relating M_{sd}, M_{rd}, N_{sd} and N_{rd} for the most common sections. For both sections we will use the recommendation for slender sections being e_n the displacement of the neutral axis of the section requested in uniform compression, which occurs when the reduced section differs from the gross.

Central section

So we will have the following equations:

$$\frac{N_{Ed}}{N_{Rd}} + \frac{M_{yEd} + N_{Ed}e_{N_y}}{M_{yRd}} + \frac{M_{zEd} + N_{Ed}e_{N_z}}{M_{zRd}} \leq 1.0 \qquad (6.44)$$

$$\frac{N_{Ed}}{\chi_y N_{Rd}} + k_{yy}\frac{M_{yEd} + N_{Ed}e_{N_y}}{\chi_{LT,y}M_{yRd}} + k_{yz}\frac{M_{zEd} + N_{Ed}e_{N_z}}{\chi_{LT,z}M_{zRd}} \leq 1.0 \qquad (6.61)$$

$$\frac{N_{Ed}}{\chi_z N_{Rd}} + k_{zy}\frac{M_{yEd} + N_{Ed}e_{N_y}}{\chi_{LT,y}M_{yRd}} + k_{zz}\frac{M_{zEd} + N_{Ed}e_{N_z}}{\chi_{LT,z}M_{zRd}} \leq 1.0 \qquad (6.62)$$

Image 55: Recommended formulation for slender sections

NRd [kN]	My,Rd [kNm]	Mz,Rd [kNm]
490416.36	649852.92	987843.74

Ny,cr [kN]	Nz,cr [kN]	Ncr,T [kN]	Ncr,TF [kN]	My,cr [kNm]	Mz,cr [kNm]
2354125.40	17279245212.97	14789.09	14789.09	27045930757.97	265275492612.44

ksi,y	ksi,z	ksiLT,y	ksiLT,z	kyy	kyz	kzy	kzz
1.000	1.000	1.000	1.000	1.000	0.688	0.523	1.033

(6.44)	(6.61)	(6.62)	NEd/Nb,Rd	My,Ed/Mby,Rd	Mz,Ed/Mbz,Rd
0.83	**0.83**	**0.48**	0.10	0.72	0.00

Image 56: Verification of the Interaction bending moment, shear strength and axial force in the central cross- section

The image shows us that the final values doesn't surpass the limit value that here is 1 so we will accomplish the requirements.

Section below the cable

Contrary here we will surpass the value as it happened with the bending moment- axial force interaction.

NRd [kN]	My,Rd [kNm]	Mz,Rd [kNm]
-490416.36	-648403.85	987843.74

Ny,cr [kN]	Nz,cr [kN]	Ncr,T [kN]	Ncr,TF [kN]	My,cr [kNm]	Mz,cr [kNm]
2354125.40	17279245212.97	14789.09	14789.09	15018601559.17	265275492612.44

ksi,y	ksi,z	ksiLT,y	ksiLT,z	kyy	kyz	kzy	kzz
0.889	1.000	1.000	1.000	1.018	0.604	0.544	0.983

(6.44)	(6.61)	(6.62)	NEd/Nb,Rd	My,Ed/Mby,Rd	Mz,Ed/Mbz,Rd
1.03	1.07	0.64	0.19	0.85	0.00

Image 57: Verification of the Interaction bending moment, shear strength and axial force in the cross – section below the cable

The calculations and verification with the new reinforced section will be made with SAPv2000

9.2.2 SAP2000

We will realize the calculation thanks to the option “design sections” and in this case we will only do the reduction of the compressed flange since we are in U.L.S. With ***SAP2000*** we will obtain the moment-curvature diagram with the presence of axial force.

9.2.2.1 Interaction bending moment - axial force

Central section

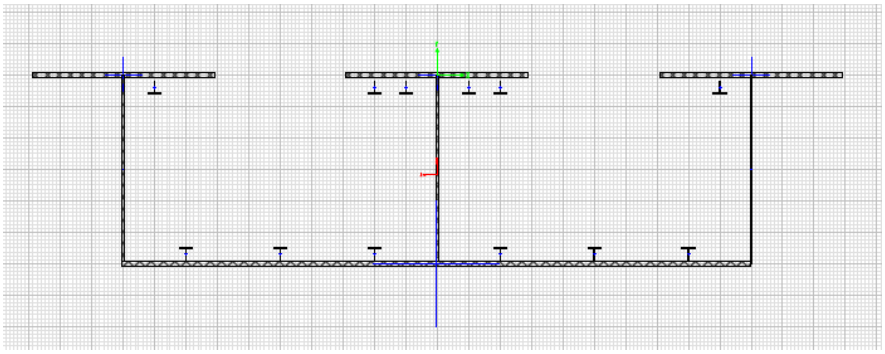

Image 58: Reduced central cross - section

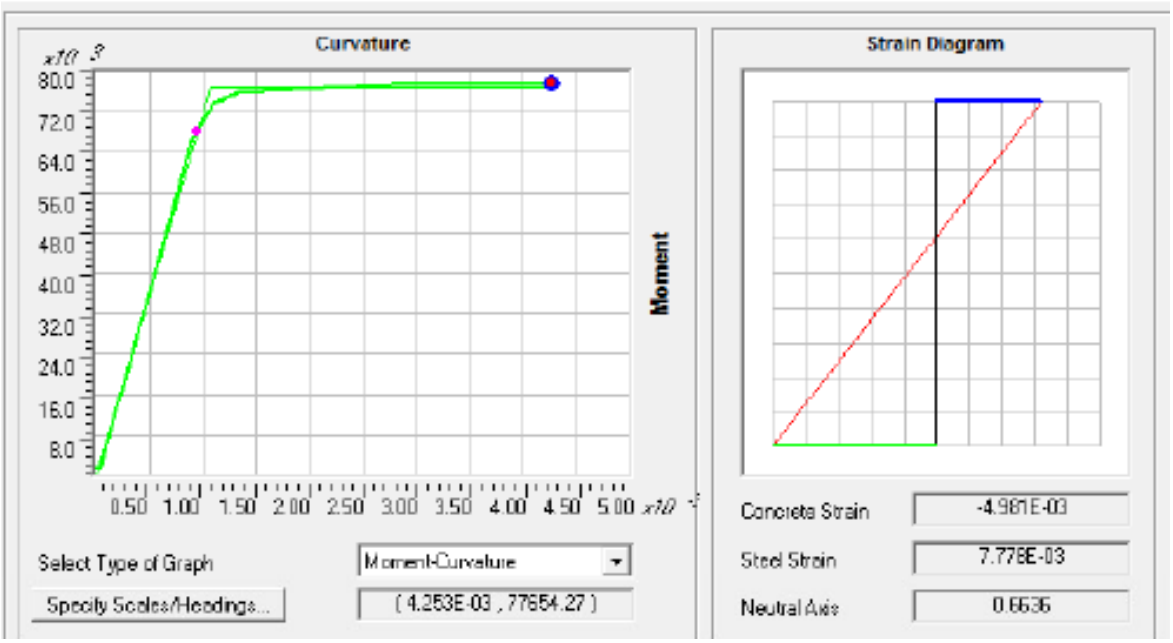

Image 59: Moment – Curvature diagram for the central cross - section

We will obtain a table with all the results corresponding with moments and curvatures in all the fibers but here we will only present the most important results:

$$\emptyset_y = 9{,}519E - 04\, rad$$

$$M_y = 68.196\, KN \cdot m$$

$$M_p = 76.898\, KN \cdot m$$

$$I_{crack} = 3{,}4116\, m^4$$

$$\emptyset_y =, .264E - 03\, rad$$

$$M_{concrete} = 77.654\, KN \cdot m$$

Finally:

$$M_u = 77.654 \frac{\mathrm{T}}{\mathrm{m}^2} > \mathrm{M}_{sd} = 46.876{,}8 \frac{\mathrm{T}}{\mathrm{m}^2} \rightarrow \mathrm{OK}$$

Section below the cable

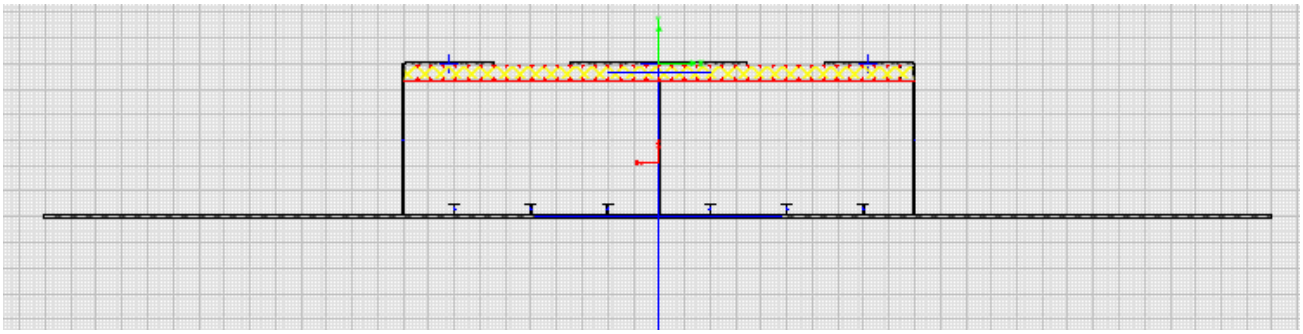

Image 60: Reduced cross – section below the cable

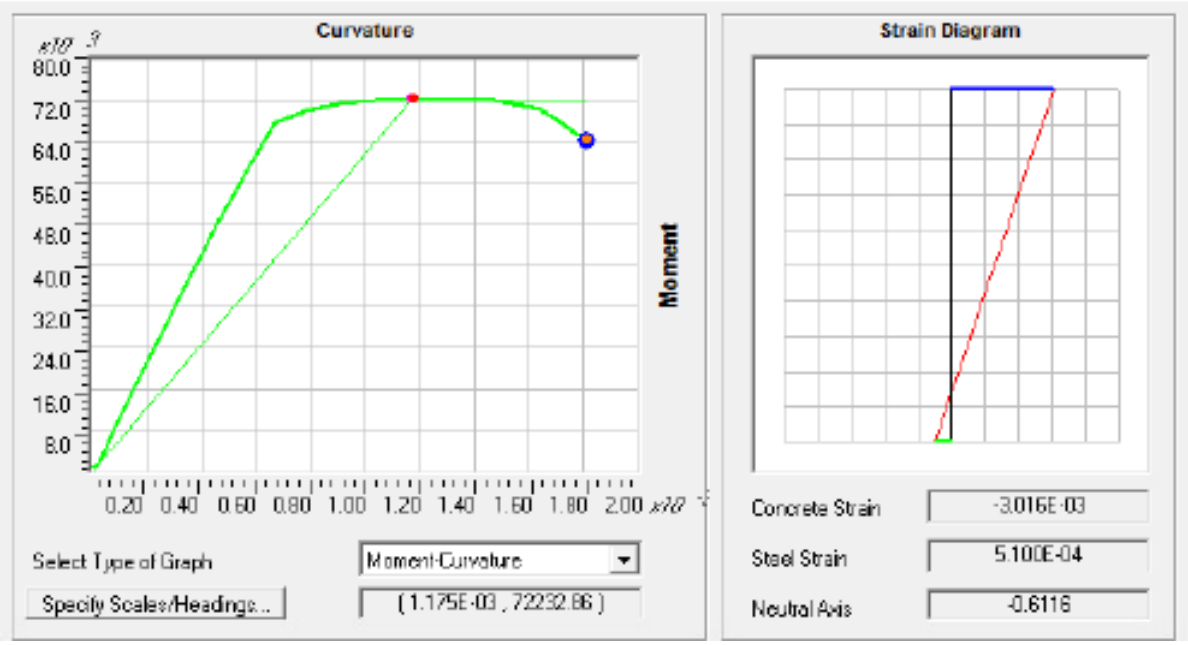

Image 61: Moment – Curvature diagram for the section below the cable

Proceeding in the same way that we have done before:

$$\emptyset_y = 9{,}170E-03\ rad$$

$$M_y = 72.225\ KN \cdot m$$

$$M_p = 72.225\ KN \cdot m$$

$$I_{crack} = 2{,}9399\ m^4$$

$$\emptyset_y = 1{,}814E-03\ rad$$

$$M_{concrete} = 64.161\ KN \cdot m$$

Finally:

$$M_u = -64.161 \frac{\mathrm{T}}{\mathrm{m}^2} > \mathrm{M}_{sd} = -55.427 \frac{\mathrm{T}}{\mathrm{m}^2} \rightarrow \mathrm{OK}$$

Therefore ***SAP2000*** will give us all the interactions as ratio values but it doesn't take into account the reduction of the flanges because of the longitudinal shear and that's why the values amply complies the requirements so these will only be reference values. We have to note too that we will have the results also for the tower. We can see them graphically in the following images.

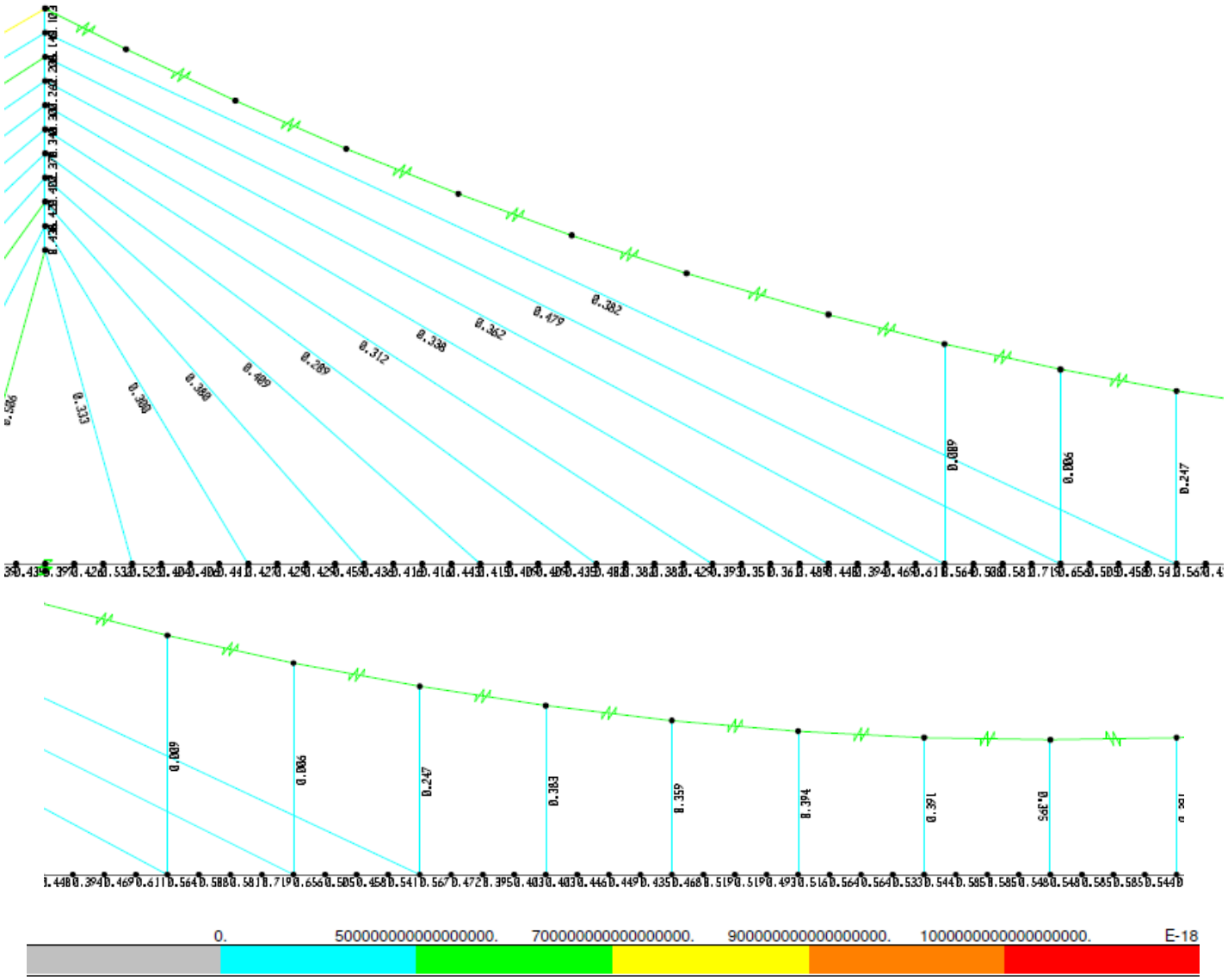

Image 62: SAP2000 interaction ratio values for the metallic components of the bridge

9.2.3 Comparison PIEM – SAP2000

S.L.S	Central section	Ultimate cable section	Central section	Ultimate cable section
σ_{top} (T/m^2)	-13.922	15.037	-12.000	14.400
σ_{bot} (T/m^2)	21.348	-27.372	19.200	-16.800
U.L.S				
M_u (T·m)	55.000	-51.000	77.654	-64.161
M_{sd} (T·m)	46.876	55.427	46.876	-55.427
		Without mixed section		With mixed section

Table 38: Comparison results between PIEM and SAP2000

The difference between both models are due to the model in SAP2000 contemplates the mixed section for the maximum negative moment whether PIEM model don't, and that's the reason why in PIEM we exceed the limit values. Anyway the results in SAP2000 are feasible and we can trust them so we can ensure its validity and therefore all the values in U.L.S are verified.

10. DYNAMIC ANALYSIS

In bridges with big spans and with very slender decks it's not enough to verify the static equilibrium and we must analyze the dynamic behavior in order to ensure the resistant capabilities of the structure.

The most important load we will have to consider in this analysis is the wind load so it will introduce bending and torsional vibrations that with small increments of the amplitudes can collapse the bridge.

Aero - elasticity

The concept of aero – elasticity its referred to the study of the interaction between airflow and the forces that it causes in a deformed solid immersed in it. This interaction may result in different forms of aero – elasticity that can provoke instabilities. These are the most important:

- Vortex shedding
- Galloping
- Wake galloping
- Flutter
- Buffering

Since the objective of this thesis is not focused exclusively in the study of the dynamic analysis we are not going to detail all this phenomena and we will only talk about flutter which is the one that has a more regular behavior. This instability appears when we arrive at certain critical speed of the wind when the forces of the airflow causes negative dampings in the structure such that the movements in the deck increases until the collapse.

As we have said before with wind loads we will have bending and torsional vibrations and the important thing in flutter will be to guarantee no coupling of these two modes trying to ward off both. It's important to know that all the following calculations are based in this phenomena.

We will study three different models:

- 2D model
- Fish-Bone beam model
- 3D model

10.1 2D Model

10.1.1 Torsional natural frequencies

The torsional frequencies are highly related with geometrical parameters of the structure. We will have two different equations depending if we have a rigid or flexible deck. First of all it's important to show the data of which shall be used in this chapter:

For section nº8 we obtain:

$$J_T = 7{,}6369\ m^4 \rightarrow torsional\ constant$$

$$J_P = 17{,}5678\ m^4 \rightarrow polar\ inertia\ per\ unit\ lenght\ of\ the\ deck$$

$$r_{min} = 1{,}4112\ m \rightarrow turning\ minimum\ radius$$
$$r_{max} = 3{,}1501\ m \rightarrow turning\ maximum\ radius$$
$$G = 8.076.923\frac{T}{m^2} \rightarrow torsional\ modulus$$

In the case of flexible decks we will use an equation derived from the Rayleigh approximation:

$$f_T = \frac{b}{2r} \cdot f_B = \frac{24}{2 \cdot 1{,}4112} \cdot 0{,}06541 = 0{,}556\ s^{-1} \rightarrow Flexible\ deck$$

In the case of rigid decks the natural frequency is obtained directly thanks to the torsional stiffness GJ_t of the cross-section by the following equation:

$$f_T = \frac{1}{2L} \cdot \left(\frac{G \cdot J_T}{J_P}\right)^{\frac{1}{2}} = 0{,}662\ s^{-1} \rightarrow Rigid\ deck$$

To calculate torsional frequencies in 2D model we can only do it analytically since SAP2000 doesn't give as torsional frequencies because we are working with frames.

10.1.2 Bending natural frequencies

There are too many methods to obtain the natural frequencies but we will use the Rayleigh method which uses the energy conservation law to find the natural frequency according to the deformations in the structure in the direction of the vibration mode. Using this methodology we will use the following equation:

$$f_B = \frac{1{,}1}{2\pi} \cdot \left(\frac{g}{v_{max}}\right)^{\frac{1}{2}}$$

Where v_{max} is the maximum static deformation of the structure due to the permanent loads acting in the direction of the corresponding vibration mode. In this case:

$$v_{max} = 99{,}75\ m \rightarrow f_B = 0{,}05493\ s^{-1}$$

Anyhow, besides the theoretical analysis the results can also be obtained by SAP2000:

$$f_B^{-1}(SAP) = 15{,}288^{-1} \rightarrow f_B = 0{,}06541 \rightarrow mode\ 19$$

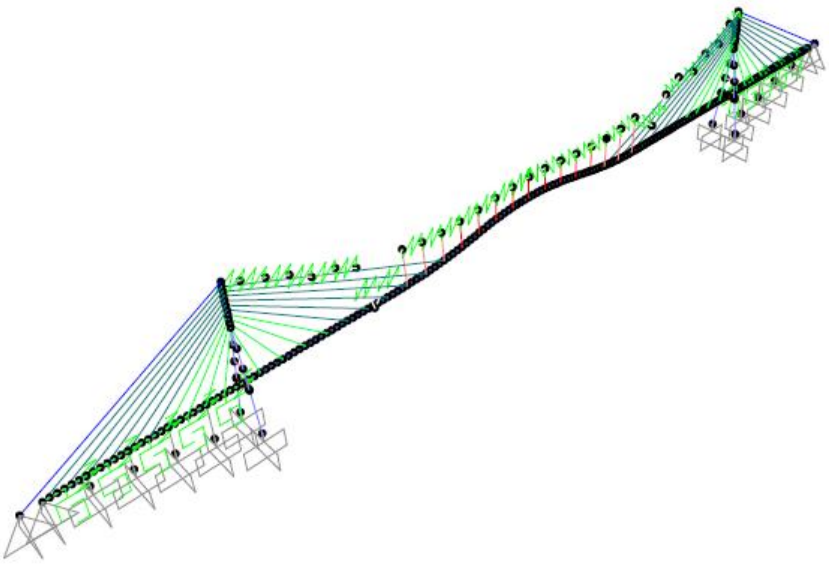

Image 63: Bending vibration mode in 2D model

10.1.3 Flutter critical speed

For the calculation of flutter critical speed we will use the Selberg approximation which serves the following equation:

$$V_{Rf} = 3{,}7\sqrt{\frac{mr}{\rho B^3}\left(1-\left(\frac{n_z}{n_\theta}\right)^2\right)}$$

This speed value (v_{Rf}) corresponds to the reduced flutter speed of a supported surface. To use it we have to attend to meet:

$$\begin{Bmatrix} n_\theta > 1{,}4 \cdot n_Z \\ \frac{mr}{\rho B^3} > 5 \end{Bmatrix}$$

Where:

$$m \rightarrow weight\ per\ unit\ length$$

$$m = m_{pp} + m_{cp} = m_{pp} + m_{pav.} + m_{rail.} = 21{,}859 \cdot 1{,}1 + 1{,}2 + 5{,}244 = 30{,}489\frac{T}{m}$$

$$\rho = 1{,}29\frac{Kg}{m^3} \rightarrow air\ density$$

$$n_\theta \rightarrow torsional\ natural\ frequency$$

$$n_Z \rightarrow bending\ natural\ frequency$$

Then:

$$V_{Rf} = 3{,}7\sqrt{\frac{30.489 \cdot 1{,}4112}{1{,}29 \cdot 24^3}\left(1 - \left(\frac{0{,}06541}{0{,}662}\right)^2\right)} = 5{,}719$$

From this value is possible to arrive to the flutter speed without any reduction:

$$V_f = V_{Rf} \cdot B \cdot n_\theta = 5{,}719 \cdot 24 \cdot 0{,}662 = 90{,}865\frac{m}{s}$$

Finally, to get the flutter critical speed we have to consider that the cross-section of the deck is not an airfoil and therefore it should be important to apply an effectiveness factor:

$$V_c = \eta \cdot V_{Rf} \cdot B \cdot n_\theta = 0{,}7 \cdot 5{,}719 \cdot 24 \cdot 0{,}662 = 63{,}604\frac{m}{s}$$

10.1.4 Top speed

$$v_c(z) = \sqrt{C_e(z)} \cdot v_b(T) = \sqrt{5{,}145} \cdot 29{,}12 = 66{,}052\ m/s$$

$$v_{crit.} = 1{,}25 \cdot v_c(z) = 1{,}25 \cdot 66{,}052 = 82{,}565\ m/s$$

$$v_{crit.} > v_c \rightarrow Not\ valid$$

$$n_\theta > 1{,}4 \cdot n_Z \rightarrow 0{,}682 > 1{,}4 \cdot 0{,}06541 = 0{,}092 \rightarrow OK$$

$$\frac{mr}{\rho B^3} = 2{,}413 < 5 \rightarrow Not\ valid$$

10.2 Fish-bone beam model

This second model allows us to obtain more accurate results as to torsional frequencies. In figure 43 we sketch the model. The grey part is the roadway, the two external cross sections in blue are fixed and the plate is hinged there. The red lines contains the barycenters of the cross section and the yellow orthogonal lines are virtual cross sections that can rotate around their barycenter.

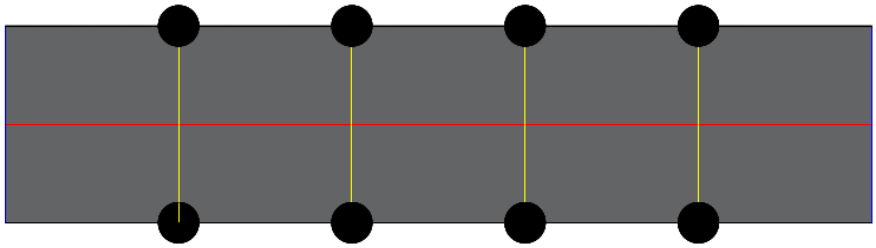

Figure 45: Fish-bone beam detail

10.2.1 Torsional natural frequencies

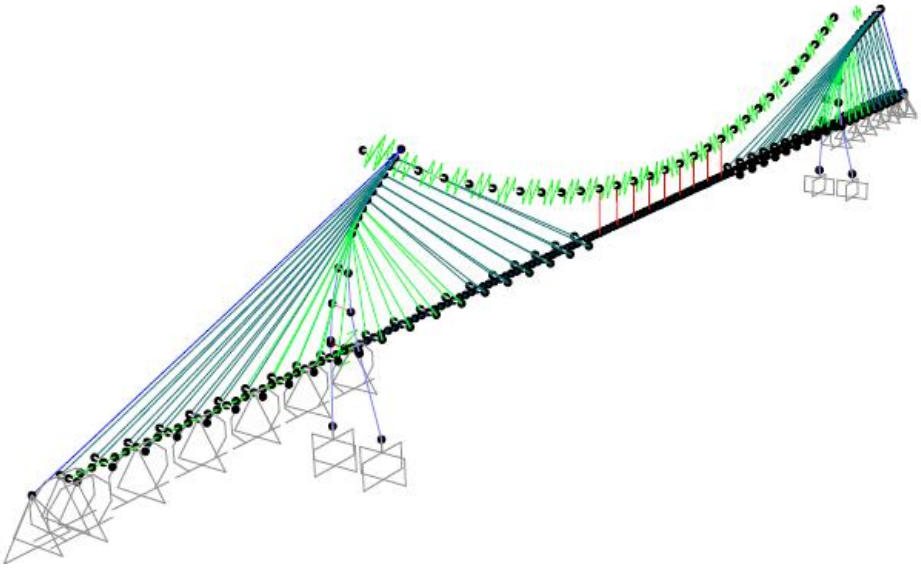

Image 64: Torsional vibration mode in fish-bone beam model

$$f_T^{-1}(SAP) = 2{,}16023 \rightarrow n_\theta = 0{,}463$$

10.2.2 Bending natural frequencies

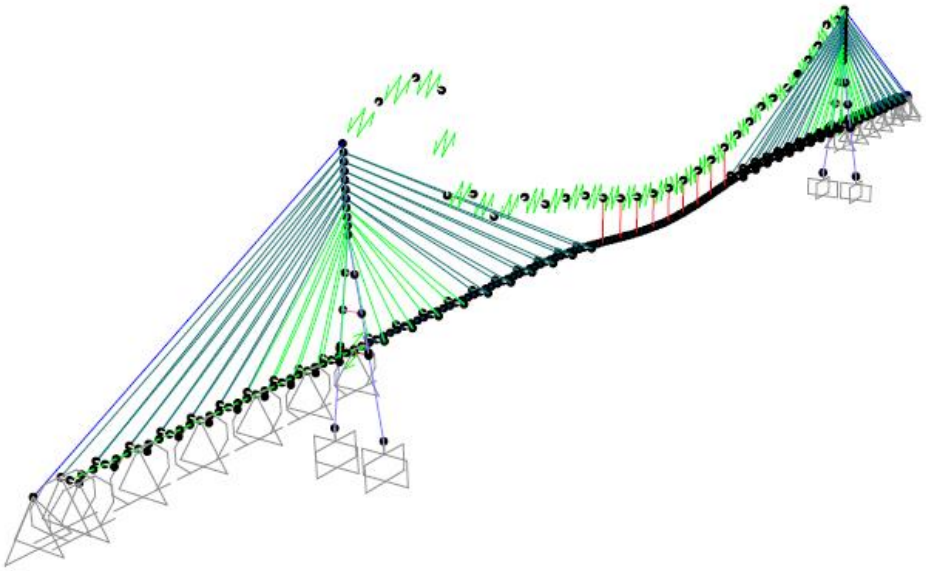

Image 65: Bending vibration mode in fish-bone beam model

$$f_B^{-1}(SAP) = 16{,}2169 \rightarrow n_B = 0{,}062$$

The fish-bone beam model gives us lower torsional natural frequencies than the 2D model. The real problem appears with torsional forces and we it's clearly represented in the towers. We can arrive at the conclusion that designing the tower with an inverted "Y" supposes to have too much high bending stresses in the transversal direction so the solution could be to design it in form of "A".

t's worthy to know what would happen if we restrict the transversal movements in the tower and then increasing it stiffness. We would have this:

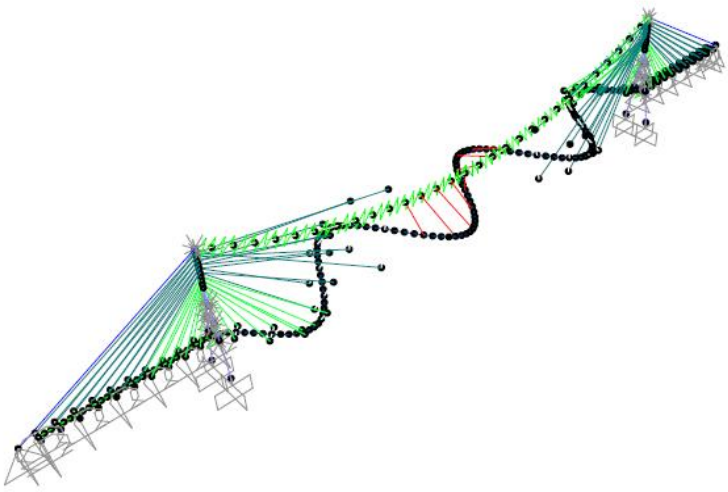

Image 66: Torsional vibration mode with restrictions in the

$$f_T^{-1} = 1{,}38229 \rightarrow n_\theta = 0{,}725$$

The objective has been reached because the torsional effects has been decreased but this is just a theoretical application to approximate the effects of a section in "A" .However, it should be necessary too to adopt a box section with a higher torsional modulus.

10.3 3D Model

In this model we will work with the same equations and methodology we have done in 2D model.

10.3.1 Torsional natural frequencies

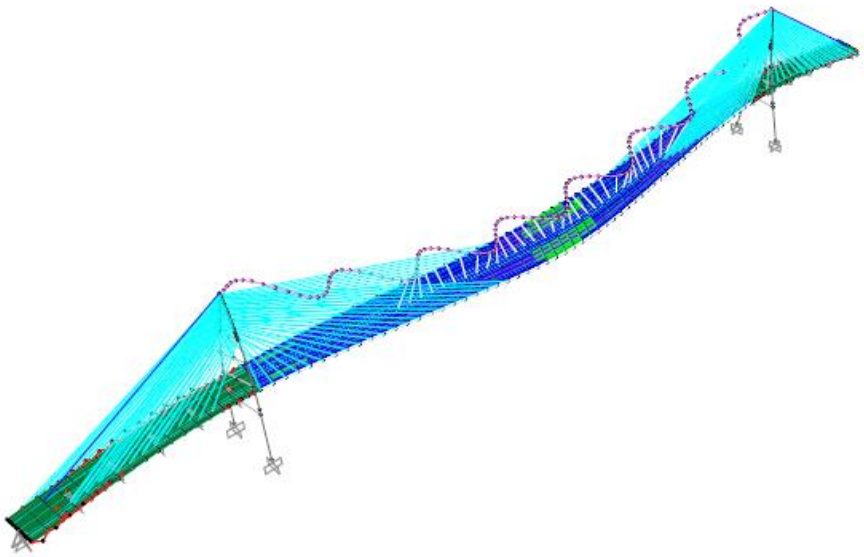

Image 67: Torsional vibration mode in 3D

$$f_T^{-1}(SAP) = 4{,}789 \rightarrow f_B = 0{,}2088$$

10.3.2 Bending natural frequencies

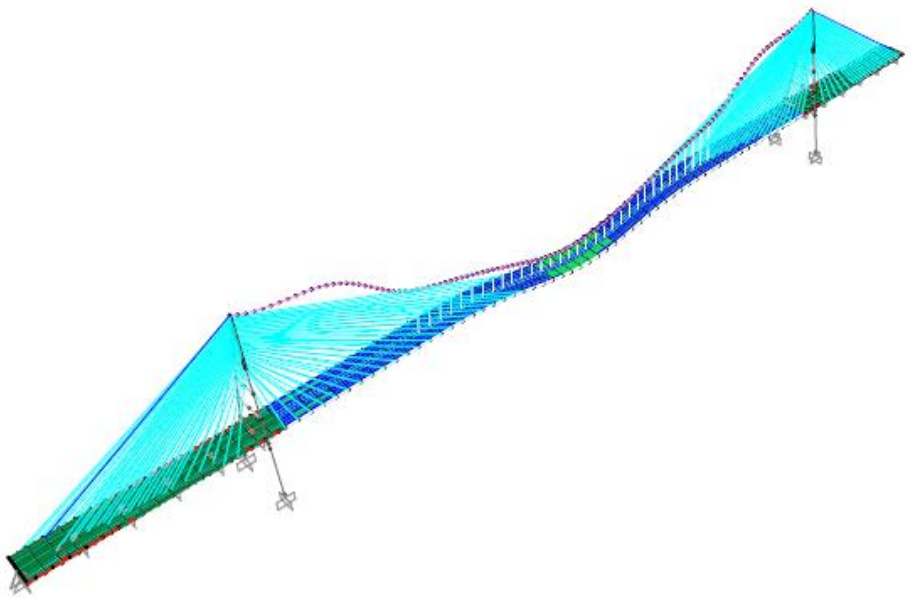

Image 68: Bending vibration mode in 3D

$$v_{max} = 70{,}57\ m$$
$$f_B = 0{,}065307$$
$$f_B^{-1}(SAP) = 14{,}507 \rightarrow f_B = 0{,}06893$$

10.3.3 Flutter critical speeds

Considering the section nº4 we have:

$$m_{pp} = (60 \cdot 0{,}04 + 60 \cdot 0{,}03 + 3 \cdot 4 \cdot 0{,}05) \cdot 7{,}85 + 60 \cdot 0{,}03 \cdot 25 = 82{,}680\ T/m^2$$

If we take into account the stiffener+ diaphragm we have to sum a 10 % more. Then:

$$m_{pp} = 82{,}680 \cdot 1{,}1 = 90{,}948 \frac{T}{m}$$

$$m = m_{pp} + m_{cp} = m_{pp} + m_{pav.} + m_{rail.} = 9{,}177 + 1{,}529 = 10{,}706 \frac{T}{m}$$

$$V_{Rf} = 3{,}7 \sqrt{\frac{mr}{\rho B^3}\left(1 - \left(\frac{n_z}{n_\theta}\right)^2\right)} = 3{,}7 \sqrt{\frac{10.706 \cdot 1{,}4302}{1{,}29 \cdot 60^3}\left(1 - \left(\frac{0{,}069}{0{,}209}\right)^2\right)} = 2{,}565 \frac{m}{s}$$

$$V_f = V_{Rf} \cdot B \cdot n_\theta = 2{,}565 \cdot 60 \cdot 0{,}209 = 32{,}161 \frac{m}{s}$$

$$V_c = \eta \cdot V_{Rf} \cdot B \cdot n_\theta = 0{,}7 \cdot 2{,}565 \cdot 60 \cdot 0{,}209 = 22{,}516 \frac{m}{s}$$

10.3.4 Top speed

$$v_c(z) = \sqrt{C_e(z)} \cdot v_b(T) = \sqrt{5{,}145} \cdot 29{,}12 = 66{,}052\ m/s$$

$$v_{crit.} = 1{,}25 \cdot v_c(z) = 1{,}25 \cdot 66{,}052 = 82{,}565\ m/s$$

$$v_{crit.} > v_c \rightarrow Not\ valid$$

$$n_\theta > 1{,}4 \cdot n_7 \rightarrow 0{,}209 > 1{,}4 \cdot 0{,}069 = 0{,}097 \rightarrow OK$$

$$\frac{mr}{\rho B^3} = 0{,}539 < 5 \rightarrow Not\ valid$$

We can arrive to the conclusion that we should increase the weight, the turning radius (and then the height of the cross-section) and the torsional natural frequency so there is no other way to accomplish all the requirements.

10.4 Comparison between the three models

	2D	Fish-bone model	3D
f_b	0,06541	0,062	0,065307
f_t	0,662	0,463	0,2088

Table 39: Comparison results between the three studied models

We can clearly see that as discretize the structure the torsional frequency values decreases whether the bending values remain almost equal. This is logical since the torsional values are referred to the transversal direction and we are adding on the one hand one more dimensions and on the other hand a fish-bone grid.

11. CONCLUSIONS

This chapter aims to assess the overall thesis and expose what may be the future research on the subject treated.

First of all it should be noted that in the last years the study of the different types of existing bridges has increased so it has been written a large number of books and documents about it. Nevertheless this information in many cases is difficult to access and in more specific aspects is even impossible to access it. That's why given the resources that have been provided the search has been quite complicated.

In terms of what is really this thesis, ignorance and lack of previous hybrid models have led to problems in implementing the model studied in the program ***SAP2000***. As we have seen, at first it has been tried to implement a 3D model but given the computational power of the computer to the excess of elements has made that the program will not reach any solution, so it has opted for the logical solution, ie implement a 2D model. In the application of this model it has seen the type of items to be used for the viability of the calculation as well as the different sections that have been tested throughout the study in order to reach consistent results.

Throughout the calculation phases process it has been observed the problems that have emerged and should highlight the laborious process to reach the calculation of the installation force on the cables in **phase 1** and the iterative process to find the necessary deformation in **phase 3**.

Then it has carried out the verification of the limit states carried out by ***PIEM*** and ***SAP2000*** in order to compare the results through two different routes. At this point we have seen the results could be considered reliable given the little difference that existed between them and verifying the static equilibrium of the bridge.

Finally it has been carried out the dynamic analysis of the bridge with which has been seen that the torsional stresses were too high. It has been concluded that the optimal design for this case would have been to use towers in "A" and the use of a fully enclosed box section.

Knowing that the dynamic study of the bridge was not the main objective of the thesis we can make the future research in conducting the same study with the sections we just have mentioned and the 3D model. To do so will require more powerful computing tools and it would be interesting also to implement more cables with respect to cable-stayed model and discretize more the structure with finite element model.

12. REFERENCES

- M.J.RYALL, G.A.R. PARKE AND J.E.HARDING, *Manual of bridge engineering, 2000.*
- HOLGER SVENSSON, Cable-Stayed Bridges: *40 Years of Experience Worldwide, 2012.*
- WAI-FAH CHEN and LIAN DUAN, *Bridge engineering handbook. Substructure design, 2014.*
- ACHE, *Manual de tirantes, 2007*
- WHITE, E.R., *Structural aspects of cable- stayed bridge design, 1975.*
- M.S. TROITSKY, *Planning and Design of Bridges, 1994.*
- DAVID COLLINGS, *Steel – Concrete Composite Bridges, 2005.*
- P DAYARATHAM, G.P. GARG, G.V.RATNAM, R.N. RAGHAVAN, *Cable Stayed, Supported and Suspension Bridges, 1999.*
- PETROS P. XANTHAKOS, *Theory and Design of Bridges, 1993.*
- CHEN, D.W., AU,F.TK., THAM,L.G. E LEE, P. K. K.., *Determination of initial cable forces in prestressed concrete cable-stayed bridges for given design profiles using the force equilibrium method, Computer and Structures, 2000.*
- GIMSING, NIELS J. *Cable Supported Bridges. Concept and Design, 2011.*
- JOSÉ M.ª GOICOLEA RUIGÓMEZ, *Cálculo de Cables, 2012*
- MARÍA F. QUINTANA YTZA, *Métodos constructivos de puentes atirantados – Estudio de la distribución de fuerzas en los tirantes, 2009.*
- A. KASUGA, J.E.GREEN, K.FURUKAWA, *Optimum cable – force adjustment in concrete cable – stayed bridges.*
- LARSEN A and ESDAHL S, *Bridge aerodynamics Balkema, 1998.*
- ELSA DE SÁ CAETANO, *Cable Vibrations in Cable – Stayed Bridges, 2007.*
- PrEN 1993 -1-11. *Eurocode 3: Design of steel structures, 2004.*
- MINISTERIO DE FOMENTO, *IAP-11: Instrucciones sobre las acciones a considerar en el proecto de puentes de carretera, 2011*